12-1-1992

Energy Storage for Power Systems with Rapidly Changing Loads

Patrick G. Lyons
Purdue University School of Electrical Engineering

Energy Storage for Power Systems with Rapidly Changing Loads

Patrick Gerard Lyons

TR-EE 92-50
December 1992

School of Electrical Engineering
Purdue University
West Lafayette, Indiana 47907-1285

Energy Storage for Power Systems with Rapidly Changing Loads

Patrick G. Lyons

School of Electrical Engineering
Purdue University
West Lafayette, IN 47907-1285

TABLE OF CONTENTS

Page

LIST OF TABLES

LIST OF FIGURES

Figure Page

Figure Page

Figure Page

ABSTRACT

In areas with rapidly changing loads of large magnitude, utility companies often experience large deviations in frequency and area control error. Inadvertent tie-line power flow also occurs. The purpose of this research is to examine the effects a large scale energy storage device has on the system response to a rapidly changing load. Two control areas connected by a tie-line are modelled and simulations are performed to determine the response to a step change in load and also to a five-stand rolling mill load. For each type of load, three cases are studied: no energy storage in the system, a superconducting magnetic energy storage device in the system, and a battery energy storage device in the system. Each case is analyzed and the improvements in system operation for each of the energy storage devices is discussed.

CHAPTER 1

INTRODUCTION

1.1 Motivation and Scope

The main objective of utility companies is to provide enough energy to meet the energy demanded. In doing this, they must concur with a set of environmental, economic, and regulatory requirements. The energy should be provided at minimum cost with minimum effect on the environment. System operation should meet all local, state, and federal requirements, along with any contractual agreements. An effort should be made to maximize safety for employees and customers and also to maximize power quality.

There are many measures of quality in the operation of power systems. For example, system reliability is an integral part of operating philosophies and procedures. Environmental impact, area control error, and cost minimization are also important parameters. One of the major concerns of both producers and consumers of power, and perhaps the most important measure of quality, is the maintenance of the proper system frequency. System frequency is a major indicator of the robustness of the system. The above measures of quality are used in developing the control strategies for system operation. Perhaps the most important of these controls is the automatic generation control.

The minimization of both area control error and inadvertent tie-line power flow and the maintenance of system Frequency are accomplished mainly through the use of automatic generation control. Area control error is defined as the required change in an

area's generation in order to restore frequency and net tie-line power flow to their desired values [33]. Inadvertent tie-line power flow occurs when an area has either too much or too little generation for its load. In simple terms, when there is too little generation, the load is met by an import of power from other areas on the tie-lines. Excess generation creates an export of power to other areas on the tie-lines.

Automatic generation control dictates the governor action at the generating plants based on certain inputs (i.e. system frequency error). The power outputs of the generating stations are set so as to force the frequency error to zero. Due to the dynamic nature of the loads on a power system, there is an ever present mismatch between generation and load. Although usually small, this mismatch means that the frequency error and the area control error are never forced to zero for an extended period of time. With this fact in mind, the North American Electric Reliability Council (NERC) has created guidelines intended to keep area control errors near zero. These guidelines are to be followed by each of the utilities holding membership in NERC.

In highly industrialized areas, there are often special challenges in system operation. Load swings on devices such as arc furnaces and rolling mills are often very large and very rapid. Due to the relatively longer time constants involved in the boiler operation, the power generated cannot meet the load instantaneously. Therefore, the energy required is taken from the rotational kinetic energy of the rotor, causing the rotor to slow and the frequency error to rise. The frequency error and corresponding area control error can be relatively large, often in violation of the NERC guidelines. A possible solution to this problem is the use of a large-scale, fast-acting energy storage device, which can meet the rapidly changing load instantaneously. This lessens the impact on the generators, thereby reducing the area control error and the frequency error.

In this chapter, the NERC area control error guidelines are presented. The use of energy storage devices on the power system is also presented. A general description of

automatic generation control systems and their implementation is provided. Also, alternative types of energy storage devices will be discussed.

1.2 Reliability Criteria

Due to the large number of interconnections in the power network as it exists today, each utility company depends on the reliable operation of neighboring utility companies in order to maintain its own reliability. It is for this reason that the North American Electric Reliability Council has created control performance criteria which apply to all North American utilities. These criteria are intended to establish minimum standards of control performance and provide a means for measuring the relative control performance for each control area [1]. The control performance criteria used by NERC consist of two distinct measurements, A1 and A2. They apply under normal operating conditions (no contingencies).

A1 Criterion

The area control error (ACE) must cross zero within any ten-minute period.

A2 Criterion

The average ACE for each of the 6 ten-minute periods during the hour must be within specified limits (Ld) that are determined from the control area's rate of change of demand [1].

These requirements are intended to keep system frequencies at desired levels, minimizing area control error and time error. They are also intended to keep a utility company from leaning on its tie-lines for any extended period of time.

1.3 Automatic Generation Control

Automatic generation control (AGC) is the means by which frequency is kept to schedule, generation is balanced with load, and the system is operated at an adequate level of security and economy [8,25,26,33]. The purpose of AGC is to replace some of the manual control operations necessary to change generation levels when there is a load change or a trip of a generating unit. Numerous papers delve into the different aspects of AGC and a brief listing is given in references [25-32].

Automatic generation control is essentially a multi-loop feedback controller [26]. It has evolved from the eras of manual and analog control to high speed digital control schemes. Within the control scheme, several inputs, such as tie-line power flows, generation operating points, valve points, and frequency deviation, may be taken [26,29]. From this input, the operating levels of the generating stations are determined. Several other factors are taken into consideration when determining the operating levels. The type of plant is an important factor to consider when faced with fluctuating loads. For example, large coal-fired plants and nuclear plants are not designed to change their operating levels very often. Economics also plays an important role in the control strategies as the lowest possible fuel cost is always desired [25].

The operating levels of the generating stations are set by sending "raise" or "lower" signals to each of the plants. The inputs for the AGC system are usually received at a central system control center. This input is processed and the operating levels of the individual plants are determined according to the criteria mentioned above. A raise or lower pulse, or no pulse, is then sent to each of the generating stations indicating, respectively, an increase, decrease, or maintenance of the current generation level. The pulse received at each station is used to set the governor, which regulates the power output at that plant. The pulse is typically sent out every two seconds [30].

Unfortunately, the purposes of **AGC** are limited by the physical processes involved. Generating stations are not able to change their power outputs instantaneously to meet a large, rapidly changing load. The inertia of the rotating shafts in the system are the only energy storage devices in most power systems so the energy required instantaneously is taken from there. Energy taken from the inertia of the rotating shafts results in their deceleration and a consequent frequency error. The effectiveness of **AGC** is also limited by deadbands that are set throughout the system. For instance, in most control areas in the United States, a frequency deviation of 0.2 Hz or more is necessary before **AGC** is activated. This means that **AGC** has a limited role in decreasing the initial frequency swing associated with a large, rapid change in demand. Trying to maintain a constant frequency or instantaneously reduce area control error to zero would be an exercise in futility. Strategies which yield an acceptable area control error trend and an acceptable range of the unavoidable inadvertent tie-line power flows are preferred [25].

1.4 Energy Storage in Electric Utility Companies

The use of energy storage devices in the electric power system is not a new concept. Thomas Edison used lead-acid batteries in his early electric power business [2,20]. They were used to store energy during the daytime for use at night when the generating stations were shut down. Ironically, the most common use of energy storage devices in utility companies today is just the opposite. Energy is stored at night when the cost is low for use during the day when the cost is high.

The need for energy storage in the power industry arises mainly due to the variations in electric power demand. Electric power demand is constantly changing. Rapidly changing loads can bring about problems with maintaining the desired system frequency, large area control errors, and with inadvertent tie-line flow. Most of the variations are periodic, with periods ranging from a few seconds to a few months [3].

Tha daily load cycle is a dramatic example of the variation of electric power demand. A typical weekly load curve is shown in Figure 1.1 [4]. The electric power demand may range from approximately 50% peak load at night to nearly 90% peak load during the day. This daily cycle presents special challenges in peak shaving and load leveling.

Large coal-fued plants and nuclear plants are designed to meet the base-load needs. These plants are created to run for extended periods of time at maximum or near-maximum power output. They are not designed to fluctuate in their power output as demand changes and frequent cycling of the plants can greatly reduce their life expectancy. As demand rises above the base-load level, it is met with older coal-fired generation, gas-fired generating stations, hydroelectric units, and oil-fired units. These types of plants are designed to better accommodate changes in their power output. Unfortunately, these plants, which are used to meet intermediate and peak loads, are relatively expensive and less efficient to operate [3].

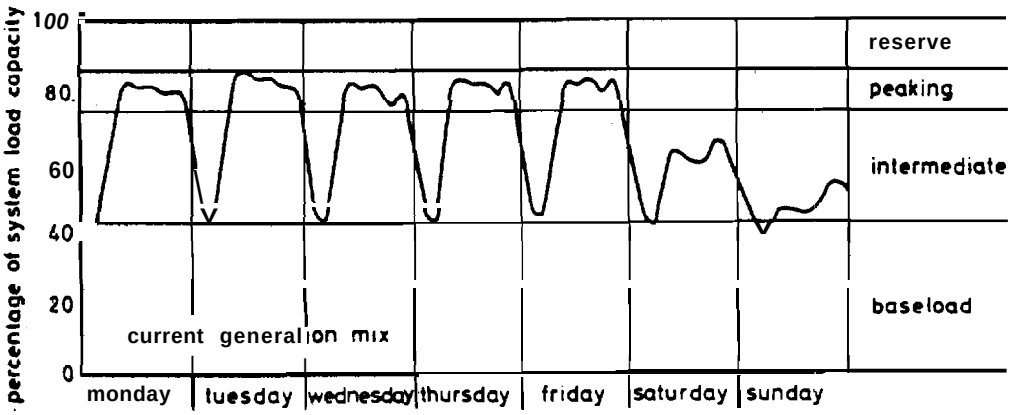

Figure 1.1 Typical Weekly Load Curve

In the United States, load factors on base-load generating stations have been declining in recent years, while peak demands have risen [5]. It is estimated that, on a

yearly basis, utility companies use only about 60% of their generating capacity [6]. Though some generation must be in the form of power plants to meet intermediate and peak loads, a portion of it could be in the form of energy storage plants [3].

The major application of energy storage devices in the power industry today is the use of pumped-hydro stations for load leveling. Presently, about 38 pumped-hydro stations are in operation or being planned in the United States. This represents about 3% of the total generating capacity in the United States [7]. It has been estimated that between 5% and 15% of the generating capacity in the United States could be in the form of energy storage [3]. Figure 1.2 [4] shows a revised weekly load curve with a large scale energy storage device on the system.

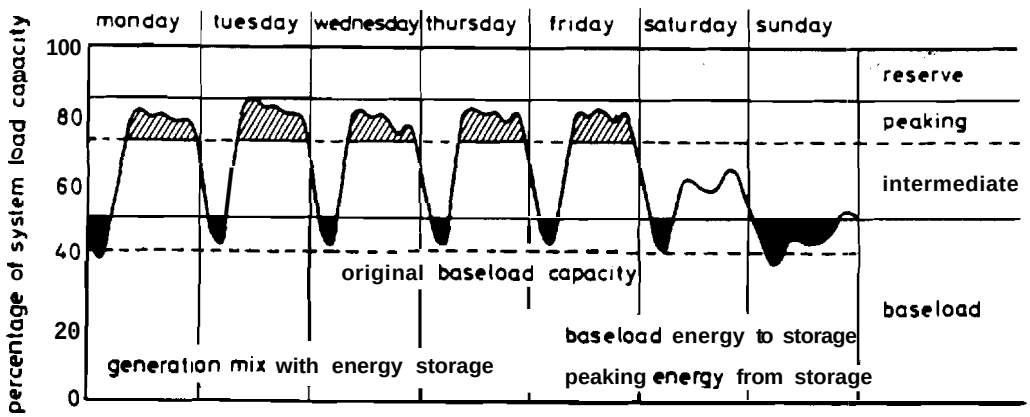

Figure 1.2 Revised Weekly Load Curve with a Large Scale Energy Storage Device on the System

With the development of new technologies (i.e. battery energy storage, superconducting magnetic energy storage), the usefulness of energy storage devices in the power industry is increasing. Battery energy storage plants and superconducting magnetic energy storage (SMES) plants with thyristor power converters provide

advantages that pumped hydro cannot offer. Thyristor control, combined with these types of storage devices, allows for nearly instantaneous change from charge to discharge mode or vice-versa. This creates a whole new set of applications for energy storage on the power system. Two of the major applications for this type of fast-acting energy storage systems are frequency regulation and area control error correction. These systems are capable of providing instantaneous reserve to meet rapidly changing loads. The perturbations caused by these sudden changes in load are absorbed by the energy storage device and not so much the kinetic energy of the rotating shaft [8]. Therefore, the effects on system frequency are lessened.

Some other applications of energy storage devices on the power system include: reactive power compensation, voltage regulation, damping of subsynchronoup oscillations, and providing black start capability [9].

1.5 Energy Storage Devices

The ability to store energy in large quantities would greatly effect the operating practices and philosophies of electric utilities. Power demand could be met instantaneously with stored energy and the system would rely less on strategies such as automatic generation control or load prediction. Large generating stations could be run at their optimum output 24 hours a day, meeting base load during the day and providing power, along with charging energy storage devices, at night. Pumped hydro plants havo already proven their worthiness, with about 38 stations existing today [7].

New technologies have arisen providing more options to electric utility companies in their use of energy storage devices. Superconducting magnetic energy storage facilities and battery energy storage facilities with thyristor controlled converters are capable of providing instantaneous supply or demand of power. This can improve

power quality and improve system operation in terms of frequency maintenance, reduction of area control error, and inadvertent tie-line flow.

The following subsections discuss the proven technology of pumped hydroelecmc storage and the largely experimental, but highly promising, technologies of SMES and battery energy storage.

1.5.1 Pumped Hydroelecmc Energy Storage

Pumped hydro technology is the only truly proven technology available for energy storage in the power industry. This technology dates back to 1879, when a unit was put into operation in Zurich, Switzerland [10]. The first pumped hydro unit installed in the United States was the Rocky River unit for Connecticut Power and Light in the year 1929 [11]. It was not until the early 1950's that pumped hydro became a widely accepted means of meeting peak demands. This acceptance coincided with the development of the reversible Francis pump-turbine. Today, there are over 150 plants worldwide with a total installed capacity of about 100,000 MW. These plants range in size from a few megawatts to over 2000 MW. In the United States, 38 plants account for 18,000 MW of capacity. This is 18% of worldwide pumped hydro capacity and 3% of the total generating capacity of the United States [7].

A pumped hydro plant uses potential energy as its means of energy storage. A diagram of the North of Scotland Hydro-Electric Board, Crauchan Station is shown in Figure 1.3 [4]. During peak demand hours, the energy contained in the water falling from the upper reservoir is converted into elecmcity by the turbines. When the demand is low, the water is pumped back up to the upper reservoir, thereby restoring its potential energy.

The main function of pumped hydro energy storage is that of load leveling. A large-scale pumped hydro plant is capable of increasing demand during the night, while in pumping mode, and meet peak demand during the day, while in generating mode. This

results in a revised load curve like the curve shown previously in Figure 1.2. Depending on the individual plant parameters, pumped hydro plants consume 1.3 - 1.4 kWh in pumping for every 1 kWh generated [10].

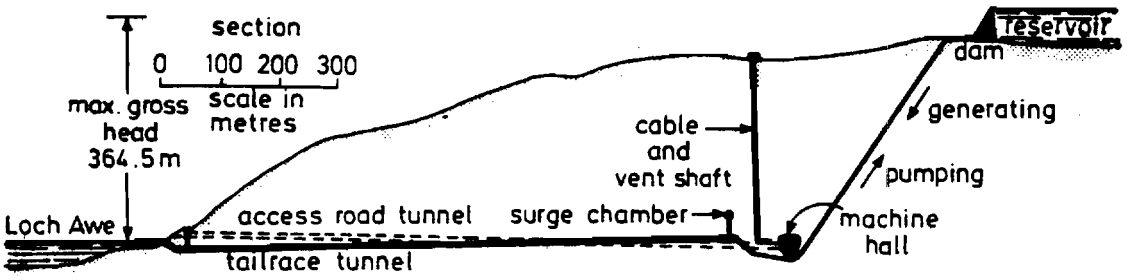

Figure 1.3 The North of Scotland Hydro-Electric Board, Crauchan Station

Some of the major pumped hydro facilities in the United States include: Northeast Utilities, 1000 MW Nonhfield Mountain Plant in Massachusetts; Pacific Gas and Electric Company, 1200 MW Helms Plant in California; and Virginia Power, 2100 MW Bath County Plant in Virginia [10].

1.5.2 Superconducting Magnetic Energy Storage

Superconducting magnetic energy storage (SMES) is a relatively new technology. An early paper by Femer [44] considers the use of a large energy storage coil for France [3]. In the United States, studies of SMES began in the early 1970's at the University of Wisconsin. Since that time, other groups have undertaken large-scale feasibility and applicability studies of SMES. These groups include: Los Alamos Scientific Laboratory, the United States Atomic Energy Commission, Bonneville Power Administration, and the Elecmc Power Research Institute among others [3].

The principles behind SMES are relatively straightforward. A coiled wire, called a solenoid, carries current and generates a magnetic field. If the ends of the wire are connected and there is no circuit resistance or sources, the resulting current does not decay [14]. The state of no resistance is achieved by using a superconducting wire. Superconductivity is achieved by cooling certain materials (i.e. Niobium or Titanium) to their critical temperatures and maintaining those temperatures. The literature on superconductivity is very extensive with references [36 - 39] being representative of the low temperature superconductivity phenomena and references [40 - 43] being representative of the high temperature type. Superconductivity has two main advantages. First, no heat is generated due to the lack of resistance, meaning large currents can be carried with little degradation of the wire. Secondly, since their are no resistive losses, the energy in the magnetic field is maintained without the need for additional energy [14].

An SMES facility would consist of several major subsystems: the superconducting coil, a Helium refrigeration system, an AC/DC converter, a structural support system, and accompanying control and protection systems [2,15,16]. The basic components of an SMES facility are shown in Figure 1.4 [8].

The transformers convert the high voltage and low current of the power system to the lower voltage and higher current required by the coil [3]. The AC/DC converter changes the alternating current from the power grid to direct current. The controller may use several inputs from both the AC system and the SMES system. These inputs are used to dictate the firing angle of the semiconductor-controlledconverter, which determines the voltage across the inductor. The firing angle may be changed rapidly, allowing an SMES unit to change from full charge to full discharge on the order of tens of milliseconds [3]. The voltage, shown as V_d in Figure 1.4, is positive when charging the superconducting coil, negative for discharging, and zero for maintaining a constant energy level in the superconducting coil. The current, I_d, fluctuates between maximum

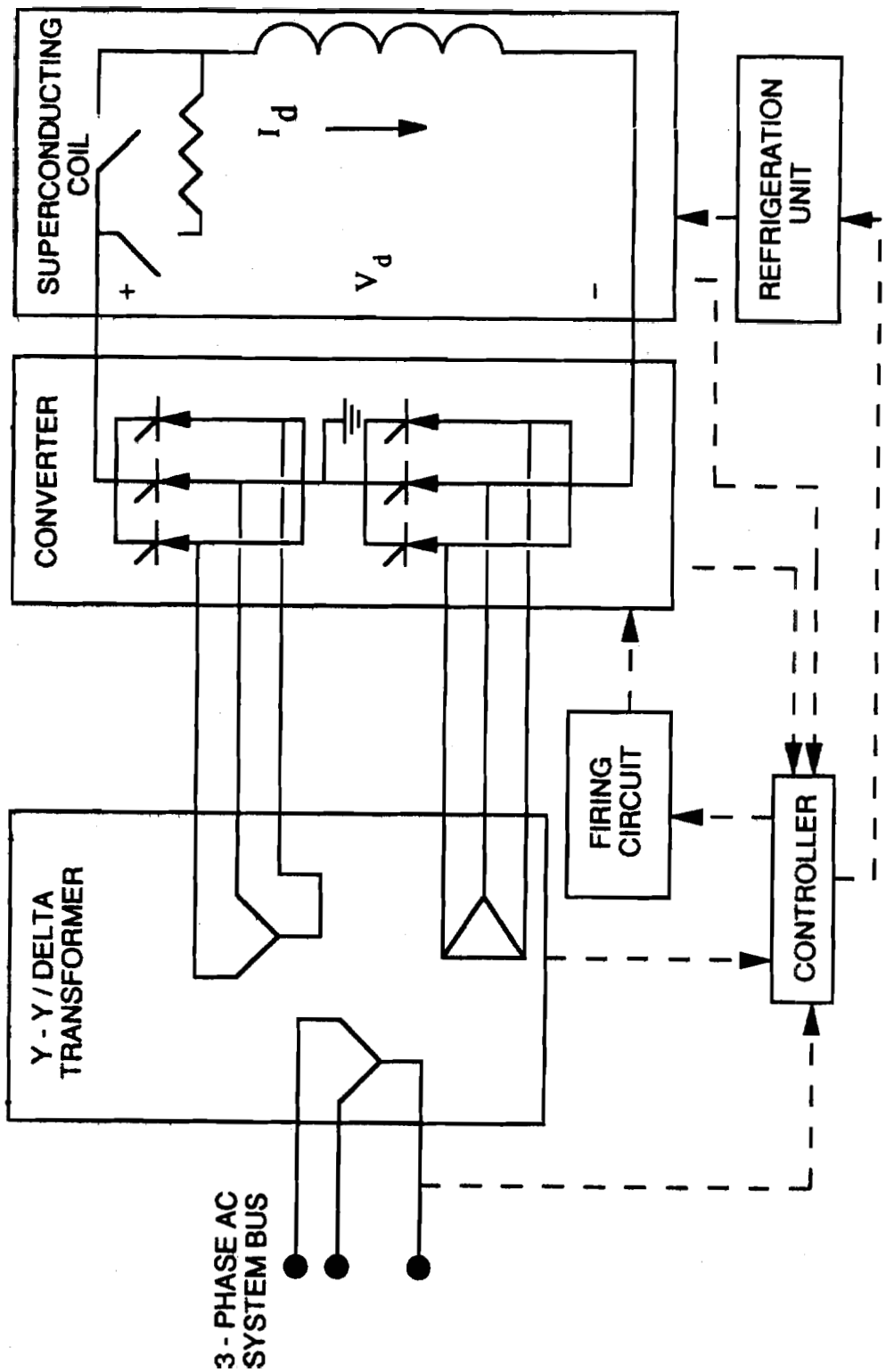

Figure 1.4 Basic Components of an SMES Facility

current and some set minimum current. The large forces associated with the electromagnetic field in the superconducting coil require a large and costly structural support system for the SMES facility. A Helium refrigeration unit is also a necessity in a low temperature SMES system to remove heat generated in the coil and maintain superconducting temperatures. The resistor shown in Figure 1.4 is the "dump" resistor. When needed, it can be switched in series with the superconducting coil causing the energy stored in the coil to be dissipated as heat through the resistor.

Obviously, the two major advantages of an SMES unit would be the fast reaction time of the AC/DC converter and the nearly lossless storage device. It has been estimated that the efficiency of an SMES unit would be in the range of 92% to 95% [3,14,16]. The losses would come in the AC/DC converter and in the power needed to run the refrigeration system.

In February of 1983, an 8.4 kWh SMES demonstration unit with a 10 MW converter was energized at the Tacoma substation of the Bonneville Power Administration [12,13,17]. It was designed to damp the dominant power swing mode of the Pacific AC Intertie [12]. The plant was the first major application of superconducting technology in the utility industry. The plant ran intermittently for over a year and was retired in March of 1984. Although in service for a relatively short time, tests on the SMES unit provided valuable information on the control-law design, electrical characteristics of the device, and its effectiveness as a power system stabilizer [12,13].

The applications of an SMES unit within a power system are numerous. The following applications are considered in this thesis: minimization of frequency deviation, minimization of area control error, and minimization of inadvertent tie-line power flow. Other applications include: load leveling, peak shaving, damping of subsynchronous oscillations, VAR control, spinning reserve, black start capability, and improvement of system transient performance [14,18].

1.5.3 Battery Energy Storage

Battery energy storage technology is nearly 200 years old. Alessandro Volta developed the galvanic battery in the year 1800 [19]. Thomas Edison used Lead-acid batteries in his early power business to store energy during the daytime for use at night [2,20]. It was not until the late 1960's though that large-scale battery energy storage units were seriously considered for use in the electric power industry in the United States.

A battery facility uses electrochemical energy storage. The operation of a basic Lead-acid battery is explained by Anderson and Carr [21].

> "Each cell of a charged Lead-acid battery comprises a positive electrode of Lead dioxide and a negative electrode of sponge Lead, separated by a microporous material. When these electrodes are immersed in an aqueous sulfuric acid electrolyte, contained in a plastic case, a nominal open circuit voltage of 2 volts is created. When the circuit between the two electrodes is closed, the battery discharges its stored energy; the Lead dioxide on the positive electrode is reduced to Lead oxide, which reacts with sulfuric acid to form lead sulfate; and the sponge Lead on the negative electrode is oxidized to lead ions that react with sulfuric acid to form Lead sulfate. In this way, chemical energy stored in the battery is converted to electrical energy."

A block diagram of a battery energy storage facility is shown in Figure 1.5 [2]. It consists of several major subsystems, including: AC/DC converter, battery subsystem, and the control and protection circuitry.

The transformer converts the low current and high voltage of the AC system to a higher current and lower voltage more suitable for battery operation. The AC/DC converter is a semiconductor-controlleddevice, which changes the alternating current to direct current. The control system takes inputs from both the battery system and the AC system. From these inputs, the firing angle of the AC/DC converter is determined. The firing angle dictates the voltage across the terminals of the battery subsystem. The battery subsystem usually consists of a large number of cells in some parallel of series configuration. The series connections set the voltage of the battery subsystem, 'while the parallel connections are used to increase the storage capacity. If the AC/DC converter

voltage is set greater than the voltage of the batteries, the batteries will be charged. If the converter voltage is set lower than the voltage of the batteries, the batteries discharge.

As in SMES systems, battery energy storage systems allow for almost instantaneous reversal of power flow. Although their efficiency is not as high as an SMES system, it is still relatively good. Efficiencies have been estimated up to 84% [22].

The applications of a battery energy storage unit on the power system are numerous and well documented. This thesis focuses on applications in the areas of minimization of frequency deviation, minimization of area control error, and minimization of inadvertent tie-line power flow. Other applications include: load leveling, peak shaving, instantaneous reserve, voltage regulation, damping of subsynchronous oscillations, providing black start capabilities, and improvement of base-load efficiencies [2,5,9,23,24].

There are several major battery energy storage facilities at this time. Southern California Edison uses its Chino 10 MW, 51.2 MWh demonstration plant for load leveling. In Berlin, a 17 MW, 14.4 MWh battery energy storage facility has been used since 1987 to regulate frequency [2]. Between 1992 and 1995, the Puerto Rico Electric Power Authority is scheduled to install over 100 MW of battery energy storage capacity [21]. These examples, along with several others, point out the feasibility and growing importance of battery energy storage facilities for utility usage.

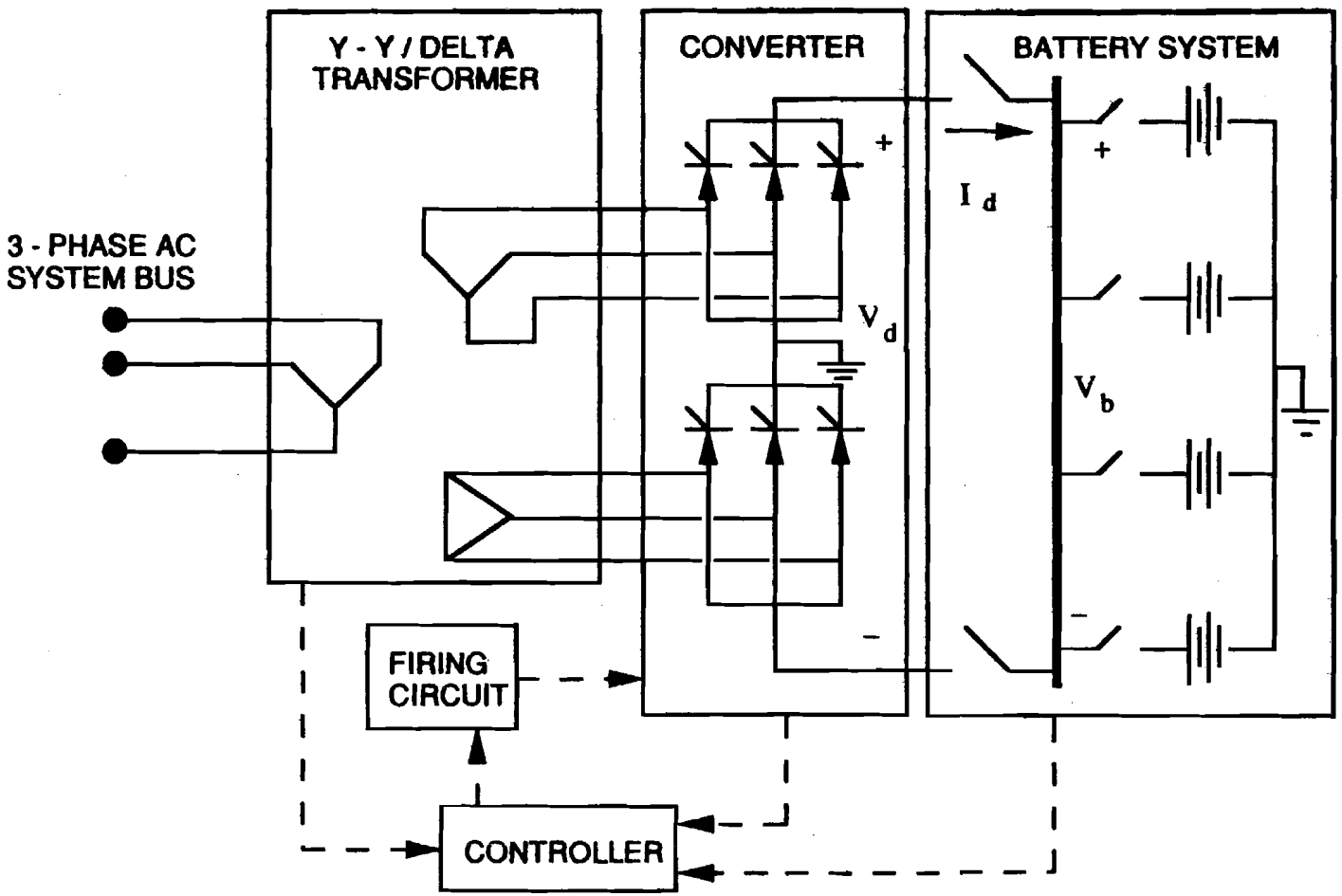

Figure 1.5 Block Diagram of a Battery Energy Storage Facility

CHAPTER 2
SYSTEM MODELING

2.1 Overall Model

In order to determine the effect of an energy storage device on a power system, it is necessary to devise a model for the system and use this model to simulate system operation. This section steps through the derivation of the different components of the overall system model. The objective is to formulate an overall model of a power system on automatic generation control.

2.1.1 Dynamic System Model

The dynamic model of the rotating mass in a power system essentially relates the frequency of the system and the net power in the system. It is necessary to assume that within a specified control area, the ties are strong enough to allow a single frequency to characterize the entire area [27]. Following a disturbance ΔP_d, the net surplus of power in the area will be $\Delta P_g - \Delta P_l$ MW, where P_g is the generated power and P_l is the demand power. This power mismatch is absorbed by the system in three ways: the first way is by increasing (or decreasing) the area kinetic energy. The rate of change of the kinetic energy is given by [27]

$$\frac{d}{dt}W_{kin} = \left[W^*_{kin}\left(\frac{f}{f^*}\right)^2 \right] \qquad (2.1)$$

$$\cong \frac{d}{dt}\left[W^*_{kin}\left(1+2\frac{\Delta f}{f^*}\right)\right] \tag{2.2}$$

$$= 2\frac{W^*_{kin}}{f^*}\frac{d}{dt}\Delta f \tag{2.3}$$

where W_{kin} is the system total kinetic energy, W^*_{kin} is the rated kinetic energy of the system (i.e. at rated frequency), f is the area frequency, and f^* is the rated frequency (60 Hz).

A second way the power mismatch is absorbed by the system is by increased (or decreased) load consumption. Since motor loads are a major part of the total demand, their change in load due to change in frequency must be modeled [33]. The relationship is characterized by a constant D, where

$$\Delta P_l = D\Delta f. \tag{2.4}$$

The third means of absorbing the changing load in the system is by varying the export of power over the tie-lines by an amount ΔP_{tie}.

Therefore, an overall equation can be used to describe the system response following a disturbance ΔP_d [27]

$$\Delta P_g - \Delta P_l = 2\frac{W^*_{kin}}{f^*}\frac{d}{dt}(\Delta f) + D\Delta f + \Delta P_{tie}. \tag{2.5}$$

Dividing by P_r, the total rated power in the specified area, the AP terms are written in per unit and the equation becomes

$$\Delta P_g - \Delta P_l - \Delta P_{tie} = 2\frac{H}{f^*}\frac{d}{dt}(\Delta f) - D(\Delta f). \tag{2.6}$$

where H is the inertia constant in seconds. Taking the Laplace transform,

$$\Delta f(s) = \frac{K_p}{1 + sT_p}[\Delta P_g(s) - \Delta P_l(s) - \Delta P_{tie}(s)]. \tag{2.7}$$

The block diagram form is shown in Figure 2.1 where

$$K_p = \frac{1}{D} \quad \text{and} \quad T_p = 2\left(\frac{H}{f^*}\right)\left(\frac{1}{D}\right) \tag{2.8) - (2.9}$$

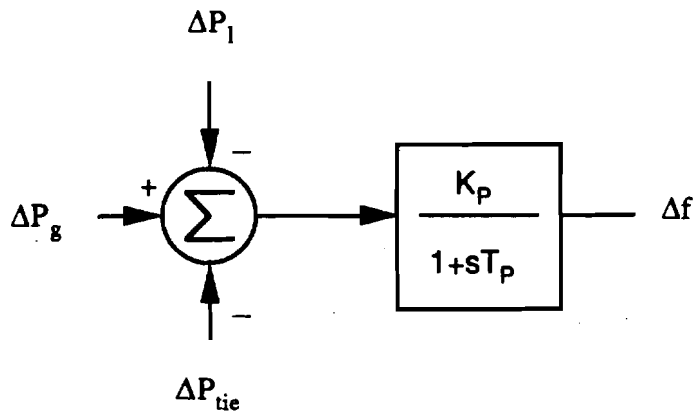

Figure 2.1 Block Diagram of the Dynamic System Model

2.1.2 Governor Model

The governor is a device which adjusts the input valve that controls the steam flow to the prime mover. The governor control action is usually set by the system frequency. The governor action increases or decreases the mechanical power output to

restore the system frequency to its desired value. The block diagram of a governor model is given in Figure 2.2. The load reference input allows the governor characteristic to be set to give reference frequency at any desired unit output [33]. The value of R1 determines the change in the generating unit output for a given change in frequency. The time constant T_g represents the delays inherent in the opening or closing of the valve. The output, ΔP_{valve}, determines the setting of the mechanical power output of the prime mover.

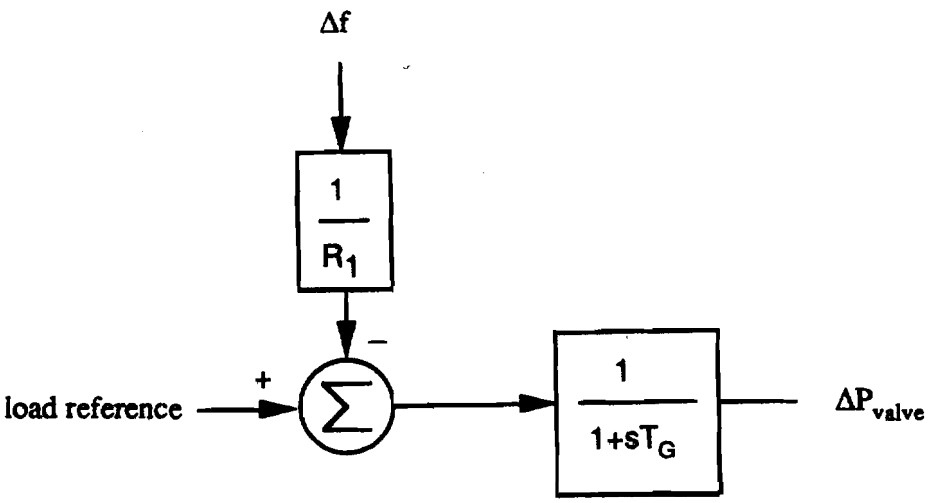

Figure 2.2 Block Diagram of the Governor Model

2.1.3 Steam Turbine System Model

Steam turbine system models vary widely depending on the type of system (i.e. single reheat, double reheat) and the amount of detail desired. A common simplified model used to represent a steam system with reheat turbines is shown in Figure 2.3.

The input to the system is ΔP_{valve}, which represents the opening or closing of the governor-controlled valves. The time constants T_t and T_r are representative of the

delays introduced by the steam chest, inlet piping, reheaters, and crossover piping [34]. The output, ΔP_g, is the mechanical power output of the turbine. This is also assumed to be the electrical generator output.

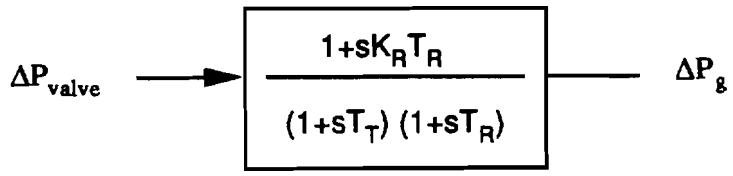

Figure 2.3 Block Diagram of the Steam Turbine System

2.1.4 Tie-Line Model

Using the DC load flow method [33], the power flow between two areas across a tie-line is expressed as

$$P_{tie} = \frac{1}{X_{tie}}(\Theta_1 - \Theta_2). \tag{2.9}$$

where P_{tie} is the power flowing from area 1 to area 2, Xtie is the impedence of the tie-line, and Θ_1 and % are the phase angles of the respective areas. If a disturbance is applied, the equation becomes

$$P_{tie} + \Delta P_{tie} = \frac{1}{X_{tie}}[(\Theta_1 + \Delta\Theta_1) - (\Theta_2 + \Delta\Theta_2)] \tag{2.10}$$

$$= \frac{1}{X_{tie}}(\Theta_1 - \Theta_2) + \frac{1}{X_{tie}}(\Delta\Theta_1 - \Delta\Theta_2). \tag{2.11}$$

Then

$$\Delta P_{tie} = \frac{1}{X_{tie}}(\Delta\Theta_1 - \Delta\Theta_2). \tag{2.12}$$

The difference of the change in the angles is found by integrating the difference of the change in frequencies. The new equation becomes

$$\Delta P_{tie}(s) = \frac{2\pi T_{12}}{s}[\Delta f_1(s) - \Delta f_2(s)]. \tag{2.13}$$

If the two systems have different power ratings and if Equation (2.13) is expressed in per-unit on a distinctive control area base, a constant must be included to account for these distinct bases. The block diagram for the tie-line power flow is shown in Figure 2.4. The term a_{12} is defined by the power ratings of the two systems

$$\Delta P_{tie,2} = \frac{-P_{rated,1}}{P_{rated,2}}\Delta P_{tie,1} \tag{2.14}$$

$$a_{12} = \frac{-P_{rated,1}}{P_{rated,2}} \tag{2.15}$$

$$\Delta P_{tie,2} = a_{12}(\Delta P_{tie,1}). \tag{2.16}$$

2.1.5 Automatic Generation Control Model

Automatic generation control (AGC) is the control system whose major function on the power system is to match generated power with demand. There are numerous factors which could contribute to the AGC configuration. These include: reducing the static frequency error following a step change in load; keeping the time error within

certain maximum and minimum values; maintaining the correct value of interchange power between control areas; reducing the area control error to zero in the steady state [25,27,33].

The selected control scheme was one in which each area control error is driven to zero in the steady state. The area control error is defined as

$$ACE = -B_1(\Delta f) - \Delta P_{tie} \tag{2.17}$$

where B_1 is the frequency bias factor, Δf_1 is the frequency deviation in the specified area, and ΔP_{tie} is the change in tie-line power flowing into the area. In order to reduce the ACE to zero in the steady state, the ACE is integrated and the resulting signal is used as the load reference signal to the governor. This signal input can be seen in Figure 2.2. Ideally, this sets the unit output so as to force the ACE to zero. A block diagram of the automatic generation control logic is shown in Figure 2.5.

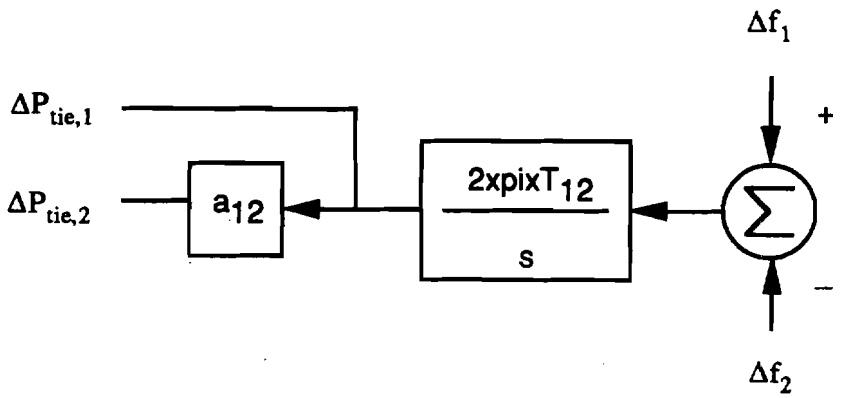

Figure 2.4 Block Diagram of the Tie-Line Power Flow

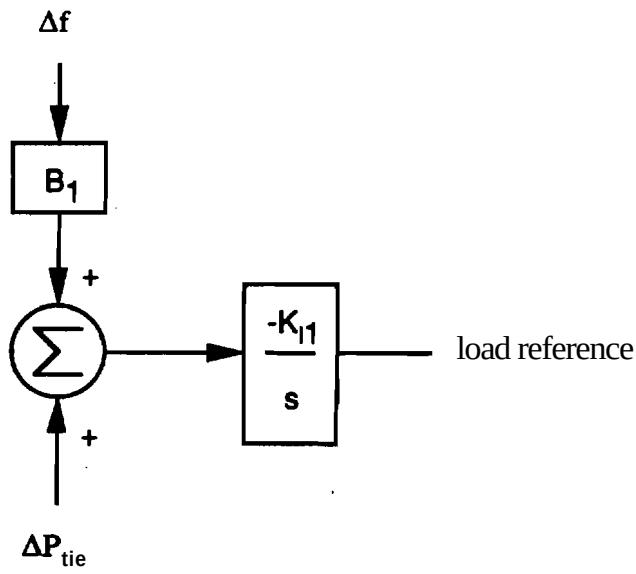

Figure 2.5 Automatic Generation Control Logic

2.1.6 Load Model

Two different load models were used in the studies. The first model is a simple step change in load of 0.025 **p.u.**. and it is shown in Figure **2.6.** This load was applied to the system in order to observe the system response to a rapid change in load. The second load models a 5-stand rolling mill with a maximum change in load of 0.025 **p.u.**. This type of load is common in the steel **industry.** The model, shown in Figure 2.7, is based on the strip chart recording of the real power demand of an actual 5-stand rolling mill.

2.1 Overall Model

The models of the different parts of the power system are brought together to form the overall model. This overall model is a **model** of two different control areas connected by a tie-line and it is used in the simulations described in this thesis. Area 1

has 1000 MW of generating capacity and this is used as a per unit base in this area. Area 2 has 3000 MW of generating capacity and its per unit terms are on a 3000 MW base. A block diagram of the overall model is shown in Figure 2.8. The values for the constants in the overall model are shown in Table 2.1.

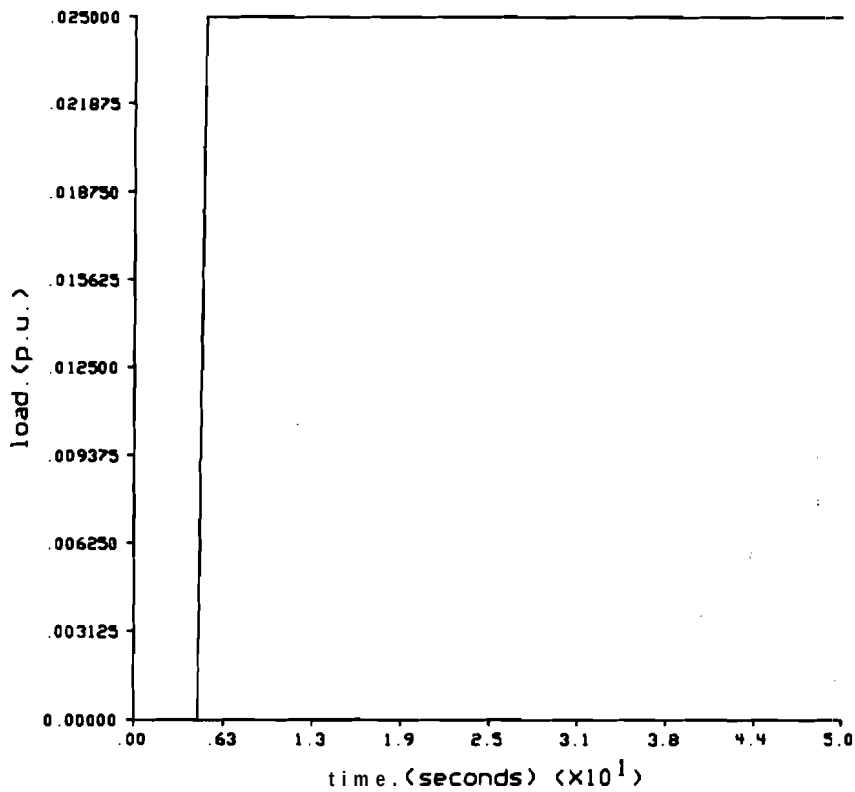

Figure 2.6 Step Change in Load

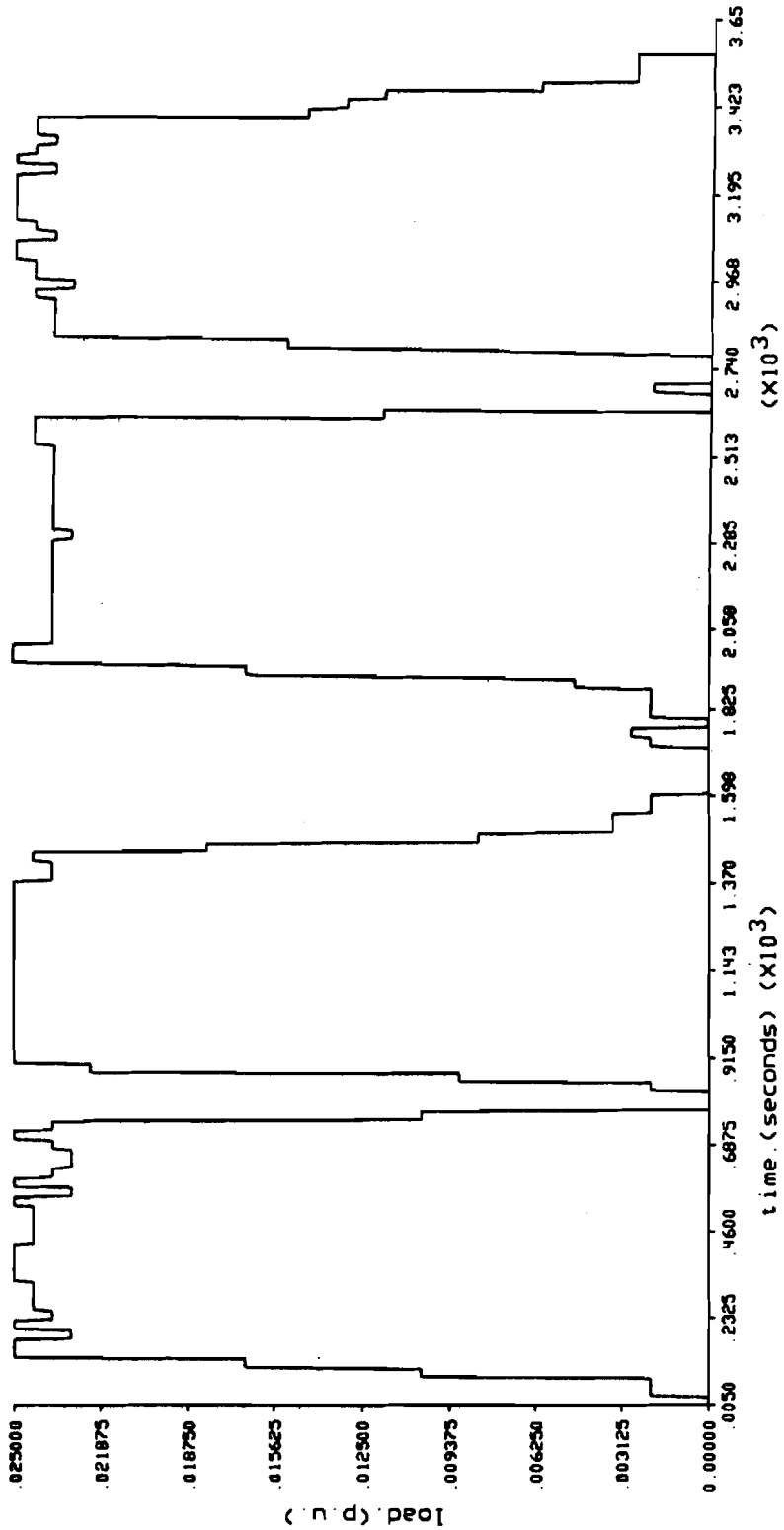

Figure 2.7 Five-Stand Rolling Mill Load

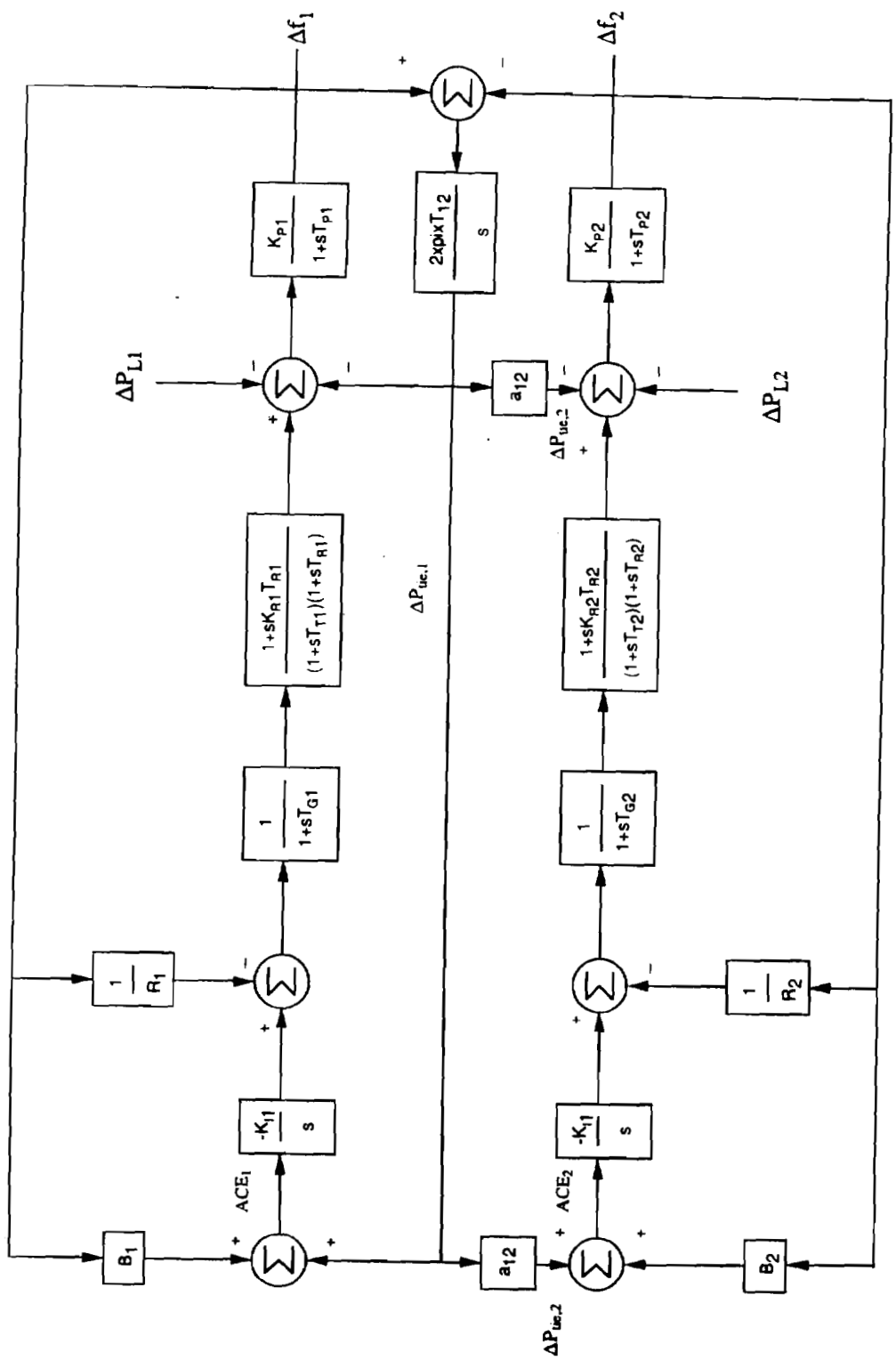

Figure 2.8 Block Diagram of the Overall System Model

Table 2.1 Values of Constants in the Overall System Model

Constant	Units	Value
Pr1	MW	1000
Pr2	MW	3000
Kp1, Kp2	Hz/p.u. MW	100
Tp1, Tp2	seconds	20
Tg1, Tg2	seconds	0.08
Tt1, Tt2	seconds	0.3
Kr1, Kr2		0.5
Tr1, Tr2	seconds	10
R1, R2	Hz/p.u. MW	2.4
B1, B2		0.425
T12		0.0866
a12		-0.333
Ki1, Ki2	Hz/p.u. ACE	0.3

2.2 Energy Storage System Models

In order to simulate the effect of an energy storage device on a power system, it is necessary to devise a model for the energy storage device and incorporate this model into the overall system model shown in Figure 2.8. All of the energy storage devices discussed in this thesis use an AC/DC converters as the interface between the energy storage device and the electric power system. A typical configuration is a cascaded bridge converter. The thyristors in the converter are controlled by a firing circuit. The firing circuit sends pulses to the thyristors, causing them to conduct. The pulse is sent at a specific time during the 16.67 millisecond cycle. This is done to keep the average voltage across the converter DC terminals at the desired level [3]. The firing angle, which can vary over a range of 0 to 180 degrees, determines the value of the average voltage across the DC terminals of the converter. This average voltage is given by the equation

$$V_d = V_o \cos\alpha \tag{2.18}$$

where a is the firing angle and V_o is the maximum value of the average voltage. By changing the firing angle, the average voltage across the energy storage device can be changed the from maximum positive value to the maximum negative value within a few milliseconds. Since the voltage across the energy storage device dictates the direction and magnitude of the power flow, the device can go from maximum charge to maximum discharge nearly instantaneously.

In the energy storage system models, the voltage across the converter is a function of the frequency deviation. The Laplace transform of the equation [8] is

$$\Delta V_d(s) = \frac{K_o}{1 + sT_d} \Delta f(s) \tag{2.19}$$

where ΔV_d is the change in voltage across the energy storage device and Af is the frequency deviation. The constants are K_o = 30 kV/Hz and T_d = 0.026 seconds. The voltage is set so that when the frequency deviation is negative, the change in the average voltage across the energy storage device is negative. Therefore, the average voltage, V_d, decreases and the device discharges. When the frequency deviation is positive, the change in the average voltage across the energy storage device is positive, the average voltage increases, and the device charges. In order to avoid operation of the energy storage device in response to small frequency deviations, a deadband of $\pm$ 0.005 Hz was set. The new overall system model with the energy storage device in place is shown in Figure 2.9. The output of the energy storage device, ΔP_d, is the charge or discharge power.

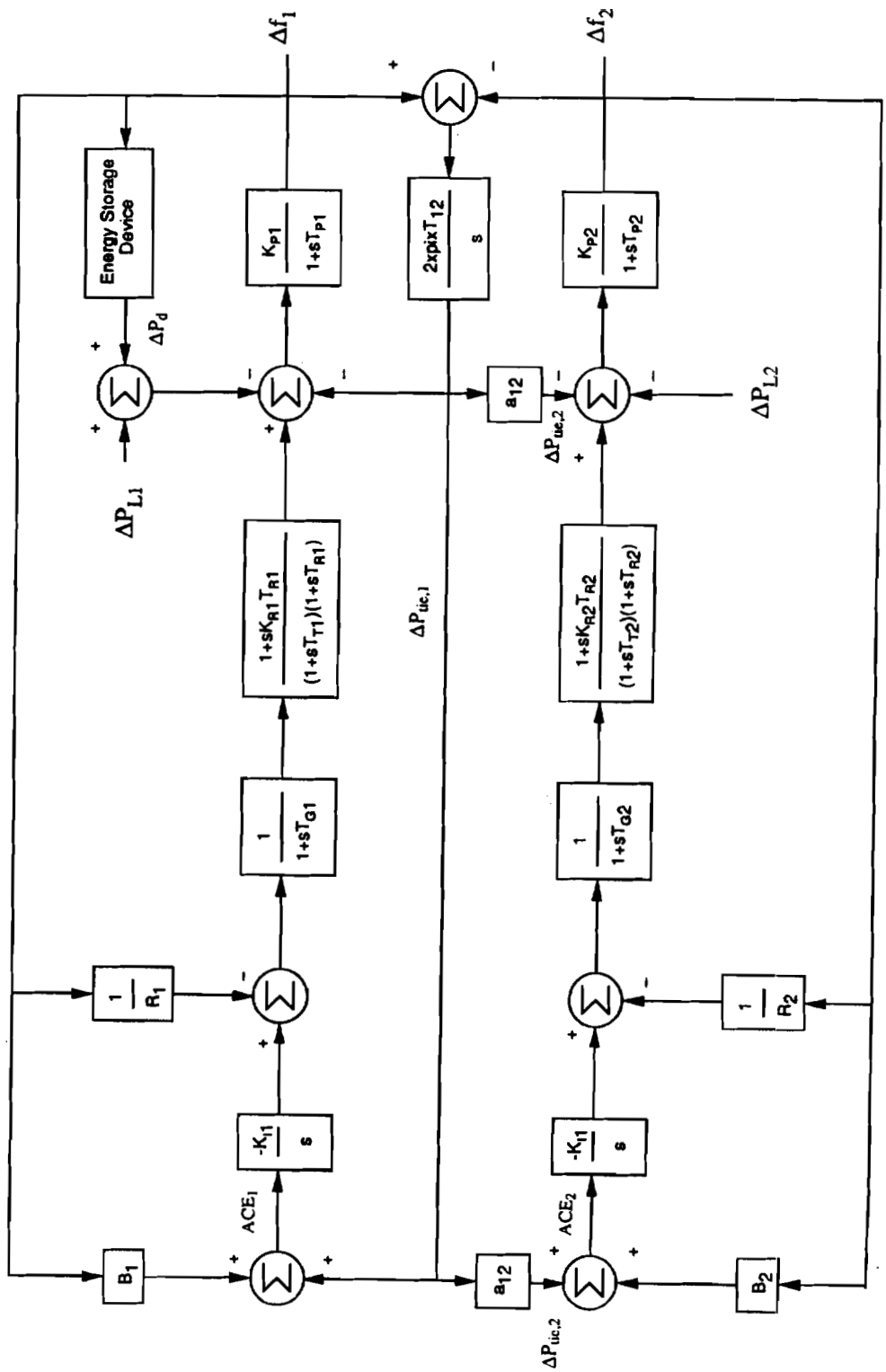

Figure 2.9 Block Diagram of the System Model with an Energy Storage Device

2.2.1 Superconducting Magnetic Energy Storage Model

A diagram of a superconducting magnetic energy storage (SMES) unit is shown in Figure 1.4.

As shown in Equation (2.19), the voltage across the superconducting coil is continuously controlled by the frequency deviation (unless the frequency deviation lies within the ± 0.005 Hz deadband). A rapid increase in load causes the area frequency to drop. Subsequently, the voltage across the inductor becomes negative and it discharges. The act of discharging causes the inductor current to drop. The equation

$$V_d = L\frac{dI_d}{dt} \tag{2.20}$$

applies. By taking the Laplace transform of the relaxed system and rearranging, the equation becomes

$$\Delta I_d(s) = \left(\frac{1}{sL}\right)\Delta V_d \tag{2.21}$$

where ΔI_d is the deviation in inductor current, L is the inductance of the coil, and ΔV_d is the deviation in the average voltage across the superconducting coil given by Equation (2.19). The equations for the voltage across the DC terminals of the converter, V_d, and the current in the superconducting coil, I_d, are

$$V_d = V_d + \Delta V_d \tag{2.22}$$

and

$$I_d = I_d + \Delta I_d. \tag{2.23}$$

The charging or discharging power is given by

$$P_d = V_d I_d. \tag{2.24}$$

The parameters of the SMES unit were based on typical parameters found in references [3, 8, 12]. The SMES unit is typically a low voltage, high current device. The upper and lower limits on the converter voltage were chosen as 500 volts and -500 volts respectively. The maximum power output of this energy storage device is chosen to best match the type of loads on the system. In this study, the maximum power during charge or discharge is 25 MW. For the maximum desired power, the maximum current is found using the equation

$$P_{max}=V_{max}I_{max}. \tag{2.25}$$

The maximum current is found to be 50 kA. In practice, the inductor current, I_d, should not be allowed to reach zero. This prevents the possibility of discontinuous conduction in the case of a large disturbance [8]. A lower limit of 30% of I_{do}, which is the rated conductor current, was chosen. An upper limit on the conductor current must also be chosen. It is chosen such that the maximum allowable energy absorption is equal to the maximum allowable energy discharge. Using the equal energy charge/discharge criterion [8] and knowing that the minimum inductor current is $0.3\ I_{do}$, the maximum inductor current is found to be $1.38\ I_{do}$. For the SMES system, I_{do} is chosen as 36 kA. The maximum current is then 50 kA and the minimum current is 10.8 kA.

The application of this energy storage device for frequency control does not require a large amount of energy storage capacity. A maximum storage capacity of 2 MWh is sufficient to supply frequency control for loads such as the, rolling mill load shown in Figure 2.7. Based on the maximum amount of energy storage capacity required and the maximum current in the inductor, the inductance of the superconducting coil is found. The equation is

$$W_{max} = \frac{1}{2} L(I_{max})^2 \tag{2.26}$$

and the inductance, L, is 5.76 H.

The limits set on the SMES unit effect the energy storage device operation. When the frequency is within the $\pm$0.005 Hz deadband, the voltage across the inductor is set to zero and the device is neither charging nor discharging. In this mode, the energy stored in the magnetic field remains constant because the superconducting coil has zero resistance. If the current, I_d, reaches the maximum value, the voltage across the inductor, V_d, is set to zero until the frequency deviation is negative once again. Thereupon, the deviation of the voltage, ΔV_d, is once again dependent on the frequency deviation. If the current, Id, reaches the minimum allowable current, the voltage across the inductor, V_d, is set to zero until the frequency deviation is positive again. At this point, the device resumes normal operation. If the voltage, V_d, reaches its maximum positive (or negative) value, it is not allowed to increase (or decrease) beyond that value.

The "round-trip" efficiency of the device is 95%. The losses, which occur in the converter, are modelled by setting the discharge power to

$$P_d = 0.95(V_d I_d) \tag{2.27}$$

2.2.2 Battery Energy Storage Model

A diagram of a battery energy storage unit is shown in Figure 1.5. The battery energy storage unit is somewhat different in its operation than the SMES unit. In the SMES unit, the current is unidirectional and varies between some minimum and maximum positive values. The voltage across the converter is also the voltage across the superconducting coil and this voltage is positive or negative depending on whether the device is charging or discharging. In contrast, the voltage across the batteries is always

positive and is not equal to the voltage across the converter. The current is bidirectional and its direction depends on whether the unit is charging or discharging. The battery system is actually a set of 25 series connected smngs of batteries connected in parallel to a common DC bus. The voltage of the battery units is a function of their state of charge. At full charge, the batteries are at their maximum voltage level, which decrease as the state of charge of the batteries decreases.

As given in Equation (2.19), the voltage of the converter is a function of the frequency (if it lies outside the $\pm$0.005 Hz deadband). A drop in area frequency caused by a rapid increase in load causes the voltage across the converter to drop. As this voltage, V_d, drops below the voltage of the batteries, V_b, current flowsout of the battery system and the unit discharges. The equation determining the current flowing in each of the strings of batteries is given by

$$I_d = \frac{V_d - V_b}{R} \tag{2.26}$$

where R is the internal resistance of the battery system, V_d is the average voltage across the converter, and V_b is the voltage across the battery system. As current flows into or out of the battery system, its state of charge changes. The equation determining change in the energy stored in the overall battery system is

$$\Delta W = 25\left[\int_{t_0}^{t} V_b(t)\, I_d(t)\, dt\right]. \tag{2.27}$$

The factor of 25 is present because the current I_d represents the current flowing in each of the 25 strings of batteries, while AW represents the change in the overall energy stored.

The parameters of the battery energy storage unit are based on the systems described in references [22, 23, 25]. As in the SMES system, the maximum

charge/discharge power and the energy storage capabilities are tailored to fit the load. In this case, the maximum charge/discharge power is 30 MW and the maximum energy storage capability is 7200 MWs (2 MWh).

The voltage level of the common DC bus is determined by the sum of the voltages of the batteries in the parallel strings. These are typically low voltage devices with very low internal resistances (on the order of a fraction of an ohm) [22, 35]. Each string of batteries on the common bus in the battery system is modelled with an internal resistance of 1.48 ohms (total) and a voltage which varies between 1020 volts and 1200 volts. As mentioned before, the voltage across the batteries is a function of the state of charge. In actual batteries, the voltage characteristic resembles a function that is the square root of the energy stored [35]. In this thesis, the voltage characteristic is approximated as a linear function of the energy stored, W. The minimum voltage across the batteries occurs at the minimum energy storage limit of the system. This minimum voltage is set to 85% of the maximum battery voltage. Between the minimum allowable energy stored and 83% of the maximum allowable energy stored, the voltage is a linear function of the stored energy, W, and rises from 85% of maximum voltage to full maximum voltage. Above 83% of the maximum allowable energy stored, the voltage across the batteries, V_b, is set to its maximum value. The equation for V_b is given as

$$\begin{aligned} V_b &= 0.031414W + 1019.058 \qquad 30\ \text{MWs} \le W \le 6030\ \text{MWs} \\ V_b &= 1200\ \text{V} \qquad\qquad\qquad\qquad W \ge 6030\ \text{MWs} \end{aligned} \tag{2.28}$$

Note that in application, two converter bridges are used (one for charging and one for discharging) in order to accomodate the reversal of current. The voltage across the DC terminals of the converter in the simulation, V_d, is allowed to vary between 2500 volts

(charge) and -280 volts (discharge). This limits the maximum current per string of batteries to 1000 A. The equation for V_d is given by

$$V_d = V_d + \Delta V_d \tag{2.29}$$

where ΔV_d is given in Equation (2.19). The charge/discharge power of the battery system is given by

$$P_d = V_b I_d. \tag{2.30}$$

As in the SMES unit, the constraints effect the battery energy storage unit operation. When the frequency deviation is within the deadband, the voltage of the converter, V_d, is set equal to the voltage of the battery system, V_b. With the voltages equal, no current flows in the circuit and no power is transferred, If the energy stored roaches its maximum value, only energy discharge is allowed and if the energy stored reaches the minimum value, only charging is allowed. Finally, if the current flowing out of the batteries, I_d, reaches maximum value and the device continues to discharge, the voltage of the converter is set so that the current does not exceed this maximum value. Similarly, if the current flowing into the batteries reaches its maximum value and the device continues to charge, the voltage of the converter is set so that the current does not exceed this maximum value.

The "round trip" efficiency of the battery energy storage system is 81%. The losses are accounted for in the energy stored and the discharge power. The model is revised such that during charge the AW is only 90% of the lossless change in energy shown in Equation (2.27). Also, during discharge, the discharge power is only 90% of the discharge power given by Equation (2.30).

CHAPTER 3

SYSTEM RESPONSE TO RAPIDLY CHANGING LOADS

3.1 Simulation of the System Response

Consider again an interconnected power system containing two control areas. A block diagram of the two control areas and the tie-line connecting them is shown in Figure 2.8 and the derivation of the equations of the system is described in Chapter 2. An analysis of the system is accomplished using the forward Euler method to approximate the derivatives in the system equations. Thus, a set of linear difference equations describe the system. An example of this method is shown using Equation (2.7) which describes the relationship between frequency deviation and net power in the system. Equation (2.7) is repeated for convenience,

$$\Delta f(s) = \frac{K_p}{1 + sT_p}[\Delta P_g(s) - \Delta P_l(s) - \Delta P_{tie}(s)]. \tag{3.1}$$

Rearranging the terms,

$$\Delta f(s)(1 + sT_p) = K_p [\Delta P_g(s) - \Delta P_l(s) - \Delta P_{tie}(s)] \tag{3.2}$$

and

$$s\,\Delta f(s) = \frac{K_p[\Delta P_g(s) - \Delta P_l(s) - \Delta P_{tie}(s)] - \Delta f(s)}{T_p} \tag{3.3}$$

This equation can be transformed to the time domain where

$$s \leftrightarrow \frac{d}{dt}. \tag{3.4}$$

Equation **(3.3)** becomes

$$\frac{d}{dt}[\Delta f(t)] = \frac{K_p[\Delta P_g(t) - \Delta P_l(t) - \Delta P_{tie}(t)] - \Delta f(t)}{T_p} \tag{3.5}$$

The forward Euler approximation is

$$\frac{dx}{dt} \approx \frac{x(t + dt) - x(t)}{dt}. \tag{3.6}$$

Using the forward Euler **method, Equation** (3.5) is approximated as

$$\frac{f(t + dt) - f(t)}{dt} = \frac{K_p[\Delta P_g(t) - \Delta P_l(t) - \Delta P_{tie}(t)] - \Delta f(t)}{T_p} \tag{3.7}$$

Finally,

$$f(t + dt) = dt\left[\frac{K_p[\Delta P_g(t) - \Delta P_l(t) - \Delta P_{tie}(t)] - \Delta f(t)}{T_p}\right] + f(t). \tag{3.8}$$

Similar transformations were performed in order to **determine** the equations for the rest of the system parameters in the time domain. These linear difference equations were then used to perform the simulation. The time step, dt, is 0.001 seconds.

3.2 System Response to Changing Loads

In this thesis, the system response is analyzed for two different types of load inputs. These two load inputs are the step change in load, shown in Figure 2.6, and the S-stand rolling mill load, shown in Figure 2.7. For each of these types of loads, three separate simulations wen performed. The first simulation is the base case with no energy storage device present in the system. The second simulation is the cart where a superconducting magnetic energy storage device is present in area 1 of the system. The third simulation is one in which a battery energy storage system is present in area 1 of the system.

Chapter 4 contains the analysis of the system response for the step change in load input. The bast case is analyzed in section 4.2; the SMES case in section 4.3; and the battery energy storage case in section 4.4. Comparisons are also made between the different cases.

Chapter 5 contains the analysis of the system response to the 5-stand rolling mill load input. The base case is analyzed in section 5.2; the SMES case in section 5.3; the battery energy storage case in section 5.4. In this chapter, a comparison is made between the different cases also.

Due to the large number of plots that arise from the following simulations, a table has been included to simplify the search for specific plots. Table 3.1 is the main index and gives reference particular figures for each specific case.

Table 3.1 Summary of Cases Studied

Case	Load Type	Energy Storage	Figure Numbers
1	Step Load	None	4.1 - 4.7
2	Step Load	SMES	4.8 - 4.17
3	Step Load	Battery	4.18 - 4.29
4	Rolling Mill	None	5.1 - 5.7
5	Rolling Mill	SMES	5.8 - 5.17
6	Rolling Mill	Battery	5.18 - 5.29

CHAPTER 4

ANALYSIS OF THE SYSTEM RESPONSE TO A STEP CHANGE IN LOAD

4.1 Introduction

In order to provide a basic comparison between the different cases studied in this thesis, the first analysis involved a simple step change in load, shown in Figure 2.6, in area 1 and no change in load in area 2 of the system. The three cases studied for this load are: the base case with no energy storage device present, the case with an SMES device present in area 1, and the case with a battery energy storage device present in area 1. The parameters of these energy storage devices are outlined in Chapter 2.

For each of the three cases, the following plots were made:

- frequency in area 1
- frequency in area 2
- tie-line power flow
- ACE in area 1
- ACE in area 2
- change in generated power in area 1
- change in generated power in area 2.

Measurements were also taken to help determine system performance. For each case, the following measurements were taken:

- minimum and maximum frequency in area 1
- minimum and maximum frequency in area 2
- minimum and maximum ACE in area 1

- minimum and maximum ACE in area **2**
- maximum tie-line flow into area **1**
- maximum tie-line flow out of area **1**
- total energy imported to area **1** across the tie-line
- total energy exported from area **1** across the tie-line
- net energy across the tie-line.

These measurements were used to compare system performance with and without an energy storage device. These measurements are important as far as determining the robustness of the system and the effect of one area's operation on a neighboring area.

4.2 Case 1: Step Change in Load with No Energy Storage Device

Case **1** is the system response to a step change in load in area **1** with no energy storage device present in the system. The step load is applied at t = **5** seconds and the simulation is run for **89.5** seconds. The plots mentioned above (frequency, tie-line power, ACE, change in generated power) are shown in Figures **4.1 - 4.7.** The system measurements mentioned above (i.e. maximum frequencies, minimum frequencies, maximum ACE, etc.) are shown in Table **4.1.**

The following observations can be made about the system response:

- The frequency in area **1** begins its descent simultaneous with the load being applied. It reaches a minimum of **59.9414** Hertz and begins to rise again as the demand is met by increased generation and power flowing in across the tie-line (the negative tie-line power flow shown in Figure **4.3** indicates power flowing from area 2 to area **1).** The frequency overshoots the desired value of **60** Hertz due to the fact that the tie-line power and the rapid rise in generated power due to the large frequency error have exceeded the power demand. The area **1** frequency arrives at a maximum value of **60.0131** Hertz and

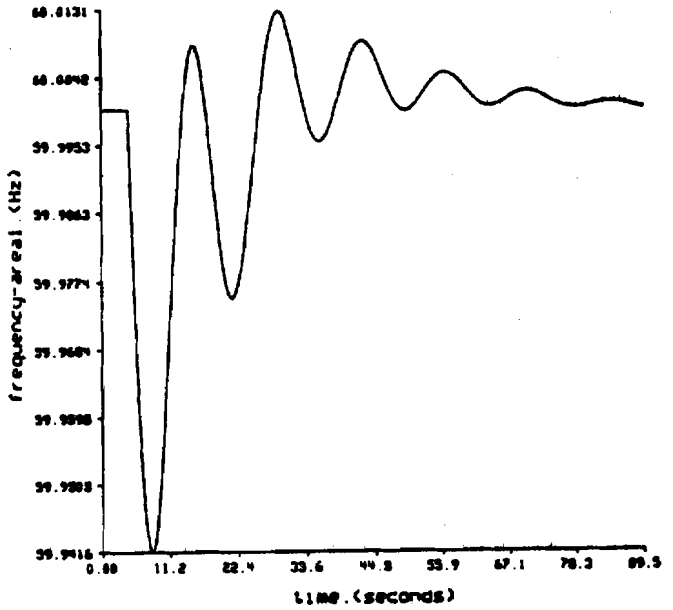

Figure 4.1 Frequency in Area 1 (Step Load - No Energy Storage)

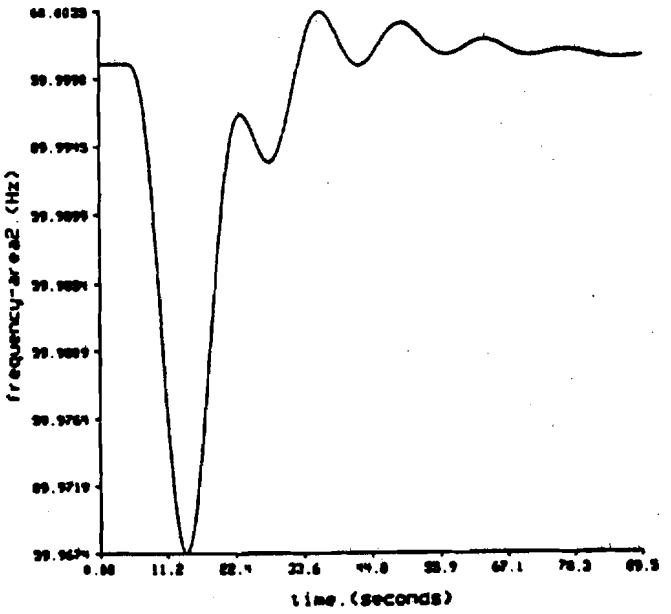

Figure 4.2 Frequency in Area 2 (Step Load - No Energy Storage)

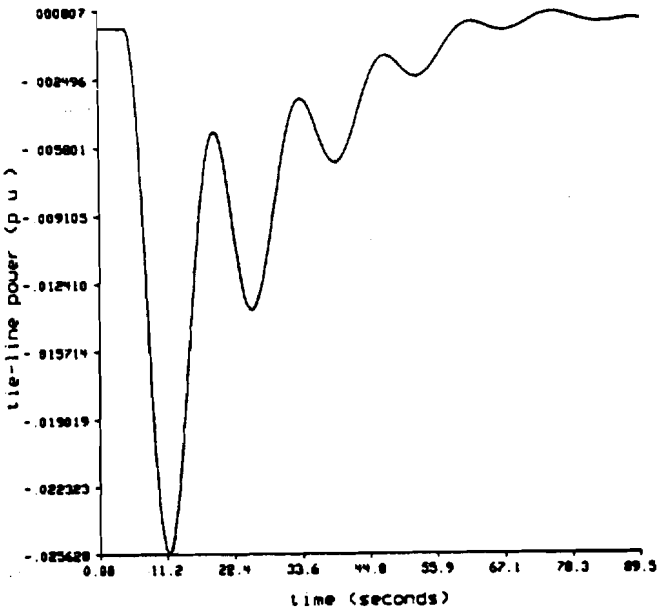

Figure 4.3 Tie-Line Power Flow (Step Load - No Energy Storage)

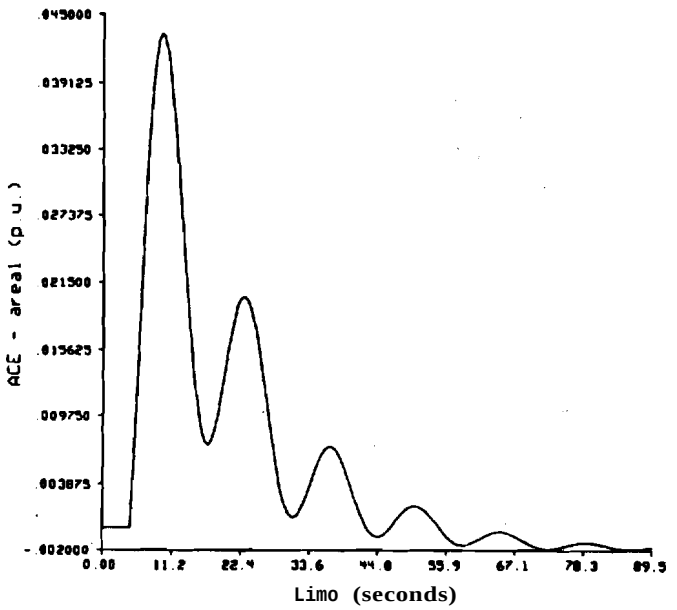

Figure 4.4 ACE in Area 1 (Step Load - No Energy Storage)

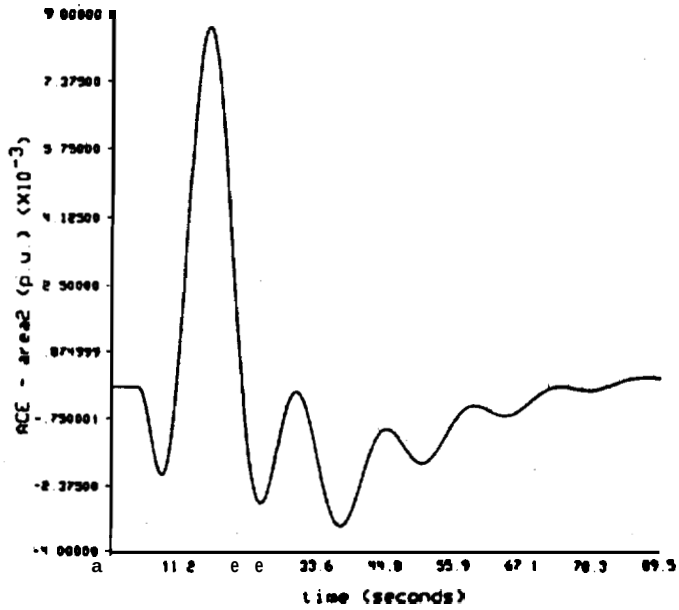

Figure 4.5 ACE in Area 2 (Step Load - No Energy Storage)

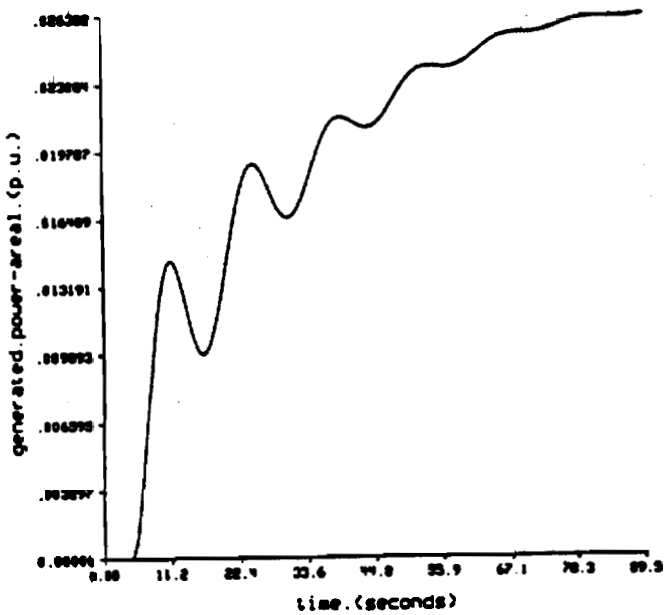

Figure 4.6 Change in Generated Power in Area 1 (Step Load - No Energy Storage)

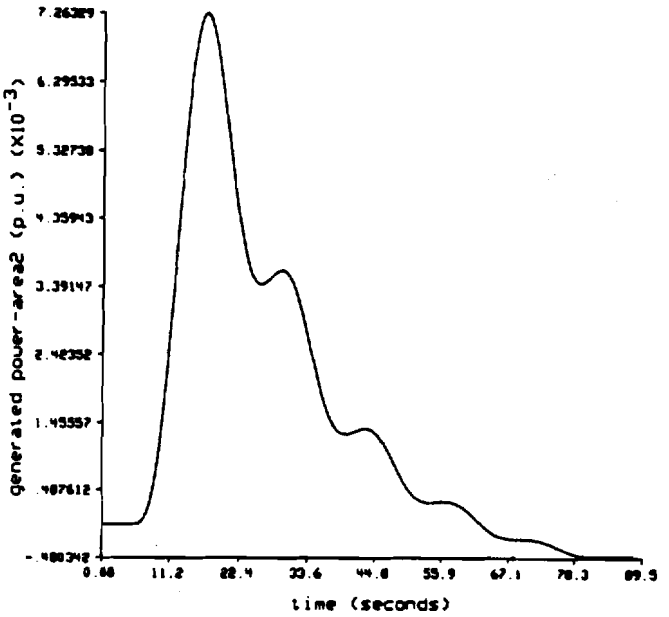

Figure 4.7 Change in Generated Power in Area 2 (Step Load - No Energy Storage)

Table 4.1 System Performance Measurements - (Step Load - No Energy Storage)

Base Case	
Parameter	Value
max f1	60.01309 Hz
min f1	59.9414 Hz
max f2	60.0035 Hz
min f2	59.9673 Hz
max ACE1	0.043378 p.u.
min ACE1	-0.001904 p.u.
max ACE2	0.008694 p.u.
min ACE2	-0.003370 p.u.
max Ptie in	-0.02563 p.u.
max Ptie out	0.001529 p.u.
Wtie import	-409.51 MWs
Wtie export	98.1249 MWs
Wtie net	-311.40 MWs

slowly oscillates back to 60 Hertz as the power generated in area 1 increases to meet the load and the tie-line flow decrease to zero.

• The large and rapid increase in tie-line flow from area 2 to area 1 is essentially the same as a large increase in load being applied to area 2. Therefore, area 2 also experiences a drop in frequency to 59.9673 Hertz, although somewhat delayed with respect to the application of the load in area 1. The change in generated power in area 2 increases as the frequency drops due to the tie-line power flow. As the demand is met in area 1 by area 1 generation, the tie-line flow decreases and the generated power in area 2 goes back to its original value.

• The shape of the ACE in area 2, shown in Figure 4.5, is interesting. As the tie-line flow out of area 2 increases with the application of the load in area 1, the ACE in area 2 decreases slightly. As mentioned above, the change in frequency in area 2 lags the tie-line power flow slightly so when the frequency in area 2 drops rapidly due to the tie-line flow, the ACE in area 2 rises to its positive maximum rapidly. As the tie-line flow decreases and the frequency in area 2 increases, the ACE increases to a positive value once again.

4.3 Case 2: Step Change in Load with an SMES Device in Area 1

Case 2 is the system response to a step change in load in area 1 with an SMES device present in area 1. The important parameters in the operation of the SMES device are plotted. These are: the voltage of the converter, which is also the voltage across the superconducting coil (V_d); the current in the superconducting coil (I_d); and the power output of the device (P_d). These plots are shown in Figures 4.8 - 4.10. The plots mentioned above (frequency, tie-line power, ACE, change in generated power) are shown in Figures 4.11 -4.17. In these figures, the base case data are superimposed on the SMES case data. This allows for a visual comparison of the different system outputs and

simplifies analysis. In each plot, the solid line represents the system output for the case with the **SMES** present and the dashed line represents the same system output for the base case. The system measurements mentioned above (i.e maximum/minimum frequencies, etc.) are shown in Table **4.2** along with the system measurements for the base case.

The following observations can be made about the response of the **SMES** device to the step change in load:

• The voltage, Vd, drops to its negative maximum value almost instantaneously in response to the rapid drop in frequency in area 1 with the application of the step load. As the frequency increases back to its steady state value of 60 Hertz, the voltage and the power output of the **SMES** device decreases. The spikes in the converter voltage and the power output are evident in Figures 4.8 and **4.10.** This occurs as a result of the **SMES** device having a **deadband** of ± 0.005 **Hertz**. As the area **1** frequency exceeds the value of ***59.995*** **Hertz,** the voltage and the power output of the **SMES** device go to zero as this frequency is within the deadband. As this power goes to zero, the power produced in area **1** no longer equals the power demand and the frequency drops again. This occurs because the time constants in the turbine-generator system are much slower than those in the **SMES** device, so the rapid initial increase in frequency back towards its steady state value is due largely in pan to the power produced by the **SMES** device and not because there is a more rapid increase in power generated. As stated above, the subsequent power mismatch occuring at the ***59.995*** Hertz limit of the **deadband** as the output power of the **SMES** device goes to zero results in a drop in frequency. This drop in frequency causes the convener to discharge again. These spikes in voltage and power output of the converter continue to occur until a point where the generated power in area **1** and the power flowing into area 1 across the tie-line is sufficient to keep the frequency in area 1 at ***59.995*** Hertz. Again, this time is limited by the slower time constants present in the turbine-generators.

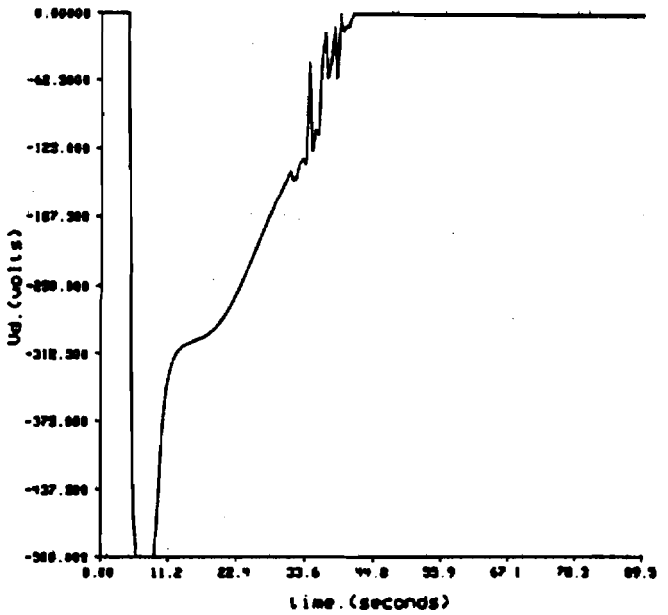

Figure 4.8 SMES Converter Voltage - V_d (Step Load)

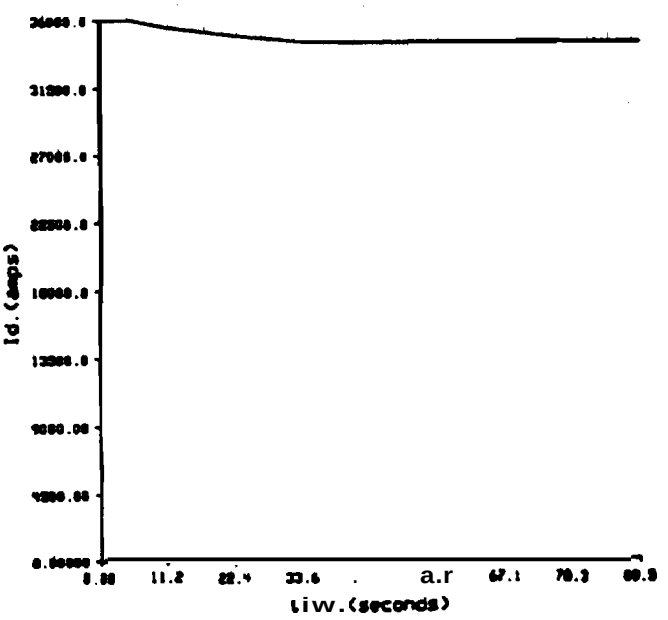

Figure 4.9 SMES Current - I_d (Step Load)

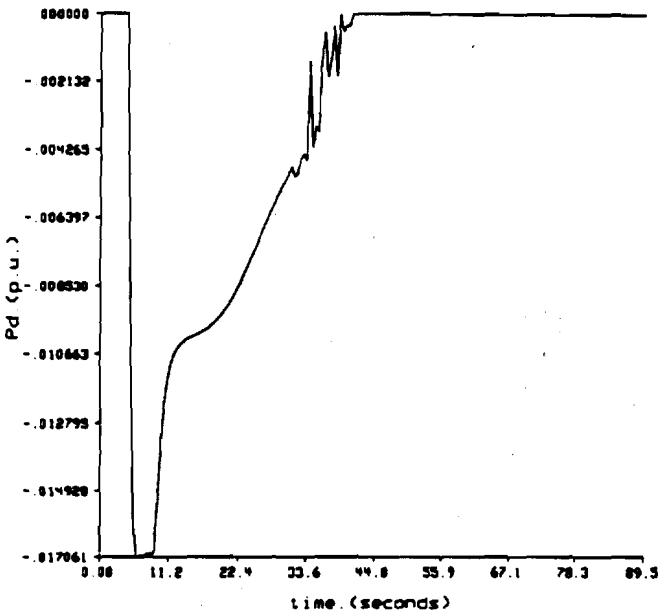

Figure 4.10 SMES Power Output - P_d (Step Load)

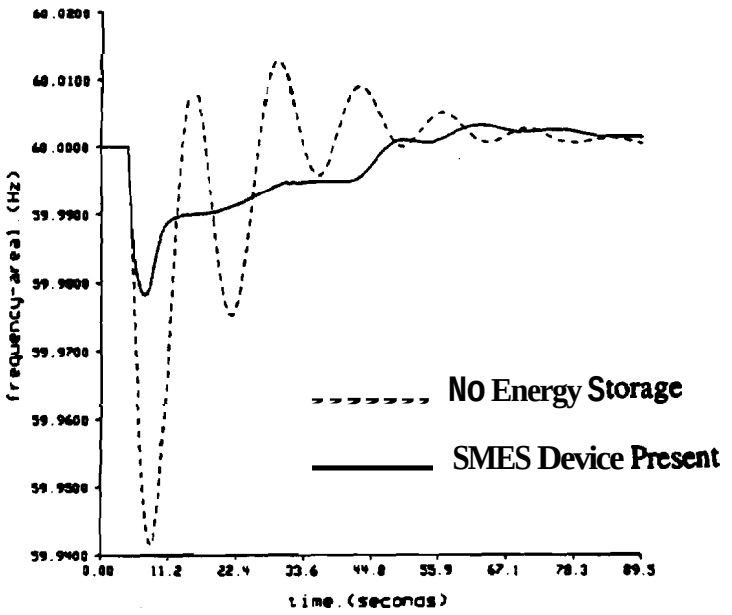

Figure 4.11 Frequency in Area 1 (Step Load - SMES Device Present)

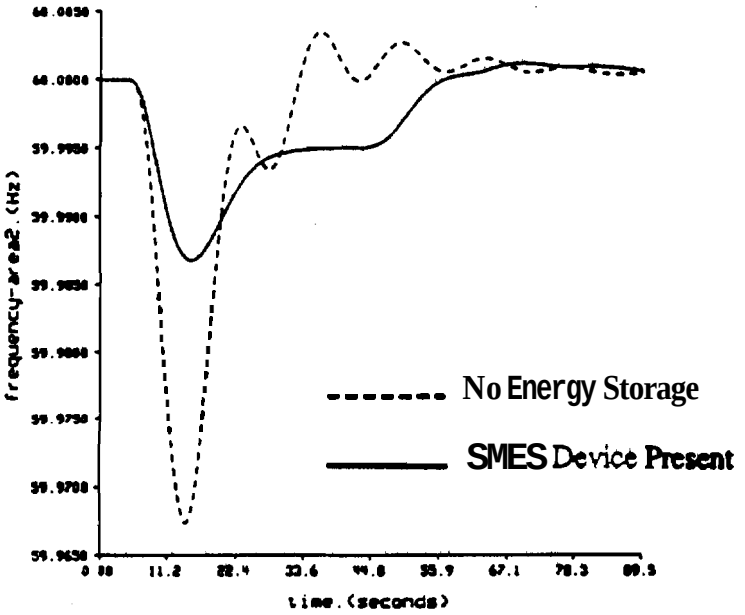

Figure 4.12 Frequency in Area 2 (Step Load - SMES Device Present)

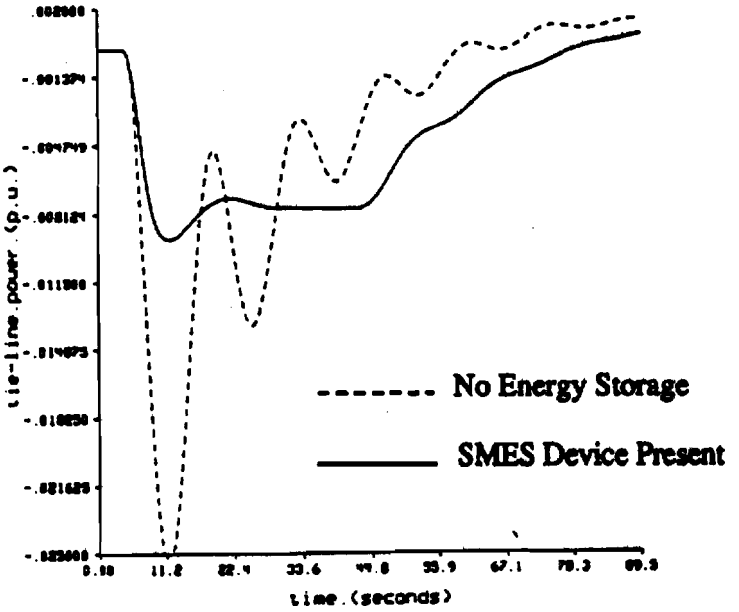

Figure 4.13 Tie-Line Power Flow (Step Load - SMES Device Present)

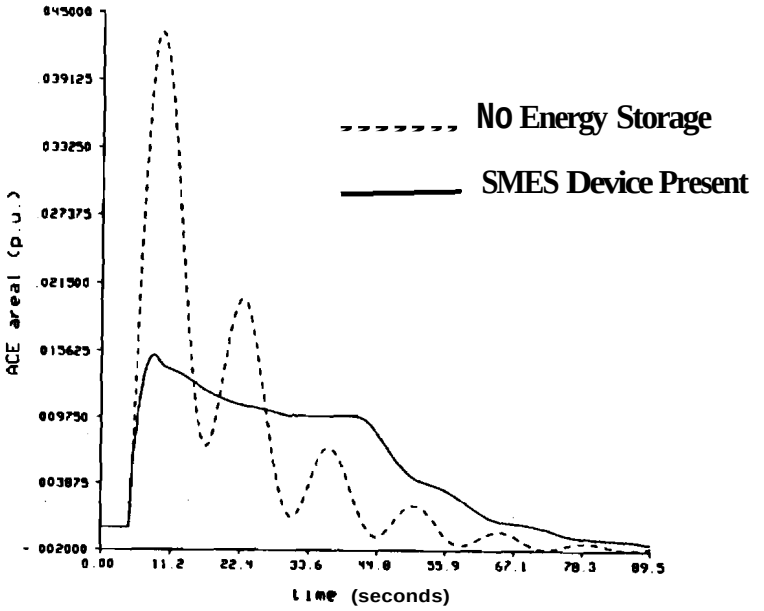

Figure 4.14 ACE in Area 1 (Step Load - SMES Device Present)

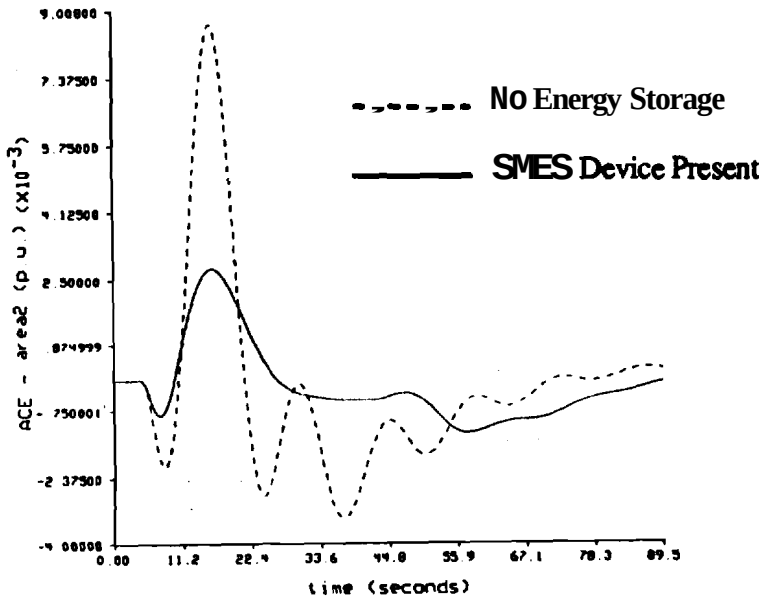

Figure 4.15 ACE in Area 2 (Step Load - SMES Device Present)

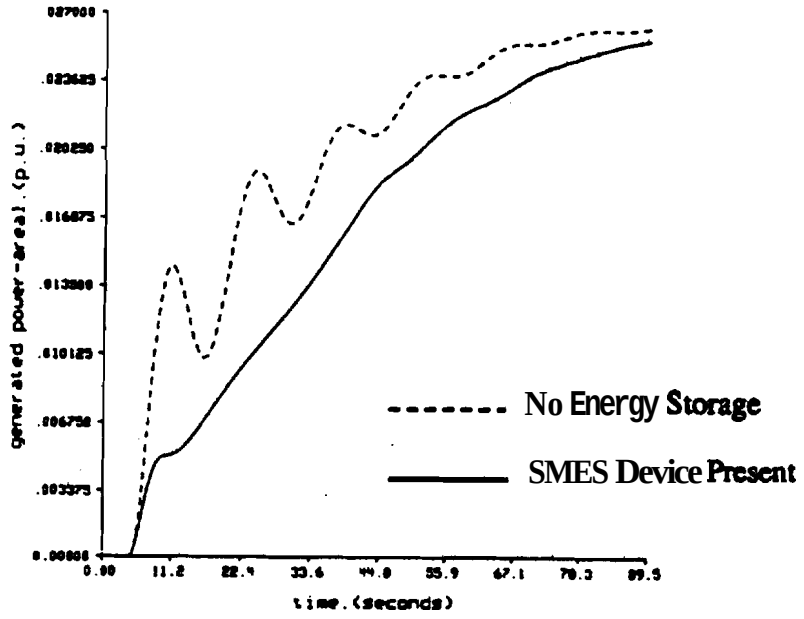

Figure 4.16 Change in Generated Power in Area 1 (Step Load - SMES Device Present)

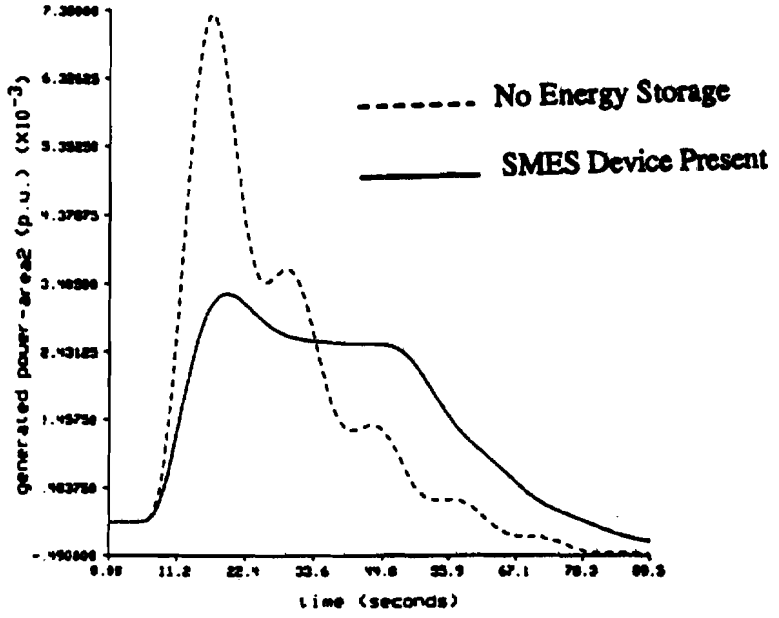

Figure 4.17 Change in Generated Power in Area 2 (Step Load - SMES Device Present)

Table 4.2 System Performance Measurements - (Step Load - SMES Device)

Parameter	Base Case	SMES Case
max f1	60.01309 Hz	60.0032 Hz
min f1	59.9414 Hz	59.9782 Hz
max f2	60.0035 Hz	60.0013 Hz
min f2	59.9673 Hz	59.9868 Hz
max ACE1	0.043378 p.u.	0.015349 p.u.
min ACE1	-0.001904 p.u.	-0.001578 p.u.
max ACE2	0.008694 p.u.	0.002774 p.u.
min ACE2	-0.003370 p.u.	-0.001297 p.u.
max Ptie in	-0.02563 p.u.	-0.00936 p.u.
max Ptie out	0.001529 p.u.	0.001337 p.u.
Wtie import	-409.51 MWs	-399.57 MWs
Wtie export	98.1249 MWs	88.814 MWs
Wtie net	-311.40 MWs	-310.769 MWs

• By observing Figure 4.9, it is evident that this step change in load reduces the current in the superconducting coil by only a small amount relative to its overall energy storage capabilities. This suggests that, for a load such as a rolling mill in which the SMES device will be continuously charging as well as discharging, the energy storage device can be smaller.

The following observations can be about the system responses when the SMES device is present in the system:

• As seen in Figure 4.11, the initial drop in frequency in area 1 is much less in this case than the case with no energy storage device in the system. The large initial frequency drop only goes to 59.9756 Hertz (as opposed to 59.9413 Hertz with no energy storage). It can also be seen that the frequency does not reach its steady state value of 60 Hertz significantly faster with the SMES device in the system than without the SMES

device. It is also evident thar the system frequency lingers at a value of 59.995 Hertz for about 12 seconds. The 59.995 Hertz value marks the lower limit of the deadband of the SMES device. At 59.995 Hertz, the SMES device produces just enough power to keep the frequency in area 1 at this value until the power generated plus the tie-line power are sufficient to keep the frequency at 59.995 Hertz. At that point, the power produced by the SMES device goes to zero.

• As the frequency in area 1 is held at 59.995 Hertz, the SMES power output is slowly decreasing while the change in power generated in area 1 is slowly increasing. This keeps the tie-line power flow fairly constant for that period where the frequency is being held at 59.995 Hertz, as seen in Figure 4.13. At this level of tie-line power flow, the power being generated in area 2 is equal to that power being exported to area 1. Because there is no mismatch in power, the frequency in area 2 remains fairly constant at approximately 59.995 Hertz as seen in Figure 4.12. Also, the ACE in areas 1 and 2 remain fairly constant for that same period when the frequency in area 1 is being held at 59.995 Hertz (Figures 4.14 and 4.15).

• By observing Figure 4.16, it is seen that the increase in power generated in area 1 with the SMES device in place is not as rapid as in the case with no energy storage device. This is due to the fact that the governor sets the valve position to increase or decrease the power output of the generator. The input signal for the governor is proportional to the ACE of the specified area. In the case with an SMES device in the system, the ACE is not as large as in the case without an energy storage device, therefore the signal that dictates the power generated will not be as large and the power generated will increase at a slower rate.

• It is evident from the plots that the SMES device acts as a "buffer" between the load and the system responses. The system responds at a slightly slower rate to the

change in load, and the oscillations in all of the responses are much smaller if not totally gone.

• It is also evident from the plots that the SMES greatly effects the system operation in the short run by reducing the initial large and rapid changes in frequency, ACE tie-line flow, and power generated. In the long run though, the system operation is still constrained by the longer time constants present in the turbine-generator. In effect, the system response does not reach steady state values faster with an SMES device in the system (perhaps actually slower), but it greatly reduces the large initial deviations in the responses.

• By observing the amount of energy imported to and exported from area 1 (shown in Table 4.2), it is evident that there is some improvement in this area. There is a drop in the total energy imported of approximately 8 MWs and a drop in the total energy exported of about 8 MWs. The net tie-line energy exchange is nearly identical for the case with an SMES device and the case without an energy storage device.

4.4 Case 3: Step Change in Load With a Battery Energy Storage Device in Area 1

Case 3 is the system response to a step change in load in area 1 with a battery energy storage (BES) device in operation in area 1. The important parameters of the BES unit are plotted. These are: the voltage of the converter (V_d); the voltage of the common DC bus of the battery system (V_b); the current flowing into or out of the device (I_d); the power output of the device (P_d); and the total energy stored in the unit (W). These plots are shown in Figures 4.18 -4.22. The system response plots (frequency, ACE, tie-line power flow, change in generated power) are shown in Figures 4.23 - 4.29. In these plots, the base case data is super-imposed on the BES case data. This allows for a visual comparison of the different system parameters and simplifies analysis. In each plot, the solid line represents the system output for the case with the BES present and the dashed

line represents the same output for the base case. The system measurements (i.e. maximum/minimum frequencies, etc.) are shown in Table 4.3 along with the measurements from the base case.

The following observations can be made about the operation of the battery energy storage unity in response to the step change in load:

• The converter voltage, shown in Figure 4.18, behaves very similarly to the converter voltage in the SMES case. Initially, the voltage drops very rapidly as the step change in load causes the frequency to drop. The spikes present in the converter voltage and also the current, Figure 4.20, and the power output of the device, Figure 4.21, once again occur as the system frequency rises back to the lower end of the deadband of the device at 59.995 Hertz.

• It is evident that the step change in load produces on a small change in the energy stored in the BES device, as seen in Figure 4.22. This suggests that the device may be smaller for a similar application, such as a rolling mill load.

The system response (i.e. frequency in area 1, frequency in area 2, ACE, tie-line power flow) is nearly identical to the system response with an SMES device on line. F a this reason, an explanation of the system response with a battery energy storage device on line will not be repeated here. An explanation of the system response is given in section 4.2.

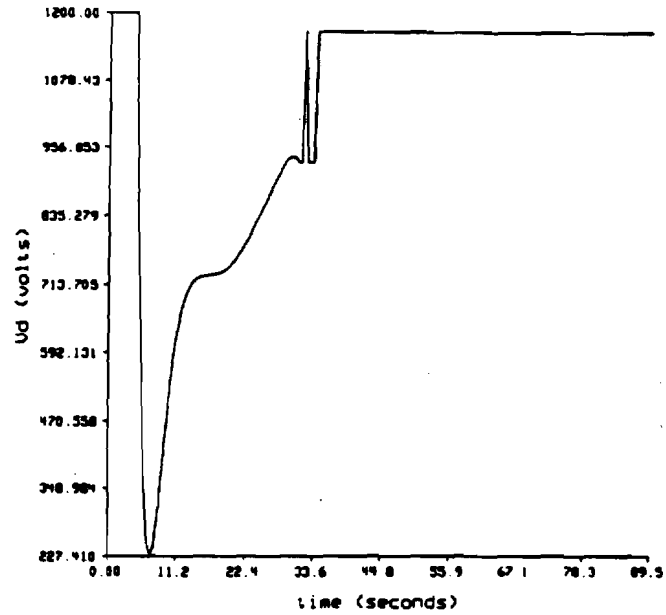

Figure 4.18 BES Converter Voltage - Vd (Step Load)

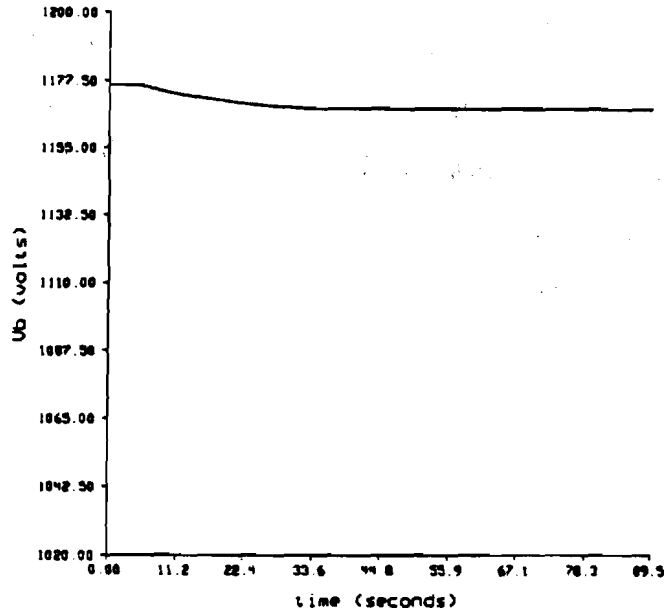

Figure 4.19 BES Common DC Bus Voltage - Vb (Step Load)

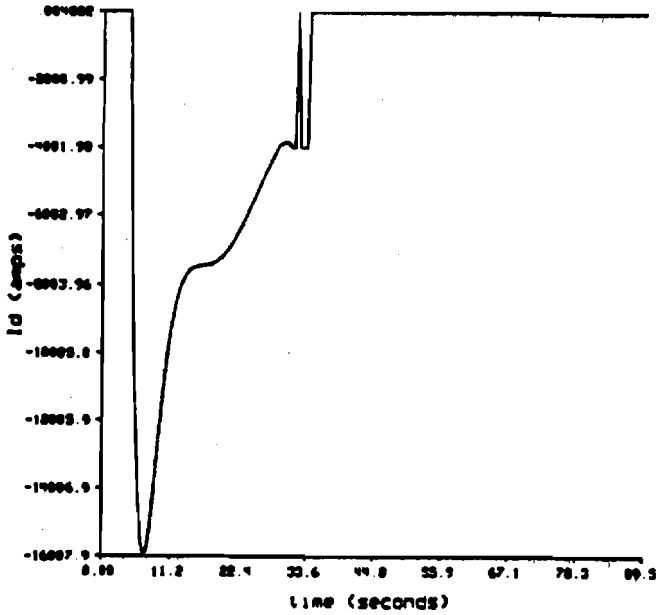

Figure 4.20 BES Current - Id (Step Load)

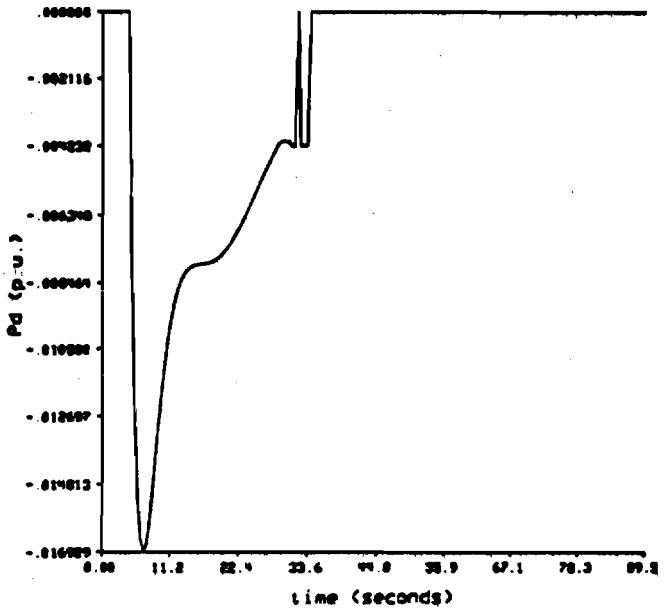

Figure 4.21 BES Power Output - Pd (Step Load)

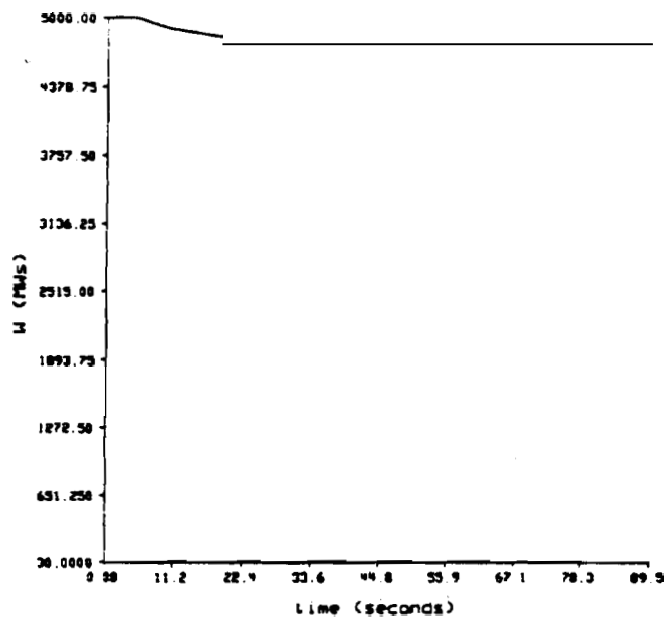

Figure **4.22** BES Energy Stored - W (Step Load)

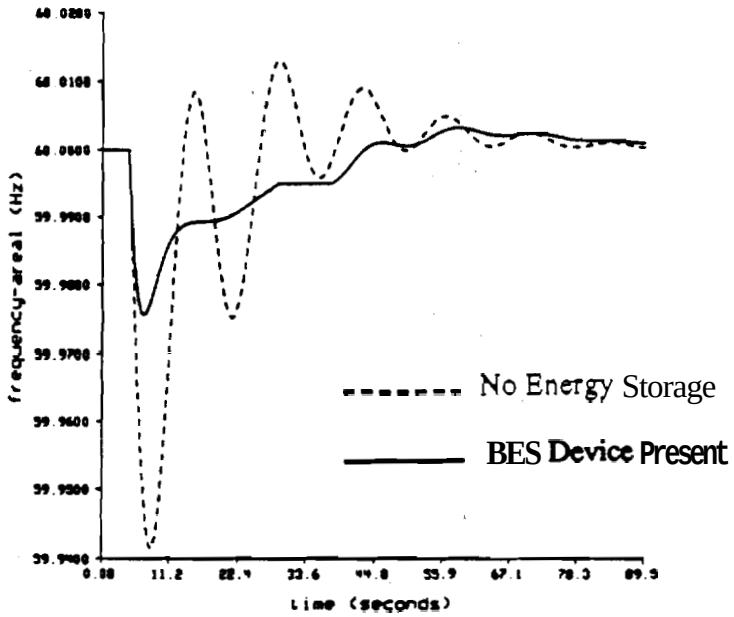

Figure **4.23** Frequency in Area 1 (Step Load - BES Device Present)

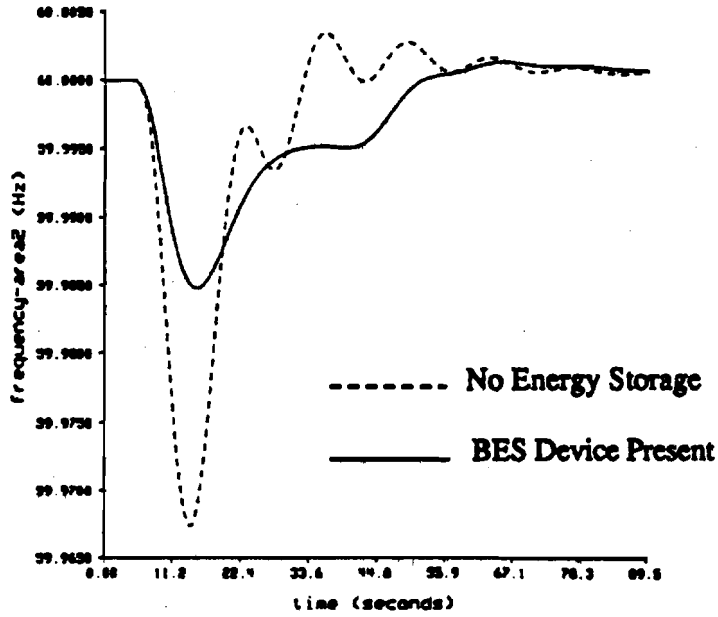

Figure 4.24 Frequency in Area 2 (Step Load - BES Device Present)

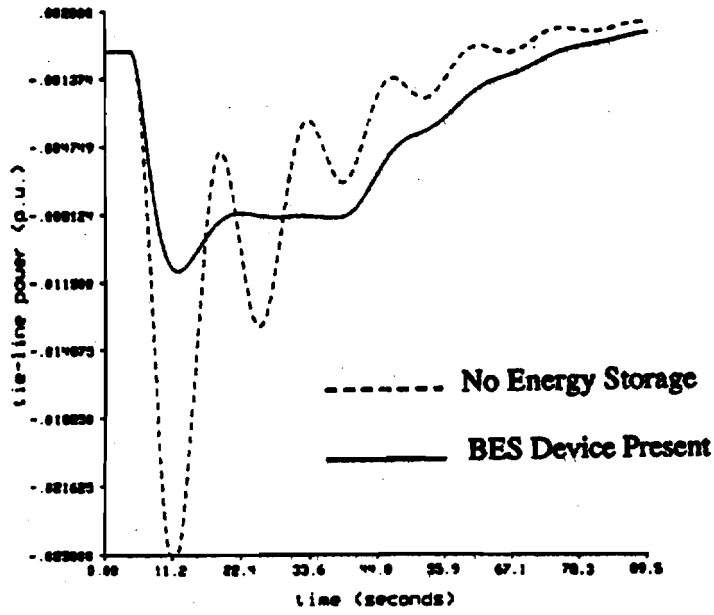

Figure 4.25 Tie-Line Power Flow (Step Load - BES Device Present)

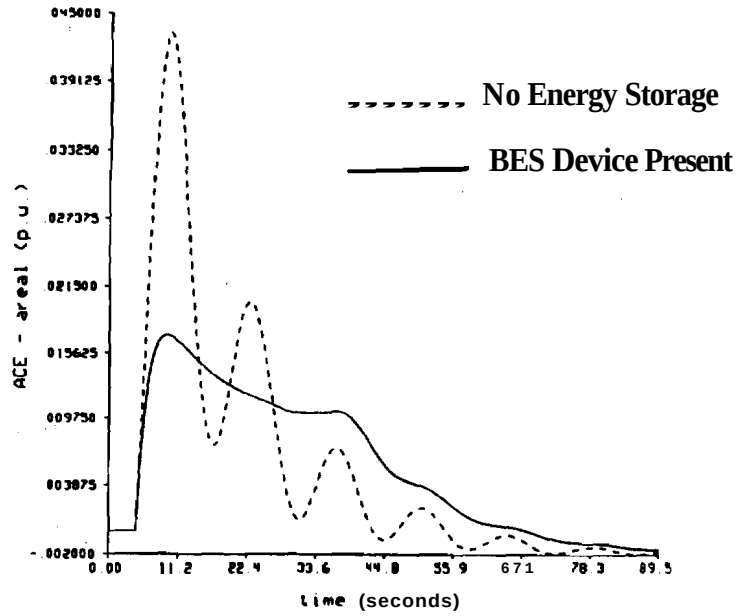

Figure 4.26 ACE in Area 1 (Step Load - BES Device Present)

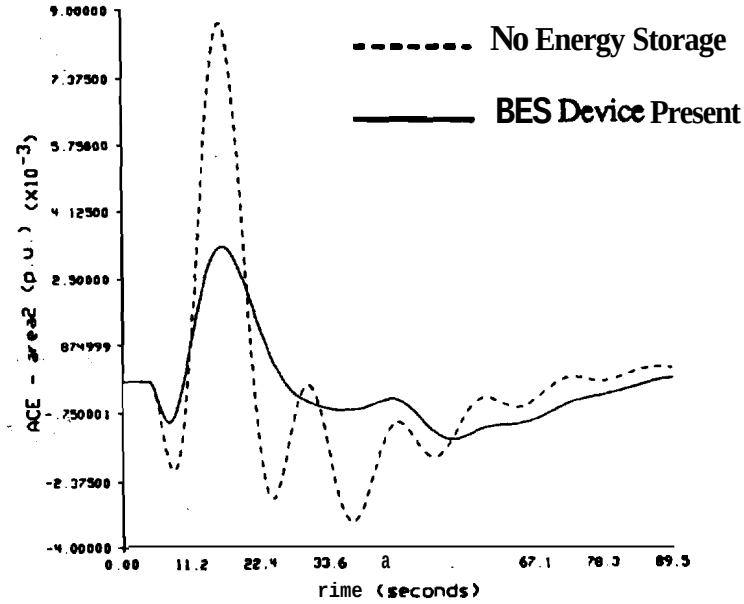

Figure 4.27 ACE in Area 2 (Step Load - BES Device Present)

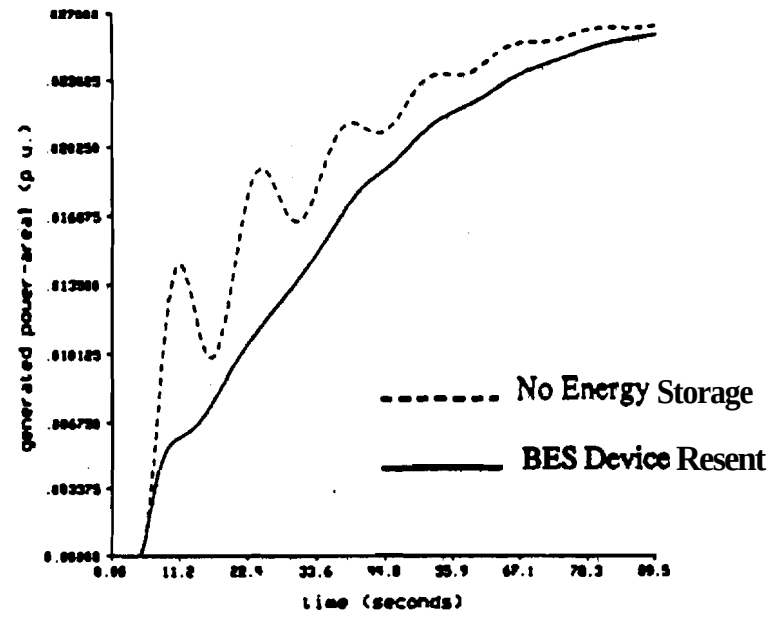

Figure 4.28 Change in Generated Power in Area 1 (Step h a d - BES Device Present)

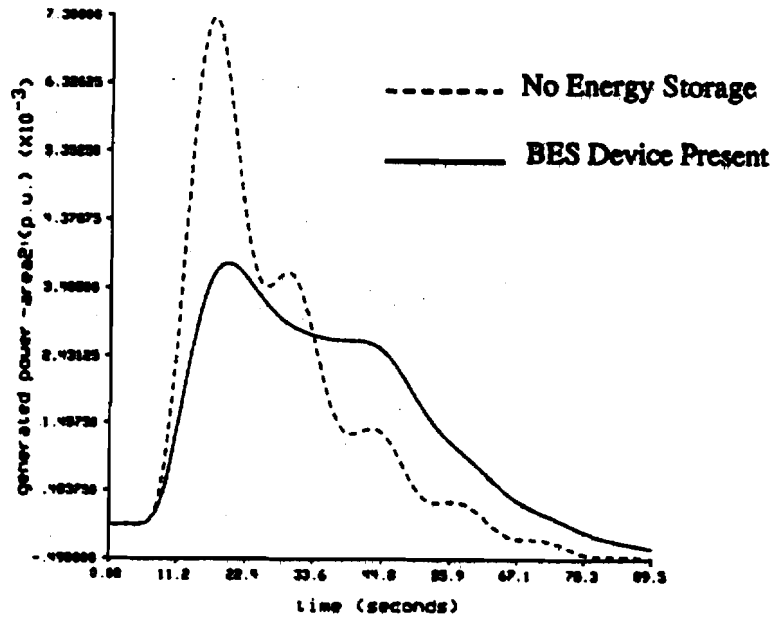

Figure 4.29 Change in Generated Power in Area 2 (Step Load - BES Device Present)

Table 4.3 System Performance Measurements - (Step Load - BES Device)

Parameter	Base Case	BES Case
max f1	60.01309 Hz	60.0034 Hz
min f1	59.9414 Hz	59.9756 Hz
max f2	60.0035 Hz	60.0013 Hz
min f2	59.9673 Hz	59.9847 Hz
max ACE1	0.043378 p.u.	0.017278 p.u.
min ACE1	-0.001904 p.u.	-0.001612 p.u.
max ACE2	0.008694 p.u.	0.003256 p.u.
min ACE2	-0.003370 p.u.	-0.001399 p.u.
max Ptie in	-0.02563 p.u.	-0.01095 p.u.
max Ptie out	0.001529 p.u.	0.001359 p.u.
Wtie import	-409.51 MWs	-401.382 MWs
Wtie export	98.1249 MWs	90.6369 MWs
Wtie net	-311.40 MWs	-310.769 MWs

CHAPTER 5

ANALYSIS OF THE SYSTEM RESPONSE TO A FIVE-STAND ROLLING MILL LOAD

5.1 Introduction

In order to provide a more realistic comparison of the different cases studied in this thesis, the second analysis involved a five-stand rolling mill load, shown in Figure 2.7, applied in area 1 and no change in load in area 2. The three cases studied for this load are: the base case with no energy storage device present in the system, the case with an SMES device present in area 1, and the case with a battery energy storage (BES) device present in area 1. The parameters of these energy storage devices are outlined in Chapter 2. As mentioned previously, the five-stand rolling mill load is based on a strip chart recording of an actual five-stand rolling mill.

For each of the three cases, the following plots were made:

- frequency in area 1
- frequency in area 2
- tie-line power flow
- ACE in area 1
- ACE in area 2
- change in generated power in area 1
- change in generated power in area 2.

Measurements were also taken to help determine system performance. For each case, the following measurements were taken:

- minimum and maximum frequency in area 1
- minimum and maximum frequency in area 2
- minimum and maximum ACE in area 1
- minimum and maximum ACE in area 2
- maximum tie-line power flow into area 1
- maximum tie-line power flow out of area 1
- total energy imported to area 1 across the tie-line
- total energy exported from area 1 across the tie-line
- net energy across the tie-line

These measurements were used to compare system performance with and without an energy storage device. These measurements are important are far as determining the robustness of the system and the effects that the energy storage device has on system operation.

5.2 Case 4: Rolling Mill Load with No Energy Storage Device

Case 4 is the system response to a rolling mill load in area 1 with no energy storage device present in the system. The rolling mill load is shown in Figure 2.7. The simulation is run for 3647.8 seconds (approximately 61 minutes). The plots mentioned above are shown in Figures 5.1 - 5.7. The system measurements mentioned above (i.e. minimum/maximum frequencies, minimum/maximum ACE, etc.) are shown in Table 5.1.

The following observations can be made about the system response:

- Since the five-stand rolling mill load resembles a series of "step up" and "step down" functions, the system behaves essentially the same as in case 1, discussed in section 4.2. With the "step up" in load, the demand in area 1 is now greater than the power produced and the frequency in area 1 decreases. This drop in frequency causes a difference in the phase angles between the two areas and causes power to flow across the

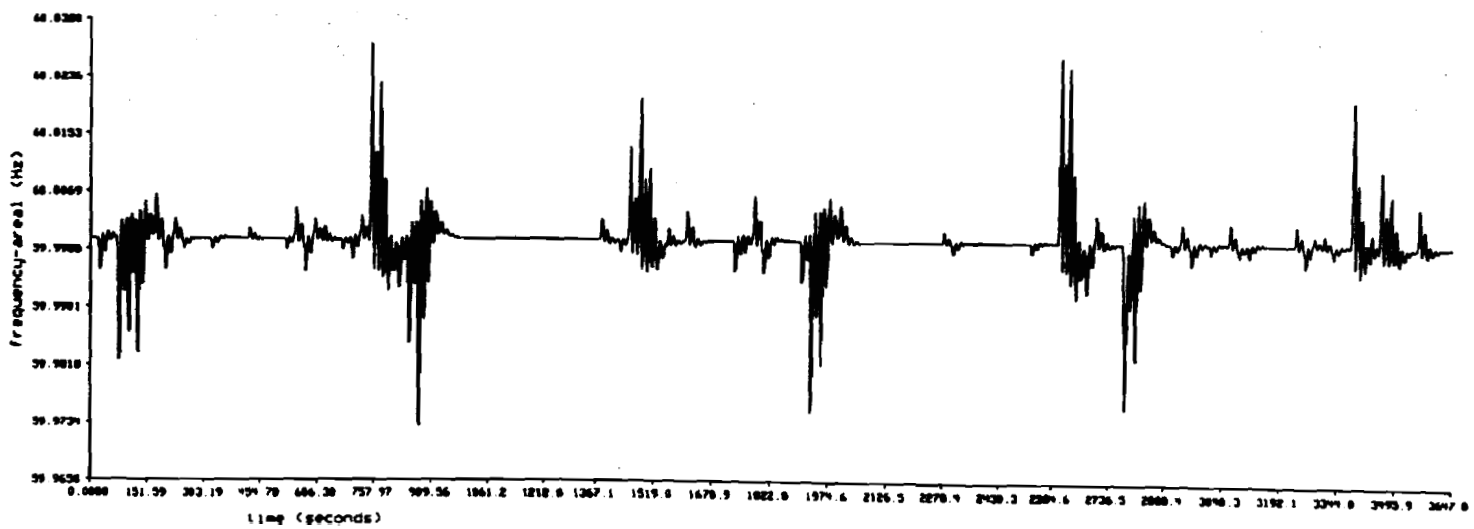

Figure 5.1 Frequency in Area 1 (Rolling Mill Load - No Energy Storage)

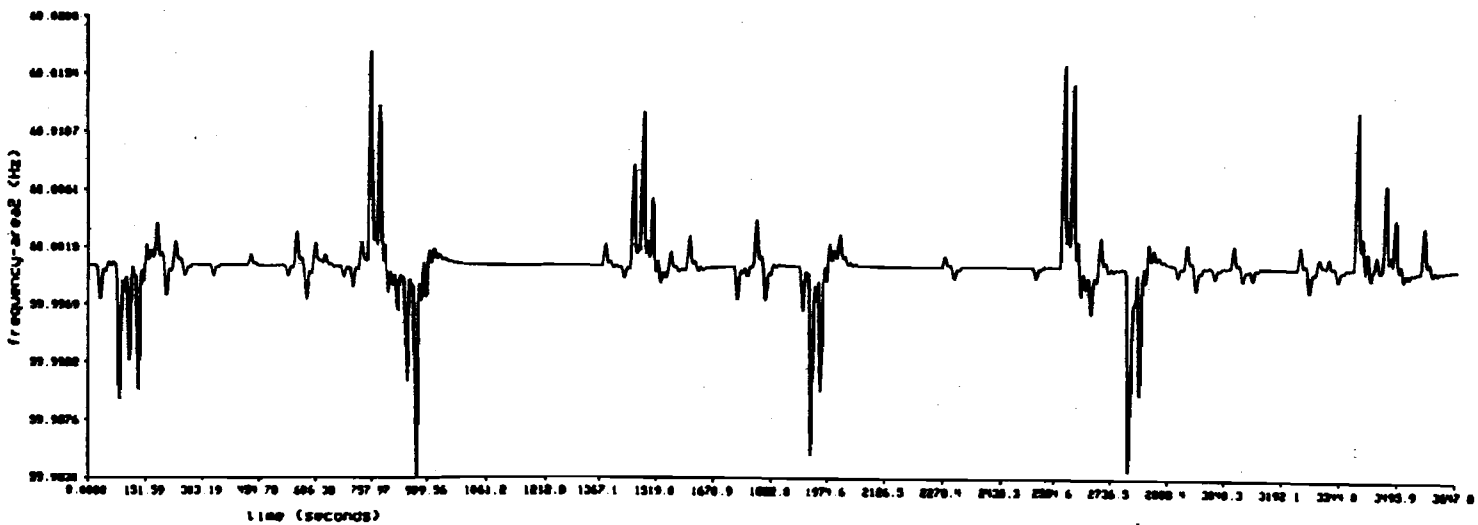

Figure 5.2 Frequency in Area 2 (Rolling Mill Load - No Energy Storage)

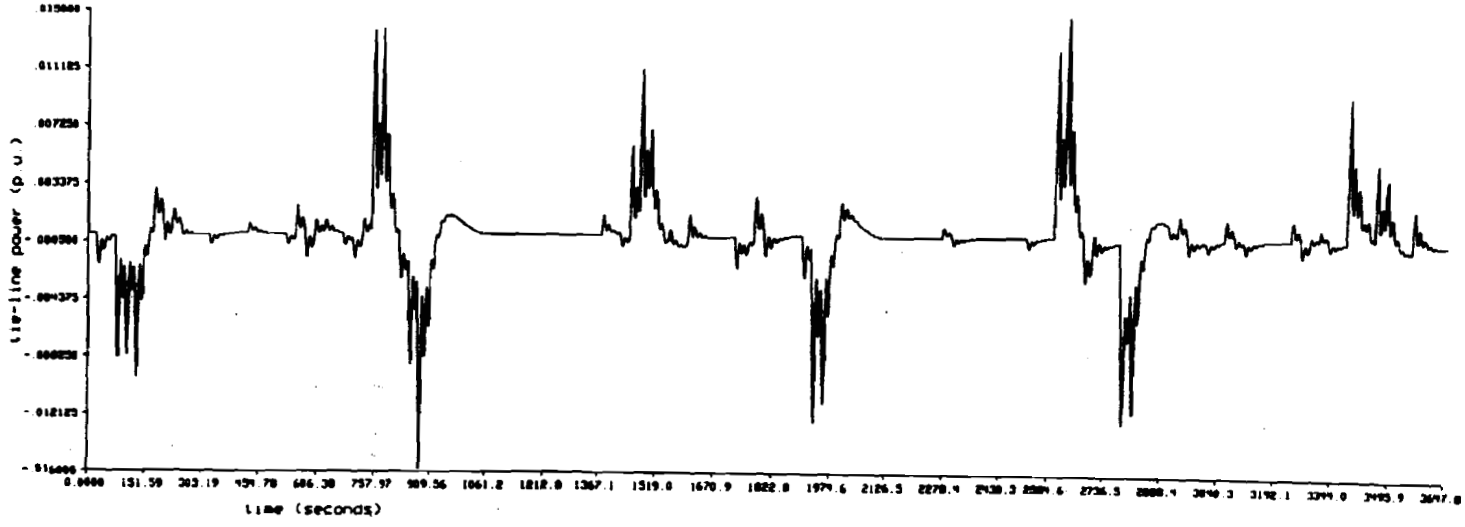

Figure 5.3 Tie-Line Power Flow (Rolling Mill Load - No Energy Storage)

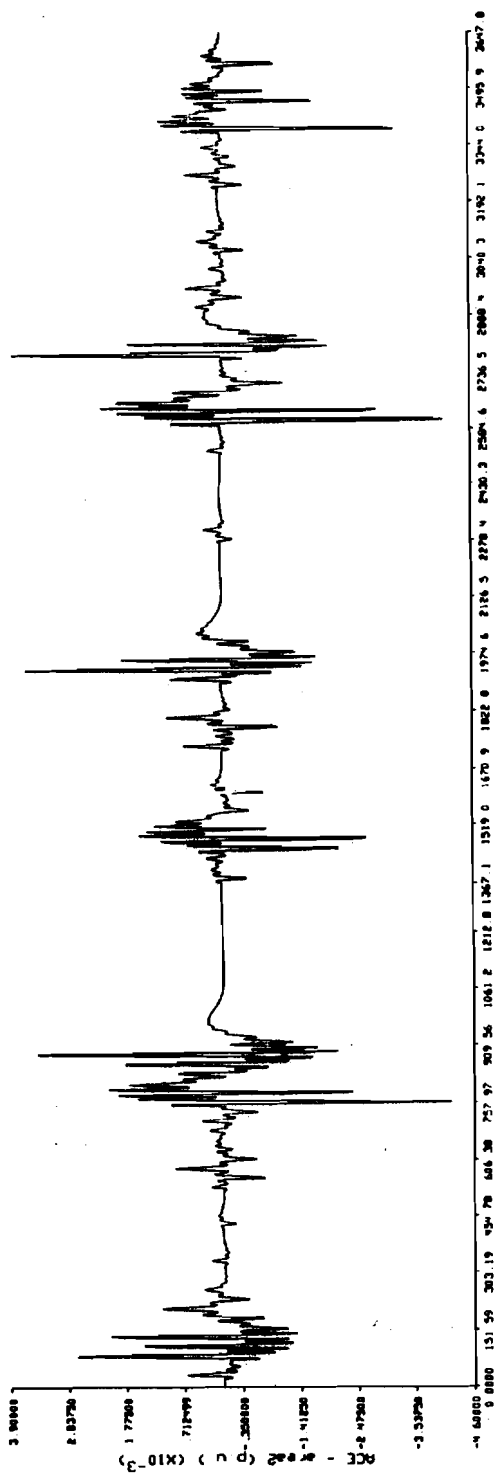

Figure 5.5 ACE in Area 2 (Rolling Mill Load - No Energy Storage)

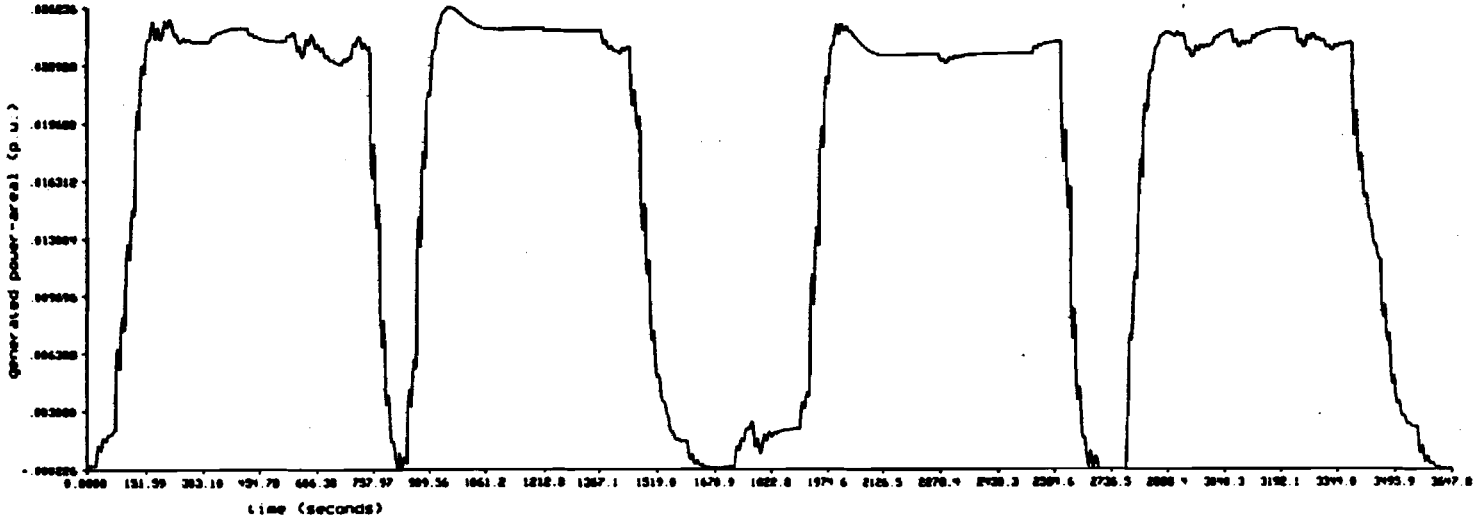

Figure 5.6 Change in Generated Power in Area 1
(Rolling Mill Load - No Energy Storage)

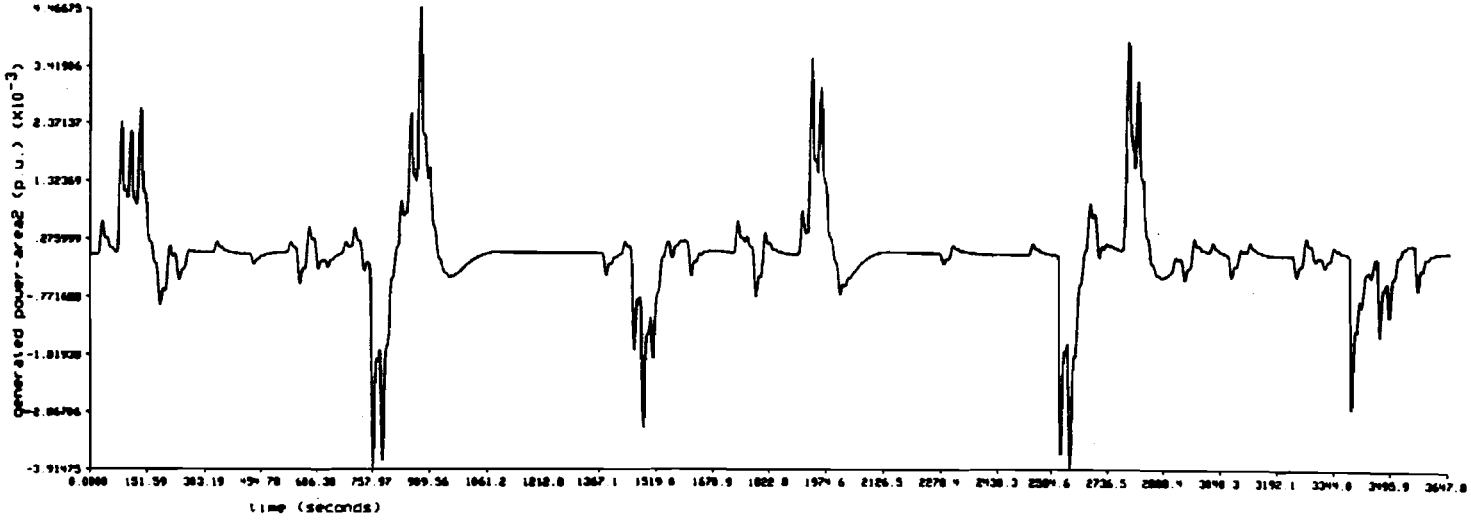

Figure 5.7 Change in Generated Power in Area 2
(Rolling Mill Load - No Energy Storage)

Table 5.1 System Performance Measurements (Rolling Mill Load - No Energy Storage)

Base	Case
Parameter	Value
max f1	60.03119 Hz
min f1	59.96936 Hz
max f2	60.01726 Hz
min f2	59.98314 Hz
max ACE1	0.025275 p.u.
min ACE1	-0.023288 p.u.
max ACE2	0.003873 p.u.
min ACE2	-0.0045009 p.u.
max Ptie in	-0.01599 p.u.
max Ptie out	0.014954 p.u.
Wtie import	-1989.879 MWs
Wtie export	1993.609 MWs
Wtie net	4.1427 MWs

tie-line from area 2 into area 1. The frequency drop also means that the input signal to the governor is no longer zero, as in steady state. The signal is now positive, producing an increase in generation. With the "step down" in load, the power generated in area 1 now exceeds the load and the power mismatch drives the frequency upward. This increased frequency and excess power force power to flow out of area 1 and into area 2 across the tie-line. The input signal to the governor is now negative and the power generated in area 1 decreases. The maximum frequency achieved in area 1 for the base case is 60.03119 Hertz and the minimum frequency is 59.96938 Hertz. The maximum tie-line power flow into area 1 is 0.01599 p.u. and the maximum tie-line flow out of area 1 is 0,01495 p.u..

•The power flowing into and out of area 2 along the tie-line produces a power mismatch in area 2 as well as area 1. Subsequently, the frequency in area 2 varies as load is applied in area 1. This is due to the fact that power flowing into or out of area 2 along

the tie-line is essentially the same as a load being applied or taken away in area 2. The maximum frequency achieved in area 2 is 60.01726 Hertz and the minimum frequency achieved in area 2 due to the changes in load in area 1 is 59.98314 Hertz.

• The sharp decrease in frequency in area 1 results in a signal to the governor to increase generation rapidly. As seen in Figure 5.6, the change in generated power in area 1 rises fairly rapidly and also oscillates as it rises. Although the generation in area 1 is rising rapidly, its increase is slow relative to the changing load and power is needed from area 2 across the tie-line in order to meet this demand. The change in generated power in area 2, shown in Figure 5.7, rises in response to the load change in area 1. As the power generated in area 1 rises (or falls) to meet the changing demand, the change in generated power in area 2 returns to zero.

5.3 Case 5: Rolling Mill Load with an SMES Device in Area 1

Case 5 is the system response to a rolling mill load in area 1 with an SMES device present in area 1. The important parameters of the SMES device are plotted. These are: the voltage of the converter, which is also the voltage across the superconducting coil (V_d); the current in the superconducting coil (Id); and the power output of the device (P_d). These plots are shown in Figures 5.8 - 5.10. The plots mentioned in 5.1 (frequency, ACE, tie-line power flow, change in generated power) are shown in Figures 5.11 - 5.17. For the sake of clarity, the base case data was not superimposed on these plots, as in Chapter 4. The figures for the SMES case have been plotted on the same scales as those in the base case. This allows for visual comparison of the two cases. The system measurements mentioned above (i.e. minimum/maximum frequencies, etc.) are shown in Table 5.2 along with the system measurements for the base case with the rolling mill load.

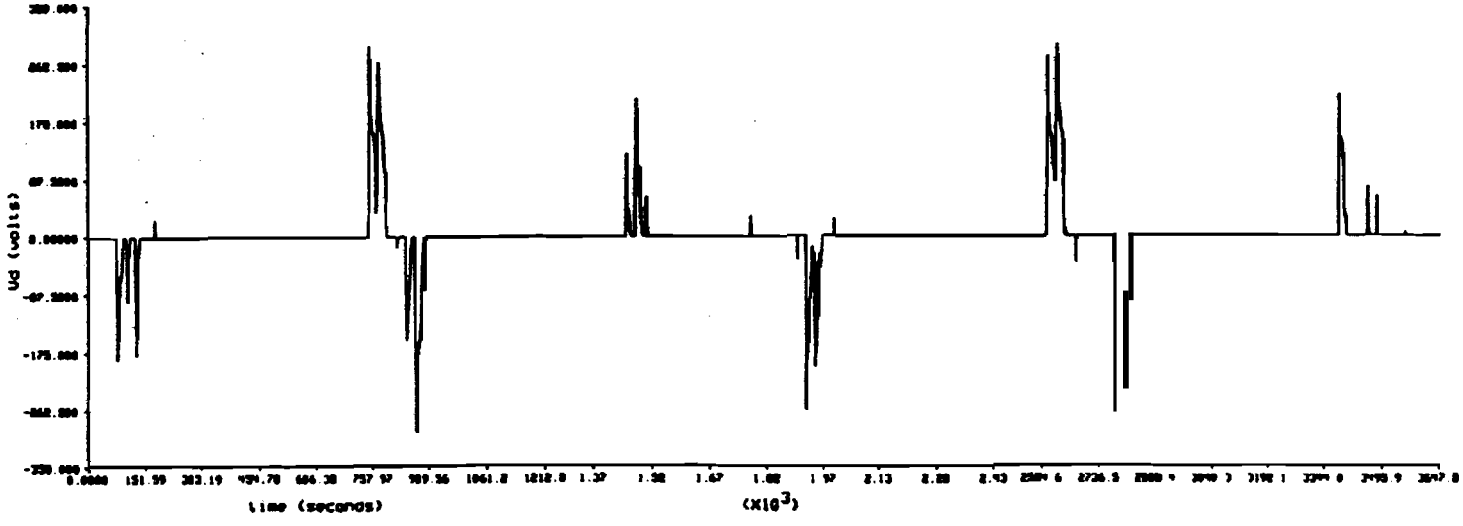

Figure 5.8 SMES Converter Voltage -V_d (Rolling Mill Load)

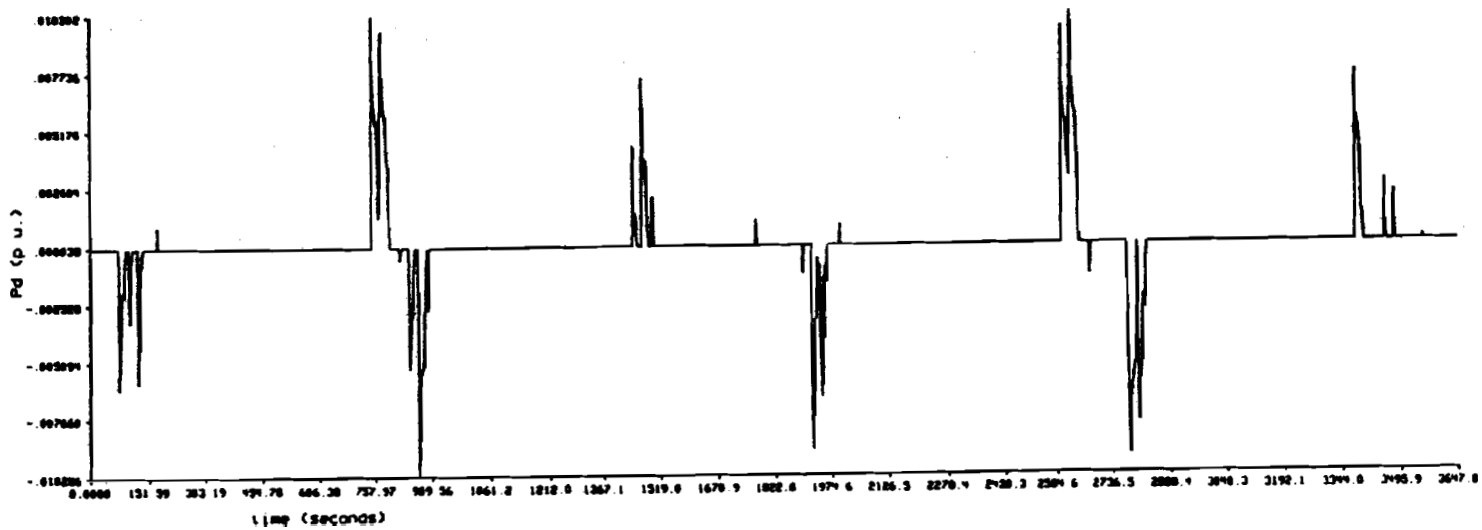

Figure 5.10 SMES Power Output - P_d (Rolling Mill Load)

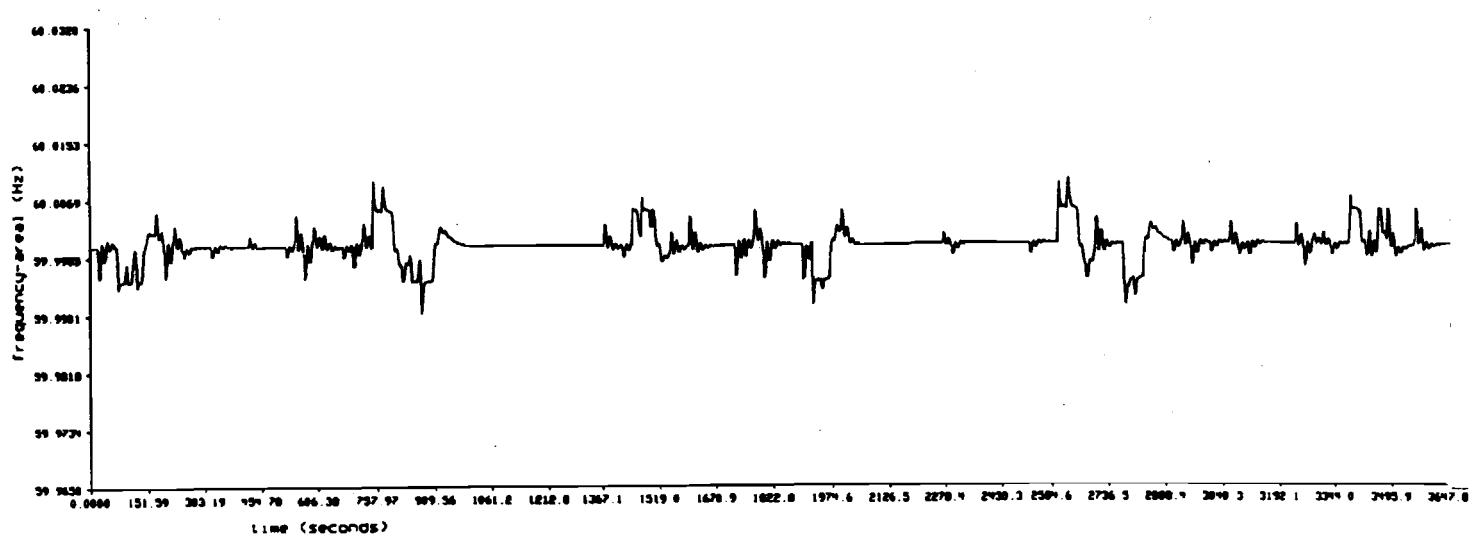

Figure 5.11 Frequency in Area 1 (Rolling Mill Load - SMES Device Present)

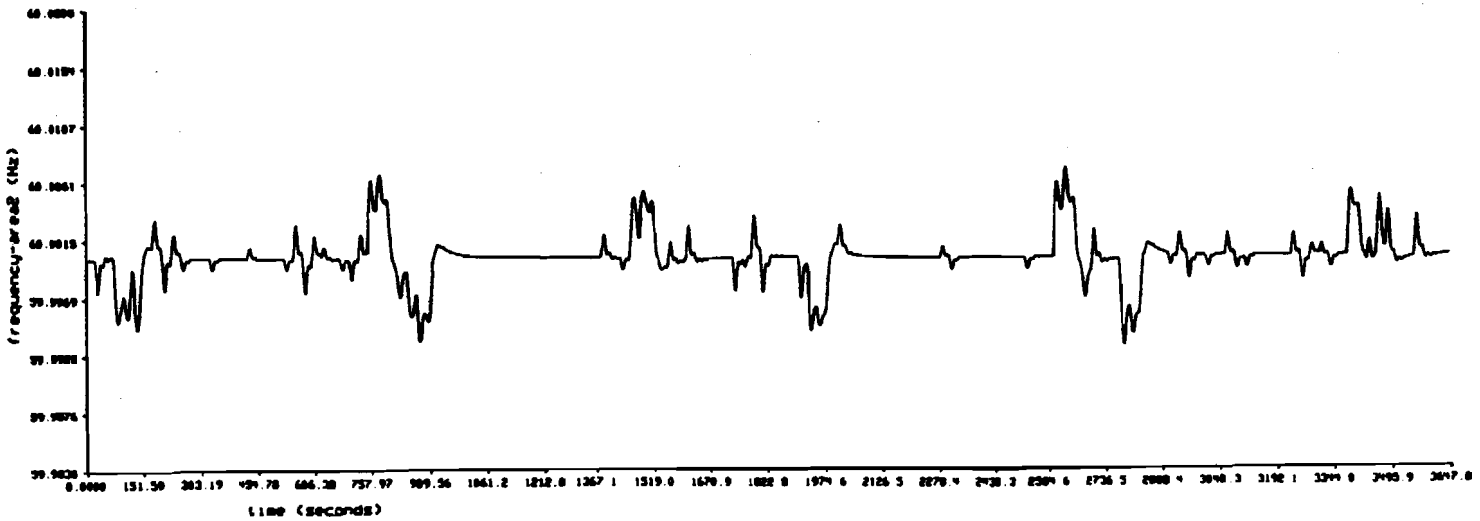

Figure 5.12 Frequency in Area 2 (Rolling Mill Load - SMES Device Present)

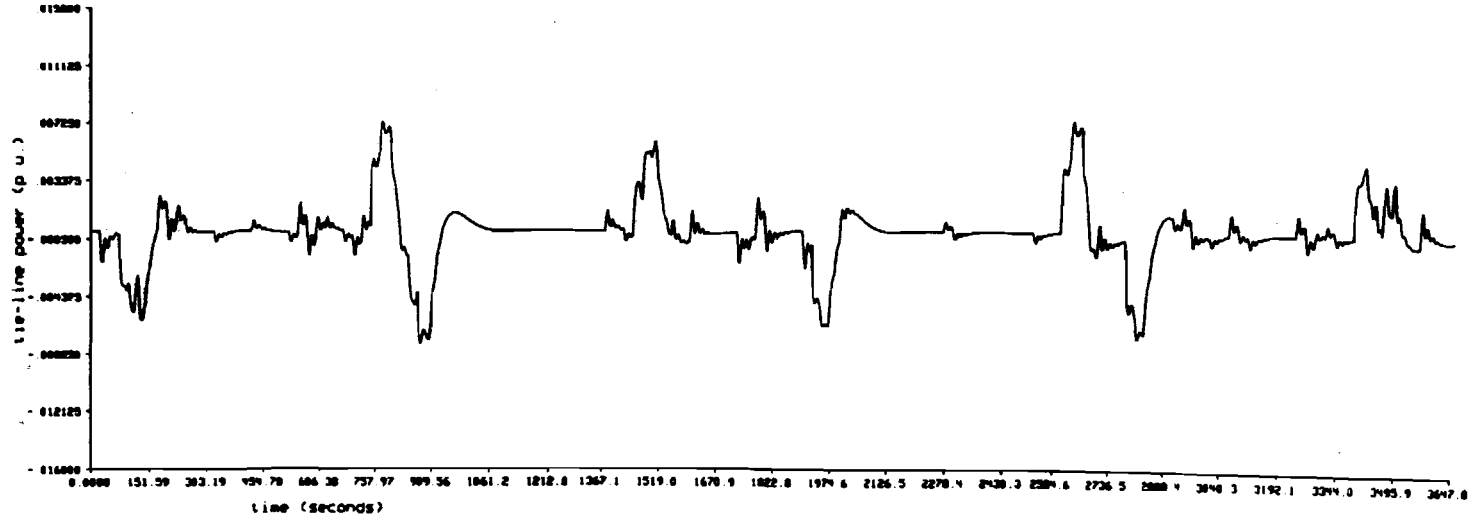

Figure 5.13 Tie-Line Power Flow (Rolling Mill Load - SMES Device Present)

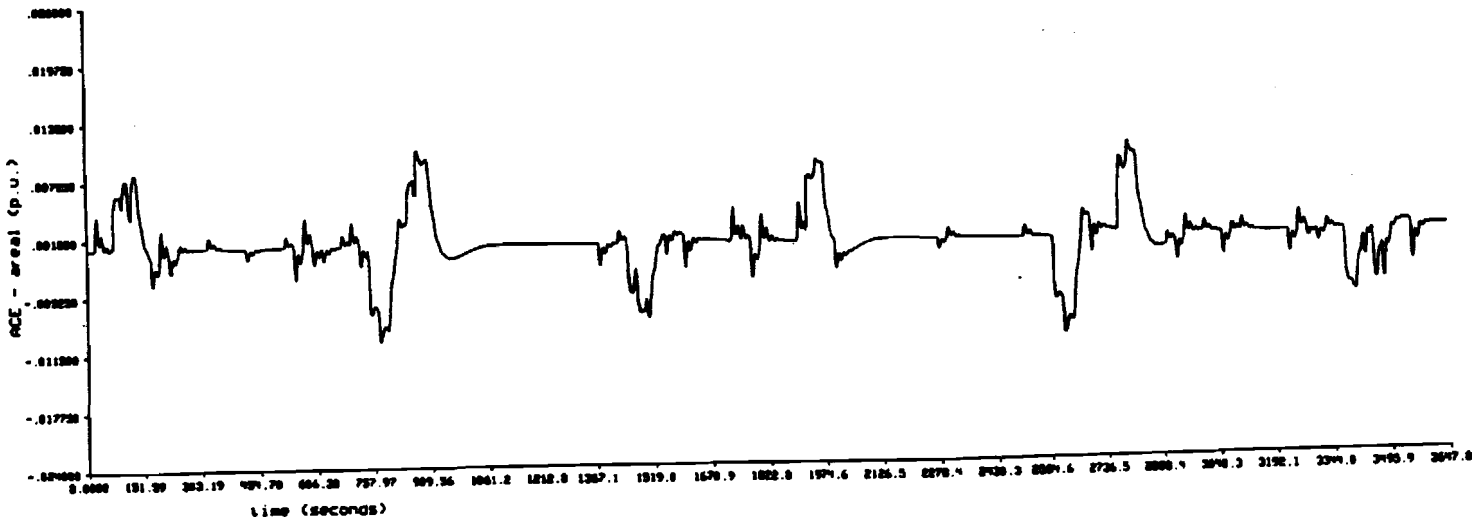

Figure 5.14 ACE in Area 1 (Rolling Mill Load - SMES Device Present)

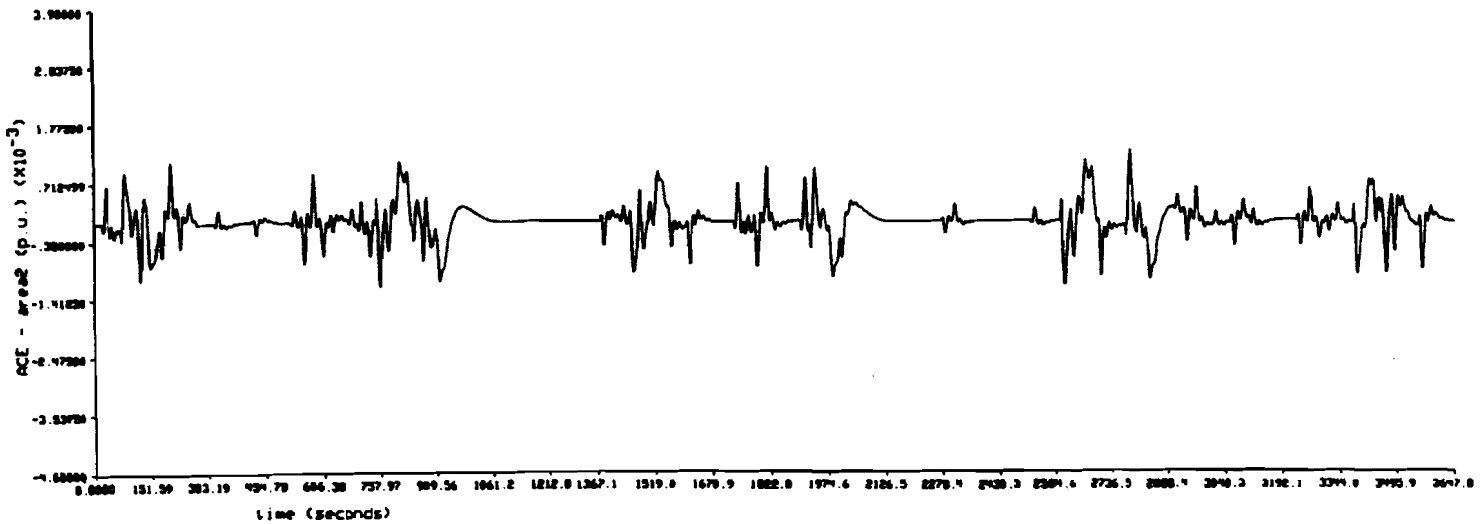

Figure 5.15 ACE in Area 2 (Rolling Mill Load - SMES Device Present)

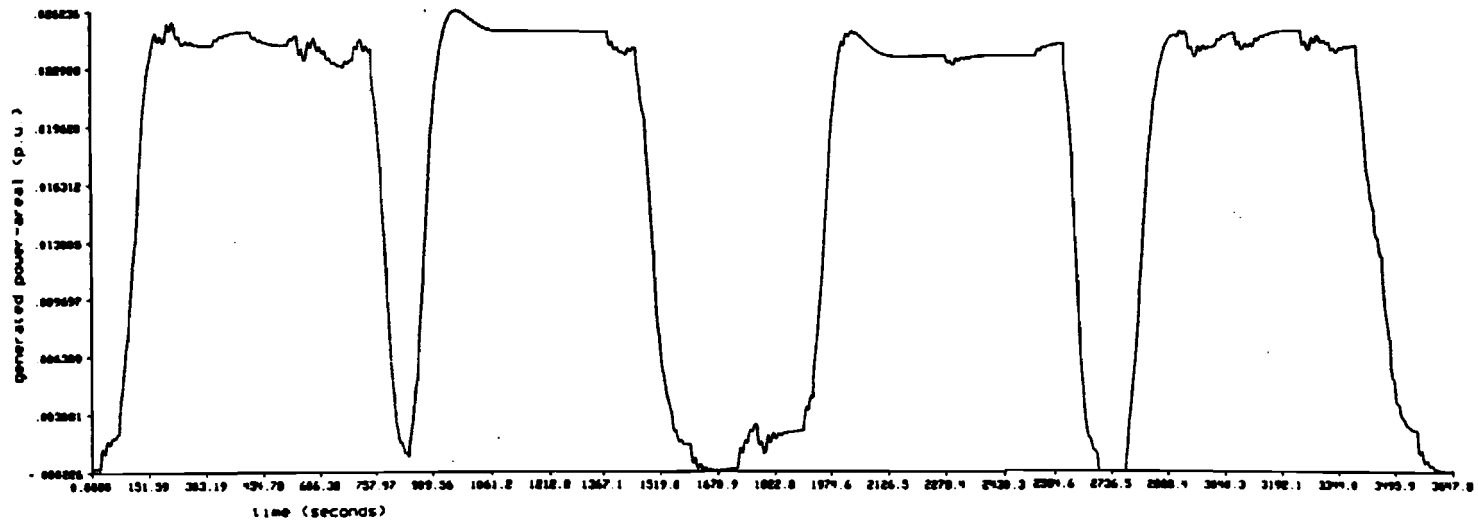

Figure 5.16 Change in Generated Power in Area 1
(Rolling Mill Load - SMES Device Present)

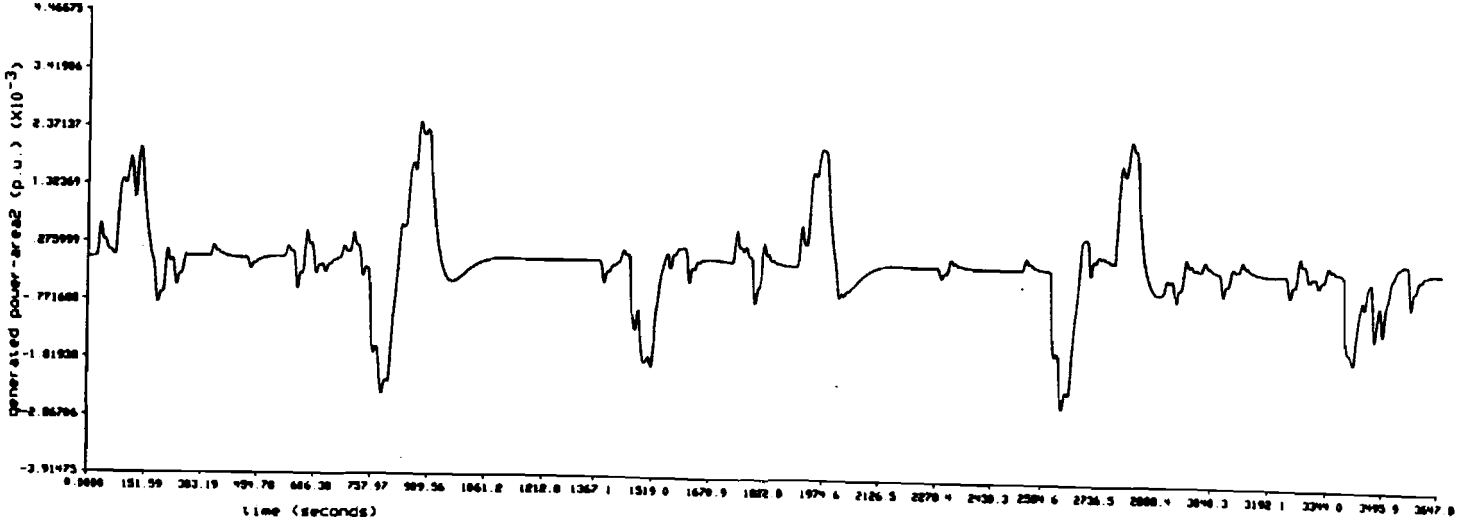

Figure 5.17 Change in Generated Power in Area 2
(Rolling Mill Load - SMES Device Present)

Table 5.2 System Performance Measurements (Rolling Mill Load -SMES Device)

Parameter	Base Case	SMES Case
max f1	60.03119 Hz	60.01022 Hz
min f1	59.96936 Hz	59.9897 Hz
max f2	60.01726 Hz	60.00723 Hz
min f2	59.98314 Hz	59.99286 Hz
max ACE1	0.025275 p.u.	0.010294 p.u.
min ACE1	-0.023288 p.u.	-0.010602 p.u.
max ACE2	0.003873 p.u.	0.001307 p.u.
min ACE2	-0.0045009 p.u.	-0.0012301 p.u.
max Ptie in	-0.01599 p.u.	-0.007593 p.u.
max Ptie out	0.014954 p.u.	0.0074762 p.u.
Wtie import	-1989.879 MWs	-1953.981 MWs
Wtie export	1993.609 MWs	1957.144 MWs
Wtie net	4.1427 MWs	3.687 MWs

The following observations can be made about the response of the SMES device to the rolling mill load:

• When the rolling mill load is applied in area 1, the SMES device responds essentially in the same way as when a step load is applied. During the "step up" portion of the rolling mill load, the converter voltage, Vd, drops in response to the dropping frequency in area 1. As in the step load case, the spikes in voltage and power output are recognizable as the frequency in area 1 increases to the lower limit of the deadband at 59.995 Hertz. These spikes occur because as the power output of the SMES device goes to zero at 59.995 Hertz, a mismatch in power in area 1 occurs. This mismatch in power causes the frequency in area 1 to drop thereby forcing the converter voltage negative again, which results in the device discharging. These spikes in voltage and power output continue until the power generated in area 1 plus the power flowing into area 1 across the

tie-line are sufficient to keep the frequency in area 1 within the frequency deadband of the SMES device.

• During the "step down" portion of the rolling mill load, the SMES device operates in an opposite manner to that described above. During the "step down" portion, the power generated in area 1 exceeds the demand and forces the frequency above 60 Hertz. The positive frequency deviation causes the converter voltage, V_d, to go positive and the device charges. Similar to what happens during the "step up" portion of the rolling mill load, during the "step down"portion, voltage spikes occur as the frequency enters the frequency deadband of the SMES device. As the frequency in area 1 enters the deadband, the power output of the device goes to zero. At this point,,there is a power mismatch in area I due to excess generation and the area 1 frequency rises above the 60.005 deadband limit and the SMES device begins to charge again. This results in the spikes present in the converter voltage and the power output of the SMES device, as seen in Figures 5.8 and 5.10. These spikes continue until the power generated in area 1 minus the power flow our of area 1 across the tie-line is sufficient to keep the frequency in area 1 at or below 60.005 Hertz.

• As in the step load case, the time between the application of the load and the time in which the area frequency is within the SMES deadband is limited by the relatively slower time constants present in the steam system.

• By observing Figure 5.10, it is evident that the SMES device is only charging or discharging during the initial change in load, which is a relatively short time compared to the overall time. For the majority of the time, the area 1 frequency is within the SMES device deadband and the device.power output is zero.

• By observing Figure 5.9, it is evident that the rolling mill load does not greatly effect the amount of current in the superconducting coil relative to its overall storage capabilities. The "step up" and "step down" nature if the load causes the SMES device to

discharge and then to charge back to approximately its original value of current. This implies that, for this application, the energy storage device can be smaller than originally estimated.

The following observations can be made about the system responses when the SMES device is present in the system:

*As seen in Figure 5.11, the frequency in area 1 tends to linger at the lower (or upper) limit of the SMES deadband after the appropriate load is applied (or removed). These lower and upper limits are 59.995 Hertz and 60.005 Hertz respectively. This occurrence was explained in section 4.2 for the step load and applies here. At these frequencies, the SMES device will discharge (or charge) just enough to keep the frequency in area 1 at the lower (or upper) limit of the deadband. The SMES device continues discharging (or charging), but by a smaller and smaller amount as the generated power is increasing. When the generated power in area 1 plus the tie-line power is sufficient to keep the frequency within the SMES deadband, the power produced (or absorbed) by the SMES device goes to zero.

• With the SMES device on line, the instantaneous power mismatch in area 1 is not as large as in the case with no energy storage device. Therefore, the frequency deviations, area control errors, and tie-line power flows do not achieve the same magnitudes as in the base case. Since the ACE is the input which essentially sets the output of the turbine-generators, the smaller magnitude in ACE results in a slower change in the generated power in each area.

• As the frequency is held at the lower limit of the SMES deadband, the SMES power output is slowly decreasing as the generated power in area 1 is slowly increasing. As a result, the tie-line power flow from area 2 during this time is held fairly constant. Since there is no change in load in area 2, this tie-line flow to area 1 is equal to the power generated in area 2. Therefore, the generated power in area 2, along with the frequency

in area 2, is held fairly constant for the period in which the frequency in area 1 is being held constant. A similar phenomenon is seen when the frequency in area 1 is being held at the upper limit of the SMES deadband.

• As mentioned above, the change in generated power is slower with the SMES device than without it. This results in the system parameters (frequencies, ACE) taking a longer time in approaching their steady state values. It is also seen in the plots that the oscillations in the responses are much smaller in the SMES case (or gone altogether) than in the base case. This is a result of the fact that the SMES device acts as a "buffer" between the rapidly changing load and the system. Its ability to respond quickly to the load eliminates the large deviations in the system parameters and many of the oscillations in the system.

• As mentioned in case 2, the SMES device effects the system operation more in the short run than in the long run. It eliminates the large deviations in frequency, ACE, and tie-line power flow. It also eliminates the oscillatory nature of rapidly increasing generation. In the long run though, the system operation is still constrained by the longer time constants present in the steam system. In effect, the SMES device does not force the system parameters to their steady state values any faster , but it greatly reduces the large initial deviations in the responses.

5.4 Case 6: Rolling Mill Load with a Battery Energy Storage Device in Area 1

Case 6 is the system response to a rolling mill load in area 1 with a battery energy storage (BES) device present in area 1. The important parameters of the BES device area plotted. These include: the voltage across the converter (Vd); the voltage of the common DC bus of the batteries (Vb); the current (Id); the power output of the device (Pd), in which a negative value indicates a discharge of power; and the total energy stored (W). These plots are shown in Figures 5.18 - 5.22. The plots of the system outputs

(frequencies, ACE, tie-line power, generation) are shown in Figures 5.23 - 5.29. As in case 5, the data from the base case was not superimposed on the the case 6 data., although the figures are plotted on the same scale as the figure from the base case. This allows for an easier visual comparison of the cases. The system measurements (minimum/maximum frequencies, etc.) are shown in Table 5.3 along with the system measurements for the base case with the rolling mill load.

The system response with the battery energy storage system in area 1 is nearly identical to the system response with the SMES device in area 1. Both are able to charge or discharge nearly instantaneously and both reduce the initial large deviations in frequency, area control error, and tie-line flow. The major changes and improvements in the system response are the same as in the SMES case so they will not be repeated here. Although it is not clearly visible in this case, the BES device does not supply as much power as the SMES device does when the initial step up in load occurs. This has several effects as far as the system response is concerned:

• The magnitude of the initial change in frequency at the points of rapidly changing load for the BES case is slightly larger than in the SMES case. This results in the initial area control errors being slightly larger and a also a larger initial tie-line power flow.

• Since the initial magnitude of the area control errors is slightly larger in the BES case than in the SMES case, the signal to increase (or decrease) generation is larger also. This results in a more rapid change in the generated power in both areas. As discussed earlier, the time constants of the steam system are the limiting factor for the frequencies, area control errors, and tie-line power flow to reach their steady state value. Therefore, the slight increase in initial frequency deviations and area control errors results in an increased rate of change of generated power and an improved settling time for the system response.

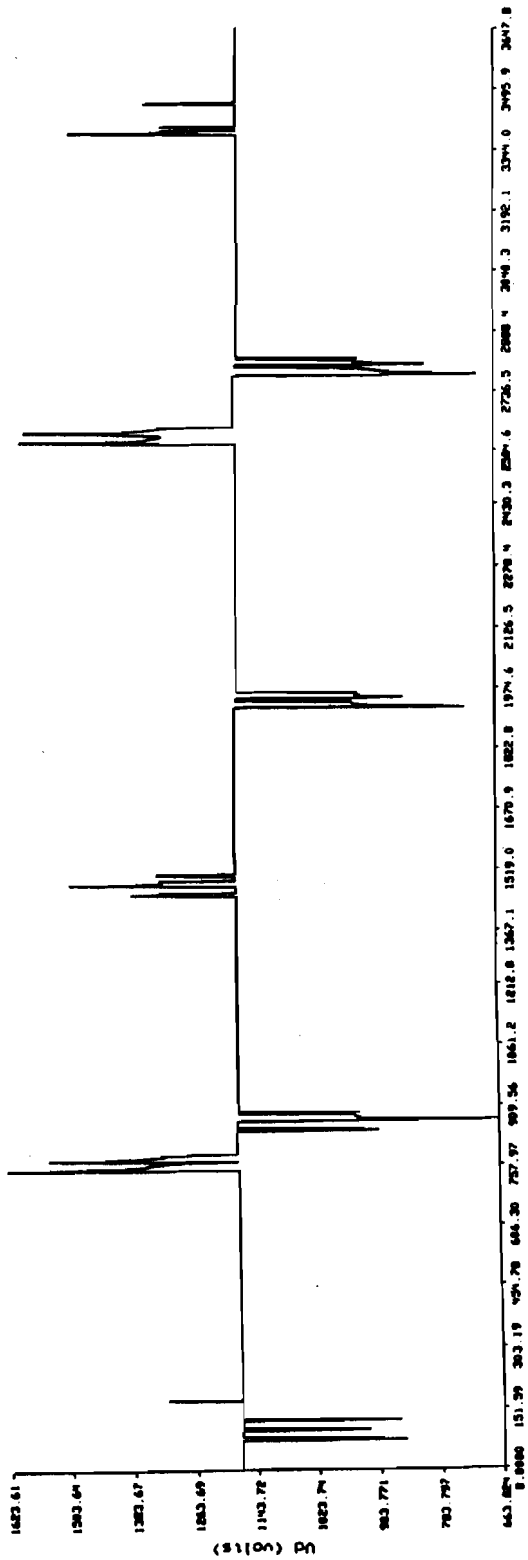

Figure 5.18 BES Converter Voltage - Vd (Rolling Mill Load)

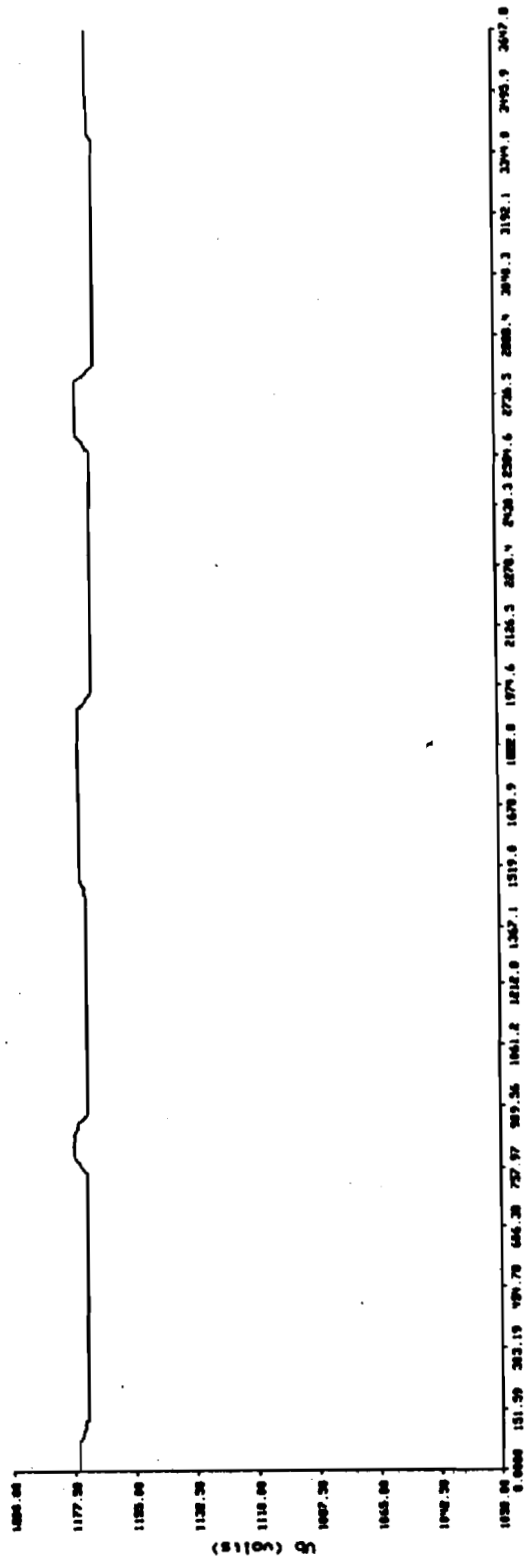

Figure 5.19 BES Common DC Bus Voltage - Vb (Rolling Mill Load)

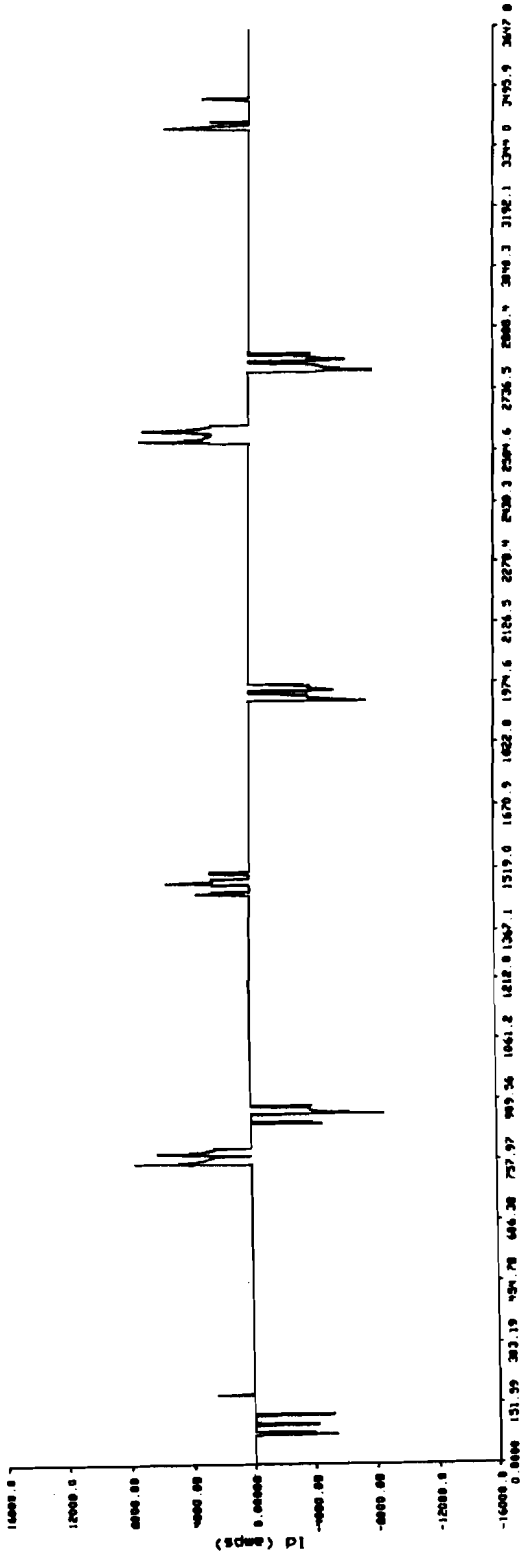

Figure 5.20 BES Current - Id (Rolling Mill Load)

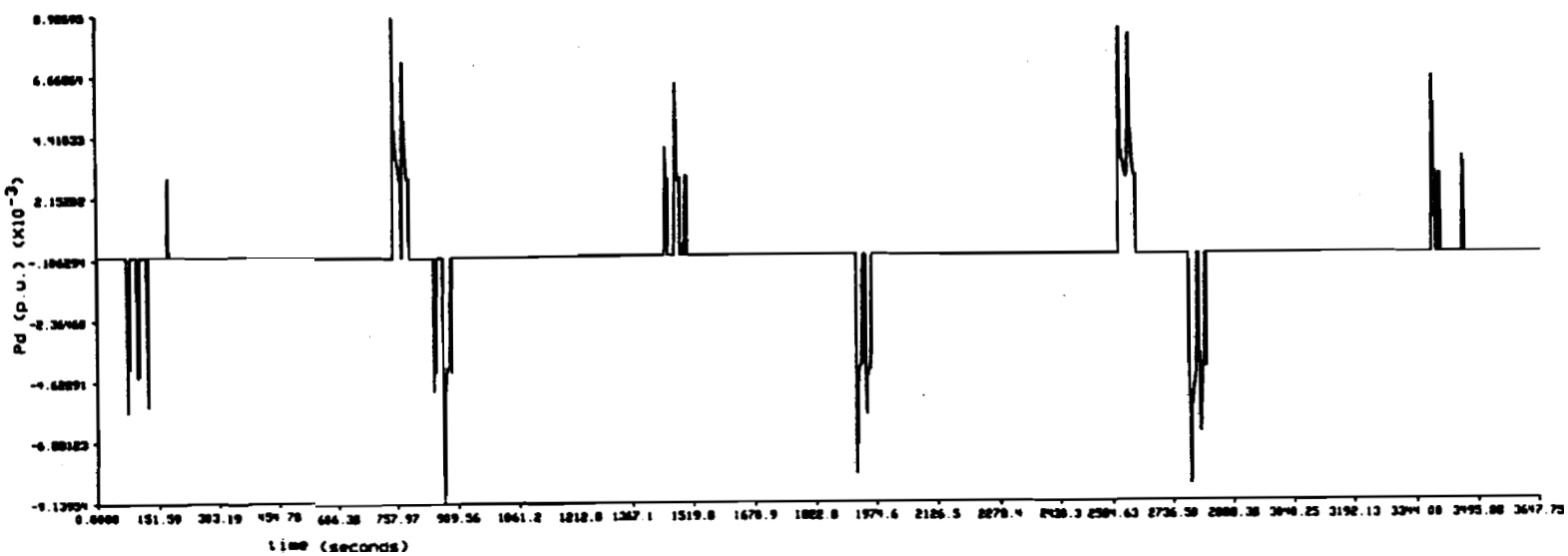

Figure 5.21 BES Power Output - P_d (Rolling Mill Load)

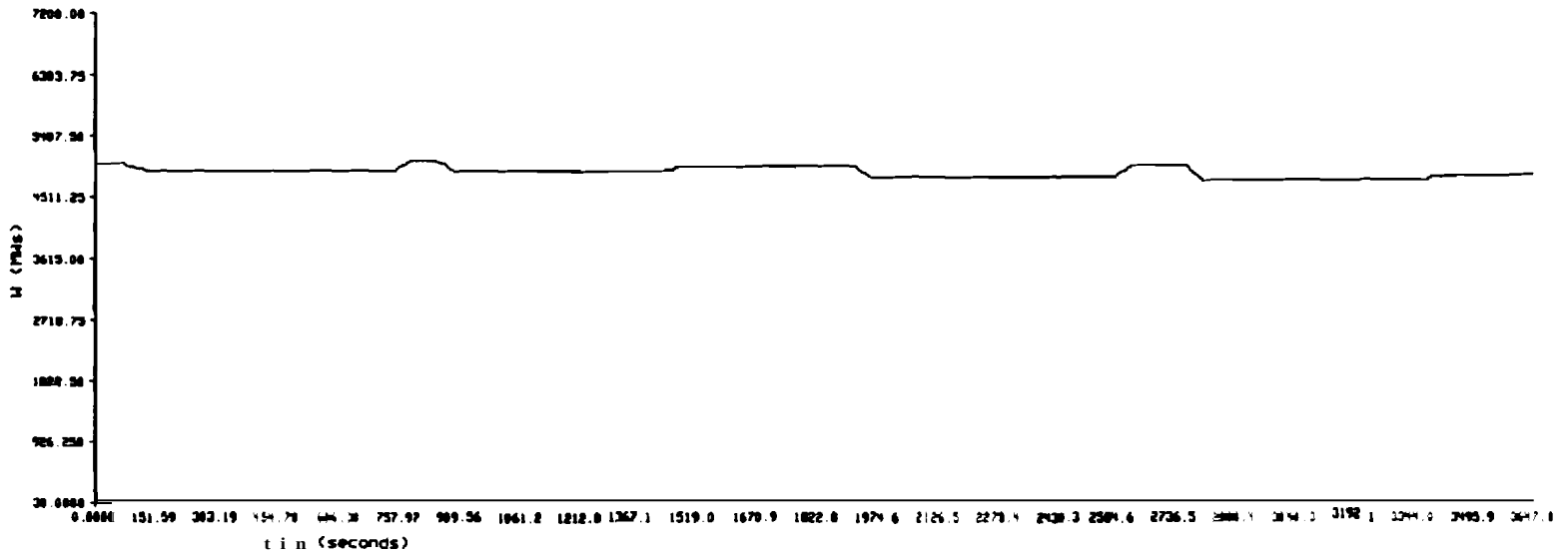

Figure 5.22 BES Energy Stored - W (Rolling Mill h a d)

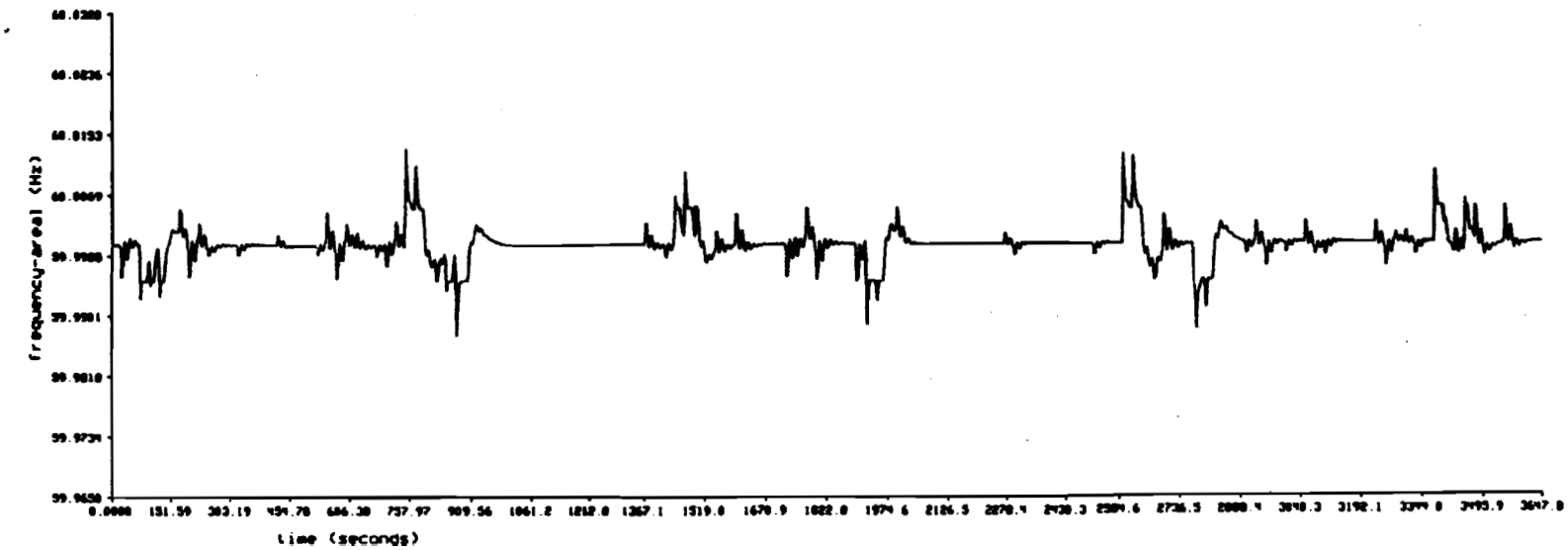

Figure 5.23 Frequency in Area 1 (Rolling Mill Load - BES Device Present)

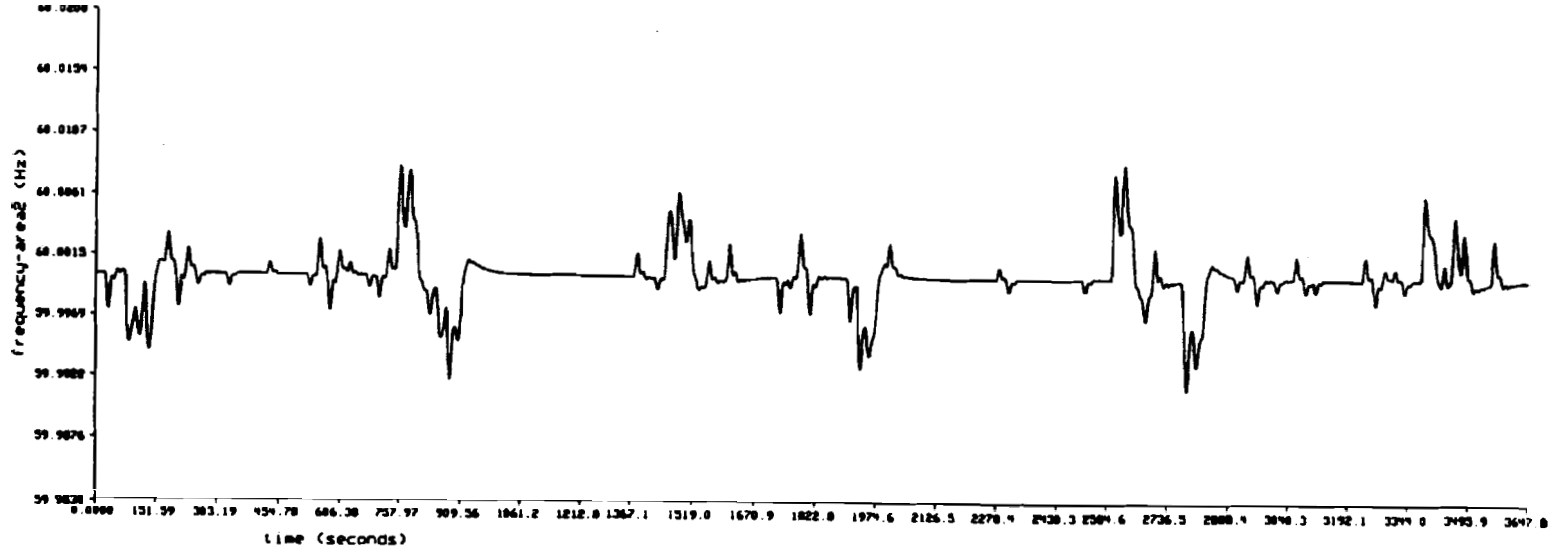

Figure 5.24 Frequency in Area 2 (Rolling Mill Load - BES Device Present)

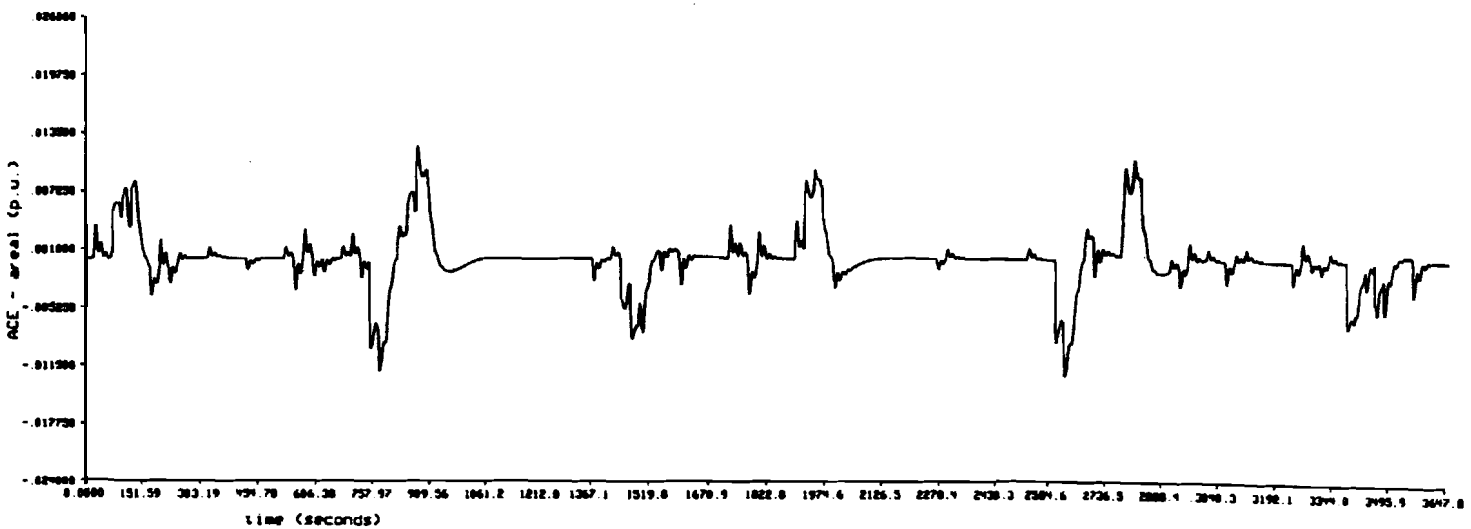

Figure 5.26 ACE in Area 1 (Rolling Mill Load - BES Device Present)

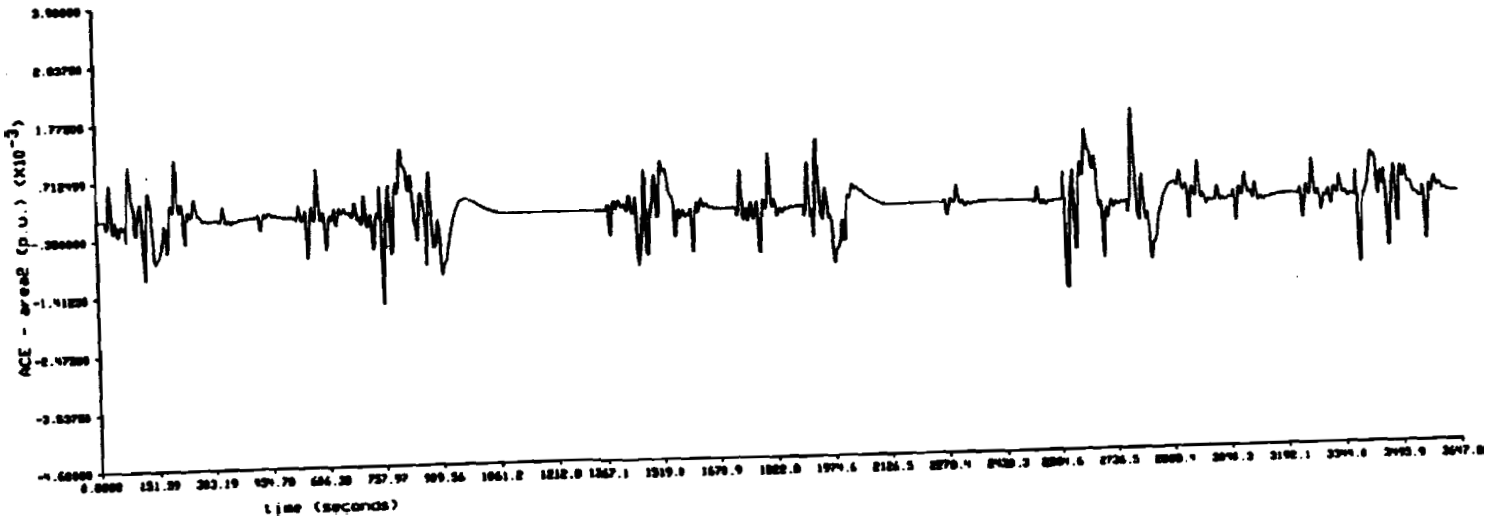

Figure 5.27 ACE in Area 2 (Rolling Mill Load - BES Device Present)

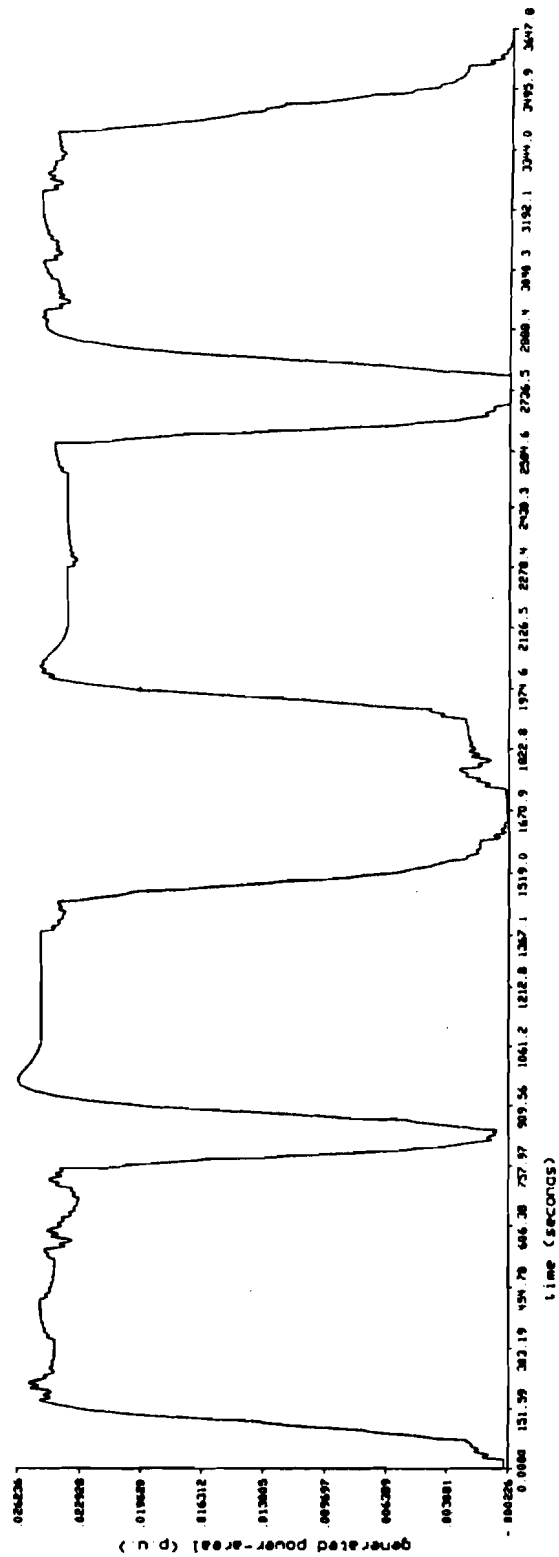

Figure 5.28 Change in Generated Power in Area 1
(Rolling Mill Load - BES Device Present)

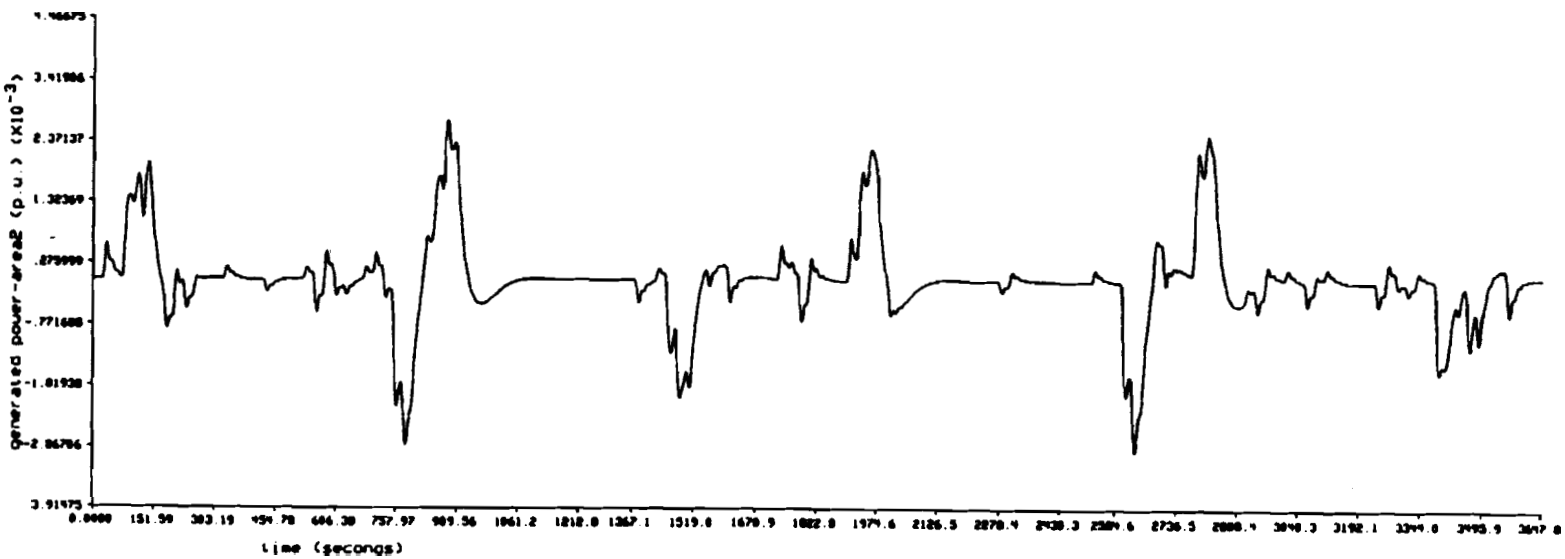

Figure 5.29 Change in Generated Power in Area 2
(Rolling Mill Load - BES Device Present)

Table 5.3 System Performance Measurements (Rolling Mill Load - BES Device)

Parameter	Base Case	BES Case
max f1	60.03119 Hz	60.01343 Hz
min f1	59.96936 Hz	59.98729 Hz
max f2	60.01726 Hz	60.00871 Hz
min f2	59.98314 Hz	59.99152 Hz
max ACE1	0.025275 p.u.	0.01207 p.u.
min ACE1	-0.023288 p.u.	-0.01278 p.u.
max ACE2	0.003873 p.u.	0.001640 p.u.
min ACE2	-0.0045009 p.u.	-0.001684 p.u.
max Ptie in	-0.01599 p.u.	-0.008596 p.u.
max Ptie out	0.014954 p.u.	0.089160 p.u.
Wtie import	-1989.879 MWs	-1969.109 MWs
Wtie export	1993.609 MWs	1972.395 MWs
Wtie net	4.1427 MWs	3.7175 MWs

CHAPTER 6
CONCLUSIONS

In areas with rapidly changing loads of large magnitude, utility companies often experience large deviations in frequency and area control error. Inadvertent tie-line power flow can also be a problem in these situations. A summary was given of automatic generation control strategies currently used in power systems to: reduce the deviations in frequency, reduce area control error, and to match the generation with the demand. Three different types of energy storage devices were discussed. The most commonly used form of energy storage in the power industry - pumped hydroelectric storage - was discussed. An old energy storage technology with new applications in the power industry - battery energy storage - was also discussed along with a relatively new technology with many possible applications - superconducting magnetic energy storage. To study these storage devices effectively requires integration of models of the devices into an overall power system model.

The focus of this research was to examine the effects that different types of energy storage devices have on power systems with rapidly changing loads. The specific loads tested were a step change in load and a five-stand rolling mill load. The three different cases for each of the two types of load were: no energy storage device in the system, a superconducting magnetic energy storage device in the system, and a battery energy storage device in the system.

There are several general conclusions that can be reached by analyzing the system response with and without an energy storage device on the system. It is

evident that the system response with an SMES device present is very similar to the system response when a battery energy storage device is present. Although they are devices with distinctly different methods of operation, they are both able to charge or discharge nearly instantaneously. The converter voltage, which regulates the power output of the energy storage device, responds in the same way to the changing loads regardless of the type of energy storage device. The power output of the two different devices is nearly identical making the system response nearly identical in both cases. From the system point of view, the energy storage device is simply a means of providing or absorbing power instantaneously regardless of what is on the DC side of the AC/DC converter.

An energy storage device in the system is able to respond very quickly to rapidly changing loads and is able to greatly effect the system operation in the short term. This means that the large initial deviations in frequency, area control error, and tie-line power flow are greatly reduced. The long term performance of the system, though, is constrained by the relatively slower time constants present in the steam system. Therefore, the system parameters (frequency, tie-line power flow, area control error) do not reach their steady state values any faster with an energy storage device in the system than without an energy storage device. In fact, they may take longer to reach their steady state values because the energy storage device reduces the large deviation in area control error. This control error is a signal which sets the area generation. Since the deviation in this signal is smaller than in the case of no energy storage, the change in generation occurs at a slower rate. Therefore, the tie-line power flow, frequencies, and area control errors may take a longer time to reach steady state.

By observing Figures 5.9 and 5.22, it is evident that the energy storage device for this application has been oversized. The rolling mill load has a "step up - step

down" pattern and allows the energy storage device to charge as well as discharge. Therefore, the energy level in the device remains fairly constant throughout the load cycle, especially in the SMES case when the losses are only on the order of 5%. For this application, it is estimated that the energy storage devices could be sized down from 2 MWh to approximately 0.25 MWh.

The system response was affected by setting a ±0.005 Hz deadband on the energy storage devices. The intent was to keep the energy storage devices from responding to small deviations in frequency, which are ever-present in the power system. This is especially important in the battery energy storage device where the batteries have a limited charge/discharge cycle life. Although the deadband reduced the effectiveness of the energy storage devices to some extent and produced "spikes" in energy charge/discharge, its elimination produces new problems in the system response. Without a deadband, the system responds to all deviations in frequency and is constantly charging or discharging in an attempt to track the system frequency. This appears to be an inappropriate mode of operation. In the case of a large, rapidly changing load, the area frequency is driven to its steady state value more rapidly without the frequency deadband than with the frequency deadband. This is because the energy storage device supplies (or demands) enough power to eliminate the power mismatch in the area and thus drives the frequency deviation and area control error to approximately zero. Recall, the area control error is a signal that increases or decreases generation. When the area control error is near zero, the effect of this input signal is to change generated power slowly. This means that the energy storage device will have to charge (or discharge) for a much longer period of time as the generation slowly increases (or decreases). This requires a larger energy storage capability for the device and a correspondingly higher cost.

There are different types of logic that can be used in controlling the firing angle of the AC/DC converter in the SMES and BES systems. One: is a scheme which uses the area control error as input instead of the frequency error. Another is a control strategy which may be helpful in reducing the size of the energy storage device. It is a control which uses the frequency or area control error to set the firing angle during periods of rapidly changing loads, but during periods of relative steady state, the energy stored is slowly driven to its initial value. At this initial value, the energy storage device is equally ready to charge or discharge. This could reduce the chance that the energy stored in the device would reach its upper or lower limit.

It is evident in Figures **4.16, 4.17, 4.28, 4.29, 5.16, 5.17, 5.28, 5.29** that the rapid increase in generation is less oscillatory when there is an energy storage device in the system. This is due to the fact that the energy storage device supplies the power demanded in the short term and the power generation is able to increase at a slower and steadier rate.

As mentioned in section 5.4, the initial power output of the BES device in response to a rapid increase in load is not as great as with the SMES device. This provides an example of the advantages and disadvantages of a rapid response. If the frequency deviation and ACE are minimal, the change in generation is slower and the system parameters take a longer time to reach steady state. If the frequency deviation and area control error are larger, the change in generation is faster and the system parameters reach steady state faster.

Although large superconducting magnetic energy storage devices are still an experimental technology, they are certainly feasible. In **1983,** the Bonneville Power Administration successfully built and tested an **8.4** kWh SMES device with a 10 MW converter. The lossless nature of the device is certainly an advantage as far as efficiency is concerned (typical estimates range from 92% to 96%), but it is also

advantageous because the lack of resistance eliminates heating of the wire and the associated degradation of the wire. The rapid response time of an SMES device would provide a new means of system control in areas with rapidly changing loads. Different control methodologies could be used to optimize the effectiveness of the device. The two major drawbacks of an SMES device are the high cost and the fact that a large-scale device has never been built. The technology exists and numerous studies have shown the feasibility and advantages of a large-scale SMES device, but the actual construction of a large-scale device has not been accomplished. Even the cost of a small-scale device is expensive. A 2800 kVAs SMES device costs on the order of 2.2 million dollars. As mentioned above, an energy storage (deviceused to reduce the detrimental effects of the rolling mill load would be approximately 0.25 MWh. Based on References [3, 15, 16], the cost of an SMES device with energy storage capacity of 0.25 MWh would be on the order of 100 million dollars.

Large-scale battery energy storage facilities have been used in several applications in recent history. A 17 MW, 14.4 MWh BES plant in Berlin is used for frequency regulation. A 10 MW, 51.2 MWh BES plant is used in California for load leveling. Also, a 20 MW, 10 MWh BES plant is being planned for frequency regulation in Puerto Rico. Although the efficiency of a BES plant (approximately 80%) is not as high as an SMES plant, battery energy storage technology has the advantage of being well established and already having several facilities in use. The BES plant is able to respond as rapidly as an SMES plant to changing loads and it can provide all of the corresponding advantages as far as new methods of system operation. One drawback of the BES facility would be the limited cycle life of the batteries. An advantage when compared to the SMES option would be the relative inexpense of a BES facility. A 0.25 MWh BES facility would cost on the order of 5 million dollars.

LIST OF REFERENCES

[1] North American Electric Reliability Council Control Performance Criteria, 1991.

[2] G.M. Cook, W.C. Spindler, G. Grefe, "Overview of Battery Power Regulation and Storage," IEEE Transactions on Energy Conversion, v. 6, No. 1, pp. 204-211, March, 1991.

[3] W. Hassenzahl, "Superconducting Magnetic Energy Storage," IEEE Transactions on Magnetics, v. 25, No. 2, pp. 750-757, March. 1989.

[4] J. Jensen, Energy Storage, Butterworth Publishers Inc., Boston, 1980.

[5] D.S. Carr, "Lead/Acid Batteries in U.S.A. Load-Levelling Applications," Journal of Power Sources, v. 31, pp. 297-310, May/June, 1990.

[6] W. Hassenzahl, Electrochemical, Electrical, and Magnetic Storage of Energy, Hutchinson Ross Publishing Co., New York, 1981.

[7] R.S. Koebbe, "Benefits and Applications of Modular Hydroelectric Pumped Storage," Proceedings of the International Conference on Hydropower, v. 1, pp. 583-592, July, 1991.

[8] S. Banerjee, J.K. Chatterjee, S.C. Tripathy, "Application of Magnetic Energy Storage Unit as Load-Frequency Stabilizer," IEEE Transactions on Energy Conversion, v. 5, No. 1, pp. 46-51, March, 1990.

[9] W.C. Spindler, "Lead/Acid Batteries in Utility Energy Storage and Power Control Applications," Journal of Power Sources, v. 35, pp. 395-398, September, 1991.

[10] T. Moore, "Pumped Hydro: Backbone of Utility Storage," EPRI Journal, v. 11, No. 1, pp. 24-31, January/February, 1986.

[11] J.G. Warnock, "Milestones in Pumped Storage Development," American Society of Civil Engineers, Proceedings of the Engineering Foundation Conference on Converting Existing Hydro-Electric Dams and Reservoirs into Pumped Storage Facilities, Rindge, NH, pp. 163-196, August 18-23, 1974.

[12] H.J. Boenig, J.F. Hauer, "Commissioning Tests of the Bonneville Power Administration 30 MJ Superconducting Magnetic Energy Storage Unit," IEEE Transactions on Power Apparatus and Systems, v. PAS-104, No. 2, pp. 302-312, February, 1985.

[13] J.F. Hauer, H.J. Boenig, "Control Aspects of the Tacoma Superconducting Magnetic Energy Storage Project," E E E Transactions on Power Systems, v. PWRS-2, No. 2, pp. 443-450, May, 1987.

[14] P.D. Baumann, "Energy Conservation and Environmental Benefits That May Be Realized from Superconducting Magnetic Energy Storage," Proceedings of the IEEE/PES 1992 Winter Meeting, New York, NY, January, 26-30, 1992.

[15] H.A. Peterson, N. Mohan, R.W. Boom, "Superconductive Energy Storage Inductor · Converter Units for Power Systems," IEEE Transactions on Power Apparatus and Systems, v. PAS-94, No. 4, pp. 1337-1346, July/August, 1975.

[16] C.A. Luongo, R.J. Loyd, "Superconducting Magnetic Energy Storage for Elecmc Utility Load Leveling: A Study of Cost vs. Stored Energy," Proceedings of the American Power Conference, v. 49, pp. 207-212, 1987.

[17] J.G. DeSteese, D.K. Kreid, J.M. Haner, W.E. Myers, "Assessment of SMES Benefits in Electric Utility Applications," Proceedings of the American Power Conference, v. 53, pp.1149-1156, 1991.

[18] K. Tam, A. Yarali, "Operation Principle and Application of Multiterminal Superconductive Energy Storage Systems," IEEE/PES 1992 Winter Meeting, New York, January 26-30, 1992.

[19] G.W. Vinal, *Storage* Batteries, John Wiley & Sons, Inc., New York, 1955.

[20] C.H. Mantell, Batteries and Energy Systems, McGraw-Hill, Inc., New York, 1983.

[21] M.D. Anderson, D.S. Carr, "Battery Energy Storage Technologies"

[22] H.J. Kunisch, K.G. Kramer, H. Dominik, "Battery Energy Storage: Another Option for Load-Frequency-Control and Instantaneous Reserve," IEEE Transactions on Energy Conversion, v. EC-1, No. 3, pp.41-46, September, 1986.

[23] S. Eckroad, B. Radimer, "Review of Engineering Design Considerations for Battery Energy Management Systems," IEEE Transactions on Energy Conversion, v. 6, No. 2, pp. 303-309, June, 1991.

[24] R.C. Reckrodt, M.D. Anderson, R.M. Kluczny, "Economic Model for Battery Energy Storage: Improvements for Existing Methods," IEEE Transactions on Energy Conversion, v. 5, No. 4, pp. 659-665, December, 1990.

[25] N. Jaleeli, L.S. VanSlyck, D.N. Ewart, L.H. Fink, A.G. Hoffmann, "Understanding Automatic Generation Control", IEEE Transactions on Power Systems, v. 7, No. 3, pp. 1106-1111, August, 1992.

[26] R. Ramabhadran, G.T. Heydt, R. Shoureshi, R. Kramer, M. Stears, "Active and Reactive Power Flow for Multiarea Systems on Automatic Generation Control", September, 1992.

[27] O.I. Elgerd, C.E. Fosha, Jr., "Optimum Megawatt Frequency Control of Multiarea Electric Energy Systems," E E E Transactions on Power Apparatus and Systems, v. PAS-89, No. 4, pp. 556-563, April, 1970.

[28] C.E. Fosha, Jr., 0.1. Elgerd, "The Megawatt-Frequency Control Problem: A New Approach Via Optimal Control Theory," JEEE Transactions on Power Apparatus and Systems, v. PAS-89, No. 4, pp. 563-577, April, 1970.

[29] F.P. deMello, R.J. Mills, W.F. B'Rells, "Automatic Generation Clontrol Part I - Process Modeling" IEEE/PES Summer Meeting, San Francisco, July 9-14, 1972.

[30] F.P. deMello, R.J. Mills, W.F. B'Rells, "Automatic Generation Control Part II - Digital Control Techniques," IEEE/PES Summer Meeting, San Francisco, July 9-14, 1972.

[31] R. Podmore, M.J. Gibbard, D.W. Ross, K.R. Anderson, R.G. Page, K. Argo, K. Coons, "Automatic Generation Control of Jointly-Owned Generating Units," IEEE Transactions on Power Apparatus and Systems, v. PAS-98, No. 1, pp. 207-215, January/February 1979.

[32] W. Prince, "Cost Aspects of AGC, Inadvenant Energy and Time Error," IEEE Transactions on Power Systems, v. PS-5, No. 1, pp.111-118, February, 1990.

[33] A.J. Wood, B.F. Wollenberg, Power Generation. Operation. and Control, John Wiley & Sons, Inc., New York, 1984.

[34] IEEE Committee Report, "Dynamic Models for Steam and Hydro Turbines in Power System Studies," IEEE Transactions on Power Apparatus and Systems, v. PAS-86, pp. 443-453, April, 1967.

[35] C.L. Mantell, Batteries and Energy Systems, McGraw-Hill, Inc., New York, 1983.

[36] W. Buckel, Superconductivity: Fundamentals and Applications, Weinheim, New York, 1991.

[37] V.Z. Kresin, S.A. Wolf, Fundamentals of Superconductivity, Plenum Press, New York , 1990.

[38] B.S. Deaver, Advances in Superconductivity, Plenum Press, New York, 1983.

[39] T. Van Duzer, C. Turner, Principles of Superconductive Devices and Circuits, Elsevier North Holland, New York, 1981.

[40] G. Burns, High Temperature Superconductivity: An Introduction, Academic Press, Boston, 1992.

[41] C.N.R. Rao, Chemistry of High Temperature Superconductors, World Scientific, River Edge, New Jersey, 1991.

[42] H.S. Kwok, P. Coppens, Y.H. Kao, Superconductivity and Its Applications, American Institute of Physics, New York, 1991.

[43] L.C.Gupta, Theoretical and Experimental Approaches to High-Tc and Conventional Superconductivity, Nova Science Publishers, New York, 1991.

[44] M. Ferrier, "Stockage d'energie dans un enroulement supraconductor," Low Temperature and Electrical Power, London, pp.425-432, 1970.